JAERI-M
83-095

JAERI TANDEM

ANNUAL REPORT

1 9 8 2

September 1, 1981 - March 31, 1983

June 1983

Department of Physics

日 本 原 子 力 研 究 所
Japan Atomic Energy Research Institute

JAERI-M レポートは，日本原子力研究所が不定期に公刊している研究報告書です。
入手の問合わせは，日本原子力研究所技術情報部情報資料課（〒319—11 茨城県那珂郡東海村）あて，お申しこしください。なお，このほかに財団法人原子力弘済会資料センター（〒319—11 茨城県那珂郡東海村日本原子力研究所内）で複写による実費頒布をおこなっております。

JAERI-M reports are issued irregularly.
Inquiries about availability of the reports should be addressed to Information Section, Division of Technical Information, Japan Atomic Energy Research Institute, Tokai-mura, Naka-gun, Ibaraki-ken 319—11, Japan.

編集兼発行　日本原子力研究所
印　　刷　日立高速印刷株式会社

JAERI-M 83-095

JAERI TANDEM
Annual Report
1982

September 1, 1981 - March 31, 1983

Department of Physics
Tokai Research Establishment, JAERI
(Received May 31, 1983)

This annual report describes research activities which have been performed with JAERI tandem accelerator from September 1, 1981 to March 31, 1983. Summary reports of 38 papers, publications, personnel and a list of co-operative researches with universities are contained.

Keywords: JAERI TANDEM, Materials Science, Nuclear Chemistry, Nuclear Physics, Fast Neutron Physics, Annual Report

Editors Kichinisuke Harada
Michio Maruyama
Kunio Ozawa
Naomoto Shikazono
Tsutomu Tamura
Shigeya Tanaka

JAERI-M 83-095

原研タンデム57年度年次報告

日本原子力研究所東海研究所
物　理　部

（１９８３年５月31日受理）

本年次報告は，原研タンデム加速器で１９８１年９月１日から１９８３年３月31日までの間に行われた研究活動をとりまとめたものである。

38篇の小論文，公表された文献，関与した職員及び大学との協力研究のリストを収録している。

（編集者）　原田吉之助・鹿園　直基・丸山　倫夫・田村　　務
小沢　国夫・田中　茂也

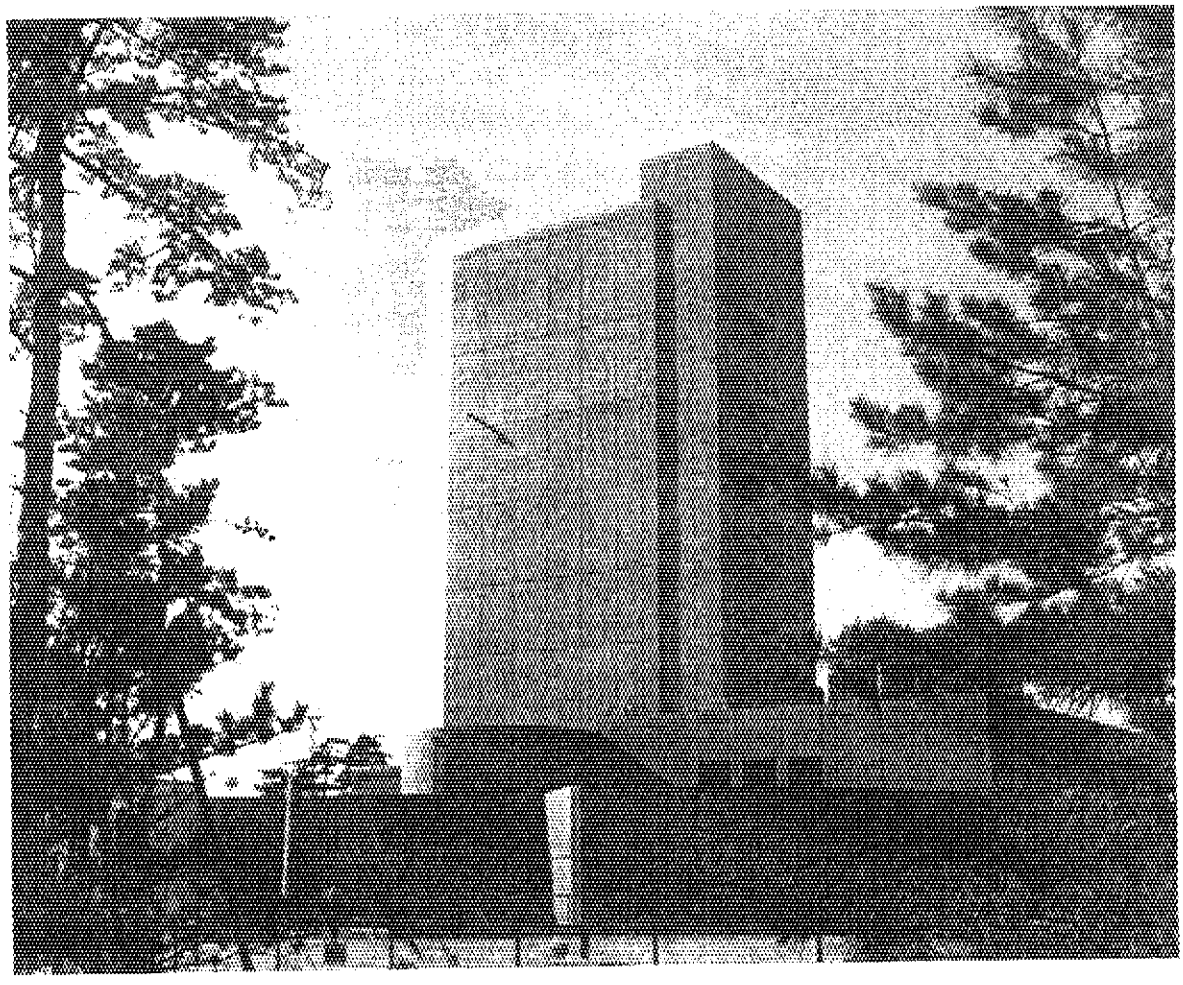

PREFACE

This is the first annual report on research activities which are going on with JAERI TANDEM. We hope this report serves in making the communication wider and deeper with domestic as well as foreign laboratories.

Installation of the JAERI tandem accelerator was completed in August, 1982. A progress record of the construction work of it has been described in "JAERI TANDEM Newsletter" No.1 to No.9. The scheduled operation of the tandem for research studies started in September, 1982. During the first six months of the operation the machine has shown a fairly stable running. At present we operate it for five whole days a week for research studies.

Our tandem accelerator will be used for manifold purpose. We will place the study emphasis on the following four subjects.

1) Materials science
2) Nuclear chemistry
3) Nuclear physics
4) Measurement of fast neutron nuclear data

At present, more than sixty staff members in JAERI have been working in the four fields of researches, and about forty colleagues of universities and institutions outside JAERI have joined and collaborated in these studies.

This volume summarizes studies on the subjects performed in a period from September, 1981 to March, 1983. There are also several reports on the developments in the accelerator technology and some theoretical studies related to the subjects.

We hope that this first issue of the annual report conveys to you enough information on our vivid activities though these are now in the beginning phase.

K. HARADA
Director, Department of Physics

CONTENTS

I ACCELERATOR OPERATION AND DEVELOPMENT

1.1 Tandem Accelerator Operation

Tandem Accelerator Group

Accelerators Division, Department of Physics,
Japan Atomic Energy Research Institute

Installation and test works of the 20MV heavy ion tandem accelerator had been continued since July, 1978 at Tokai Research Establishment of Japan Atomic Energy Research Institute. It is the Model 20UR Pelletron folded tandem accelerator manufactured by National Electrostatics Corp. in Wisconsin, U.S.A. Installation of all equipment of the system was completed and all specifications of ion beam performance were also satisfied at the terminal voltages below 18MV by June, 1982. The terminal voltage could reach 18.5MV without so intensive conditioning and the accelerator could run enough stably with both continuous and pulsed beams for heavy ion experiments. Table 1 shows some examples of the ion beam performances observed after the energy analyzing magnet. The results of the pulsed H^+ beam were obtained with the in-terminal ion source and pulsing system.

Table 1 Ion Beam Performance

Ion (Continuous)	Terminal Voltage (MV)	Energy (MeV)	Current (pμA)	Pulse Width (ns, FWHM)
H^+	18	36	5	
$^{12}C^{5+}$	14	84	0.2	
$^{16}O^{6+}$	16	112	0.35	
$^{28}Si^{8+}$	13	117	0.025	
$^{35}Cl^{9+}$	18	180	0.53	
$^{58}Ni^{10+}$	13	143	0.02	
$^{63}Cu^{10+}$	13	143	0.03	
$^{81}Br^{10+}$	13	143	0.012	
$^{127}I^{7+}$	18	144	0.54	
(Pulse, 1MHz)				
H^+	13	13	4000(peak)	0.6
	18	18	1100(peak)	0.9
$^{127}I^{8+}$	18	162	12(peak)	1.9

Considering the status of the accelerator and experimental equipments, the contract of the accelerator was terminated in August, 1982, though achievement of 20MV is left for future improvement. Schduled running of the accelerator for experiments started on September 1, 1982.

The following are summary of operation to April 8, 1983.

1) Time distribution by terminal voltage

17-18 MV	2 days	2.2 %	11-12 MV	2 days	2.2 %
16-17	11	12.0	10-11	3	3.3
15-16	28	30.3	8- 9	1	1.1
14-15	26	28.2	7- 8	1	1.1
13-14	9	9.8	3- 4	1	1.1
12-13	8	8.7			

2) Time distribution by type of projectile

H	3 days	3.3 %	D	8 days	8.7 %

C	17 days	18.4 %	Ni	13 days	14.1 %
O	23	25.0	Br	1	1.1
Cl	23	25.0	Others (Mg, In, Au etc.)	4	4.4

3) Time distribution by type of activity

Operation for research		92 days	42 %
Material test and solid state physics	24		
Nuclear chemistry	15		
Nuclear reaction and structure	38		
Neutron physics	9		
Accelerator development	6		
Voltage conditioning		9	4
Scheduled maintenance (1 tank opening)		38	17
Unscheduled maintenance (2 tank openings)		22	10
Unused time		59	27

By using the duoplasmatron source, Heinicke-Penning source, and Hiconex sputter cone source, ions of B, F, Al, S, Fe, Ge, Nb, Rh, Re and Pt are usable for experiments to add to the ions already mentioned.

JAERI type long-lived carbon foils(10 g/cm^2)[1-3] have been used as the 1st electron stripper at the exit of the low energy accelerating tube. For seven months from September, 1982 to March, 1983, 13 foils were used and their consumption times were 290, 227, 187, 99, 90, 88, 83, 59, 48, 24, 11, 10, and 5 μA·hours. Four foils of them were broken and the others still usable. Use of the 2nd foil stripper at two third potential from the tank base in the high energy accelerating tube was tried to get higher energies for ^{58}Ni ions and the results are described below.

Terminal voltage	Injected current	Charge state after 1st stripper	Charge state after 2nd stripper	Transmitted current	Ion energy
15.0 MV	450 nA	11	18	3.1 pμA	248 MeV
14.2	170	12	19	1.6	249

References

1) S. Takeuchi et al.: Nuclear Instr. and Meth. 158(1979)333.

2) S. Takeuchi and E. Takekoshi: Japan Atomic Energy Research Institute JAERI-M 9322(1981).

3) S. Takeuchi and S. kanazawa: Nuclear Instr. and Meth. 206(1983)331.

1.2 Monitoring of radiation doses and radioactive concentrations at the tandem accelerator from September 1982 to April 1983

Takeo Seki, Futao Niino and Syoji Izawa

Department of Health Physics
Japan Atomic Energy Research Institute

1. Measurements of radiation doses at the tandem accelerator building and its surroundings

For any radiation leakage, radiation doses at the points, where radiation shielding calculations were made in design, were measured by the TLD. The results are shown in Table 1.

Table 1 Radiation doses at the tandem accelerator building and its surroundings

Periods of monitoring	Numbers of monitoring points	Exposures (including B.G.)
Sept.1-Dec.4,1982	15	21.6-41.2 mR
Jan.12-Apr.9,1983	17	16.6-32.9 mR

Except in the target rooms and the accelerator tower, exposures due to tandem accelerator operation were not detected, and the radiation levels were the same as the background. The dose rate in the entrance-hall was higher than those in other places, possibly due to the radioactivity of uranium contained in the wall materials.

2. Measurements of radioactive concentrations in the target rooms during tandem accelerator operation

Because the charged particles are not introduced into the air of the target rooms, radionuclides induced in the air are due to the neutrons produced by the interaction between charged particles and target.

In the neutron target room, measurements of induced activities in the air were made from January 26 to 28, February 7 to 9 and February 21 to 22, 1983. Figure 1 shows a flow diagram of the monitoring system used for the measurements. After sampling, the filter papers were analyzed by the Ge(Li) spectrometer. The radioactivity and its decay was also measured by beta counting.

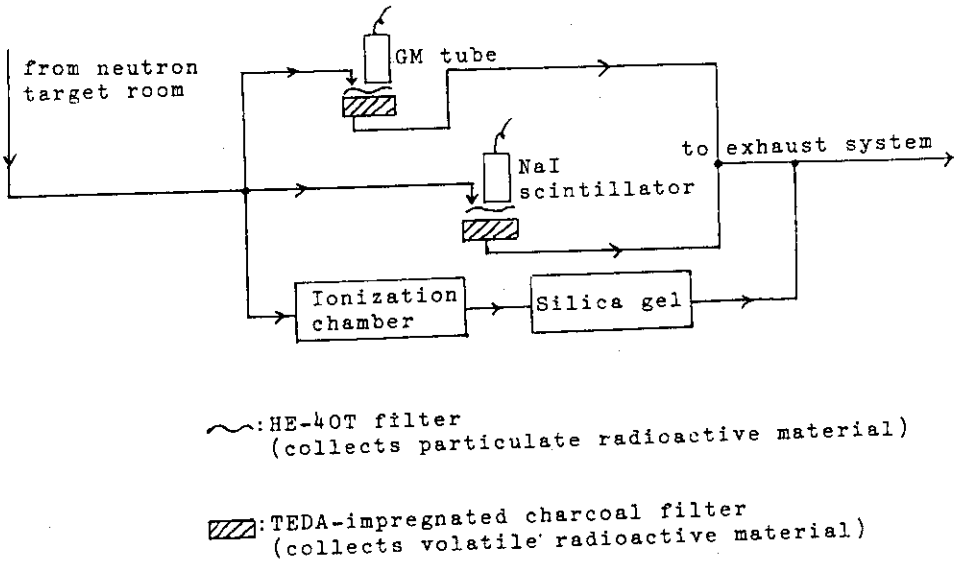

Fig.1 Air monitoring system

In the HE-40T filters, induced activities were not detected and the Ge(Li) gamma-ray spectrum was the same as the background. In the TEDA-impregnated charcoal filters, a radionuclide with a γ-ray energy peak at 0.511 Mev was trapped. The half-life of this nuclide was 110 minutes. Consequently, the nuclide was found to be ^{18}F derived from ^{19}F in (n, 2n) reaction. The radioactive concentrations were 10^{-9}~10^{-10}μCi/cm^3.

Investigations will be extended in the future for other nuclides such as ^{15}O, ^{16}N, ^{19}O and ^{41}Ar.

1.3 Production and Acceleration of Various Heavy Ions at the JAERI Tandem Accelerator

Eisuke Minehara, Shinichi Abe, Susumu Hanashima, Masumi Oshima, Chiaki Kobayashi and Shiroh Kikuchi

Accelerators Division, Department of Physics, Japan Atomic Energy Research Institute

Ions of ^{10}B, ^{19}F, ^{24}Mg, ^{27}Al, ^{32}S, ^{48}Ti, ^{56}Fe, ^{74}Ge, ^{93}Nb, ^{103}Rh, ^{115}In, ^{187}Re, $^{194,195,196}Pt$ and ^{197}Au have been successfully accelerated by the JAERI tandem accelerator. Negatively-charged atomic and molecular ions of these elements except for fluorine were obtained from a negative ion sputter source (NISS as an abbreviation) by using the cesium surface ionization gun developed in our laboratory. Details of the ion source and the gun were already reported in the previous paper[1),2)]. The fluorine ions were obtained from a Heinicke Penning ion source with radial extraction[1)] (HP as an abbreviation) by feeding F_2 gas as an ion source material.

About 100 cones and several kinds of gases were tested to know how much current we could get from them, and how stable and how long they worked. After this test, 13 cones of B, MgO, Al_2O_3, PbS, TiO, Fe_2O_3, GeO_2, Nb_2O_5, Rh, In_2O_3, Re, Pt and Au, and F_2 gas were selected and applied to accelerate B, Mg, F, Al, S, Ti, Fe, Ge, Nb, Rh, In, Re,

Table 1 Typical parameters of the ion sources, negative ion currents and ion source materials.

Ion Source	HP	Ion Source	NISS	NISS	NISS
Beam Species	F^-	Beam Species	S^-	FeO^-	Pt^-
Negative Ion Current	5000nA	Negative Ion Current	24500nA	500nA	1200nA
Ion Source Materials	F_2	Ion Source Materials	PbS	Fe_2O_3	Pt
Magnet Current	0.77A	Extraction Voltage	23KV	23KV	23KV
Extraction Voltage	3.6KV	Current	2.1mA	1.3mA	1.5mA
		Focus Voltage	12.6KV	12.8KV	13KV
Focus Voltage	2.7KV	Einzel Voltage	18.8KV	18.6KV	18.3KV
Source Pressure	620micron	Ionizer Voltage	5.8V	5.9V	5.5V
System Pressure	7.8×10^{-6}torr	Current	29A	29A	27A
		Oven Current	0.19A	0.19A	0.19A

Pt and Au ions. Typical results of the test are shown in table 1. This table contains typical parameters of the ion sources, negative ion currents and ion source materials. About 30 elements other than these 14 elements tested here were already extracted from the ion sources. Typical beam current, final energy, charge state and so on are summarized in table 2. The beam current were measured by electron-suppressed Faraday cups arranged along the beam lines.

Table 2 Beam currents and other parameters of the tandem accelerator.

Element	B	F	Mg	Al	S	Ti	Fe
Atomic Number	5	9	12	13	16	22	26
Mass Number	10	19	24	27	32	48	56
Ion Source Materials	B	F_2	MgO	Al_2O_3	PbS	TiO	Fe_2O_3
Negative Ion	B^-	F^-	MgO^-	AlO^-	S^-	TiO^-	FeO^-
Charge State	4+	7+	8+	7+	10+	10+	10+
Beam Current							
(Ion Source)	3680nA	2760nA	79nA	375nA	975nA	124nA	313nA
(Analyzing Magnet)	75.5pnA	17pnA	0.6pnA	18pnA	98pnA	1.0pnA	18pnA
Final Energy	72.3MeV	112MeV	123MeV	126MeV	182MeV	151MeV	178MeV

Element	Ge	Nb	Rh	In	Re	Pt	Au
Atomic Number	32	41	45	49	75	78	79
Mass Number	74	93	103	115	187	194,195,196	197
Ion Source Materials	GeO_2	Nb_2O_5	Rh	In_2O_3	Re	Pt	Au
Negative Ion	GeO^-	NbO^-	Rh^-	InO^-	Re	Pt^-	Au^-
Charge State	10+	9+	10+	10+	10+	11+	10+
Beam Current							
(Ion Source)	400nA	120nA	55nA	280nA	313nA	1200nA	790nA
(Analyzing Magnet)	0.8pnA	1.1pnA	0.5pnA	1.0pnA	0.4pnA	0.8pnA	2.0pnA
Final Energy	153MeV	140MeV	157MeV	155MeV	155MeV	170MeV	165MeV

References

1) E.Minehara, S.Abe, C.Kobayashi and S.Kikuchi., Proc. 4th Symp. on Ion Sources and Ion Application Technology, Tokyo, June, 24th-26th, 1981, p261.

2) S.Abe, E.Minehara, C.Kobayashi and S.Kikuchi., Proc.6th Symp. on Ion Sources and Ion-Assisted Technology, Tokyo, June, 7th-9th, 1982, p185.

1.4 Test of Terminal Potential Stabilizer for JAERI Tandem Accelerator

Susumu Hanashima, Eisuke Minehara, Isao Ohuchi, Katsuzo Horie,
Susumu Kanda and Yoshihiro Tsukihashi

Department of Physics, Japan Atomic Energy Research Institute

The terminal potential of an electrostatic accelerator must be stabilized through a negative feedback system. Figure 1 shows the terminal potential stabilizer of JAERI tandem accelerator. Beam current signals from the image slit of the analyzer magnet(in SLIT mode) or terminal voltage signals from the generating voltmeter(in GVM mode) are fed into the grid of the corona triode to give a negative feedback onto the terminal voltage. We have a trouble that the feedback system oscillates sometimes and we must select small loop gain to prevent the oscillation. The small loop gain results in a large steady state error of the system and in troublesome machine operation. To analyze this problem, we have observed the transfer function of the subsystem from the grid of the corona triode to the high voltage terminal.

A capacitive pick off(CPO) was used to detect deviation of the terminal potential. A low frequency oscillator and a lock-in-amplifier or a randum noise generator and a dual channel fast Fourier transform analyzer were used to get the transfer function. Figure 2 shows an example of the observed transfer function from the grid voltage of the triode to the terminal potential. In a frequency region less than 2 Hz, the amplitudes lie on the -6 db/oct line and the phases are near 90 degrees. This feature is well explained by the perfect integration character of the model where the grid voltage of the triode primarily controls corona needle's current. In a higher frequency region, the observed transfer function deviates from values expected by the model. The deviations in phases are just proportional to

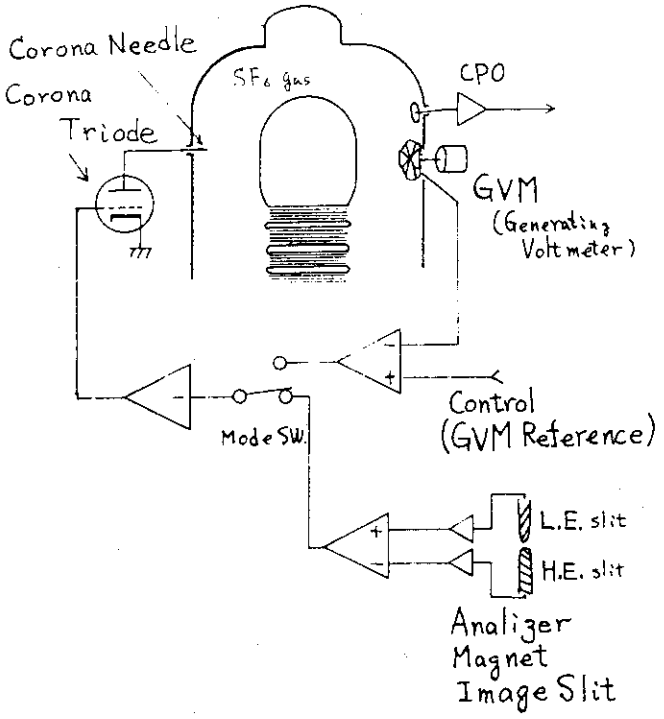

Fig. 1 Terminal potential stabilizer.

frequencies. It means that delay times of the Fourier components corresponding to the deviations are constant and independent of frequency. Terminal potential dependency of the delay times were also observed and represented in Fig. 3. They decrease with the terminal potential.

From these fact, the delay times are understood to be drift times of charges from the corona needle to the terminal. The rather large drift times mean that the charges move in the form of molecular ions. This is an important character of charge drift in SF_6 gas[1] and limits performance of the terminal potetial stabilizer in the higher frequency region. The large phase delay of the corona triode system results in a positive feedback loop and the oscillation of the terminal potential.

This work will be continued to improve the terminal potential stabilizer.

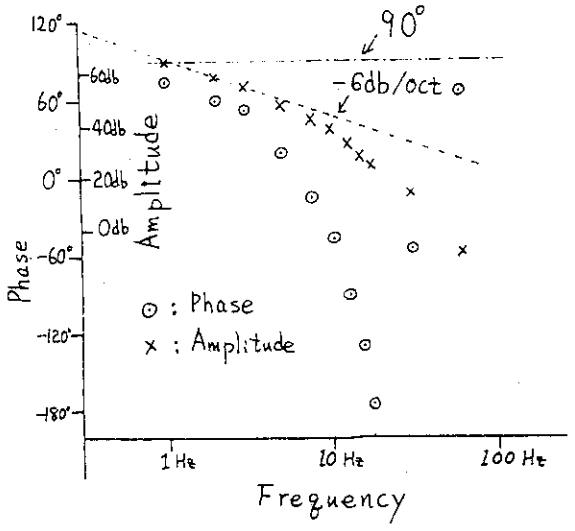

Fig. 2 Transfer function observed at the terminal potential of 16 MV, corona needle current of 25μA and SF_6 gas pressure of 5 Kg/cm^2.

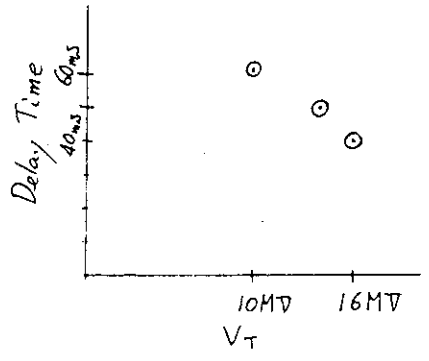

Fig. 3 Drift delay time as a function of the terminal potential observed at SF_6 gas pressure of 5 Kg/cm^2.

Reference

1) Loucas G. Christphorou(Editor), Gaseous Dielectrics II (Proceedings of the Second International Symposium on Gaseous Dielectrics, Knoxville, Tennessee, U.S.A., March 9-13, 1980), Pergamon Press, New York.

II ATOMIC AND SOLID STATE PHYSICS

2.1 Transmission Sputtering of Titanium by Energetic Carbon Ions

Teikichi A.Sasaki*, Yuji Baba*, Shin-ichi Ohno* and Takeo Aruga**

*Department of Chemistry and **Department of Fuels and Materials Research, Japan Atomic Energy Research Institute.

Transmission sputtering, particle emission from the downstream surface of solid, gives very useful information about the distribution of energy deposition. A very few works on the transmission sputtering have recently been published[1~4]. The target material used in the most experiments is confined to Au thin foil. Bay et al.[1] have measured the sputtering yield of the Au foil for 6.8 MeV Au^+ bombardment and obtained a fairly good agreement between the experimental data and calculations. Although the transmission-sputtering experiments are more direct than the back-sputtering studies to analyze, they have not been performed extensively because of experimental difficulty in preparing thin film appropriate for the ion bombardment.

This communication presents preliminary results of the transmission-sputtering experiment for 100 MeV carbon(6+) ions passing through a wedge-shaped Ti foil.

A wedge-shaped sample was prepared from Ti foil by means of automatic polishing over 2 days using diamond paste of 1/4 micron. The shiny foil was cut into a piece of ~10 mmϕ. Ag used as a catcher foil was also finished into the shiny surface with the thickness of ~120 μm. The Ti target was put on the Ag foil and mounted on a sample holder made of stainless steel. Before the irradiation the sample was annealed at 400 °C in a vacuum chamber of 1×10^{-8} Torr. To remove adsorbed contaminants from the target foil surface, sputter cleaning by 8 keV Ar ions was employed.

A detailed description about the experimental arrangement of irradiation systems and the sputtering-yield measurements will be reported elsewhere[5].

Figure 1 represents the discrepancies in the oxidation behavior of the Ti atoms on the target foil and the catcher foil. Following the irradiation the taget was exposed to dry air for 2 minutes at room temperature. The X-ray photoelectron spectra obtained for the Ti2p region show that the oxidation behavior of the target surface is almost the same as thatof Ti surface cleaned in the UHV by means of filing. On the other hand, the Ti atoms sputtered on the catcher foil appear to be resistant to the oxidation.

Relative sputtering-yield obtained by the Auger electron spectroscopy is plotted as a function of the distance from the edge of the catcher foil in Fig.2. The intensity of the beam current becomes fainter with going to an edge of the beam profile. As far as the uniformal-intensity area of ∿4 mmϕ is concerned, it could be concluded that the sputtering yield increases as the ion energy is slowing down.

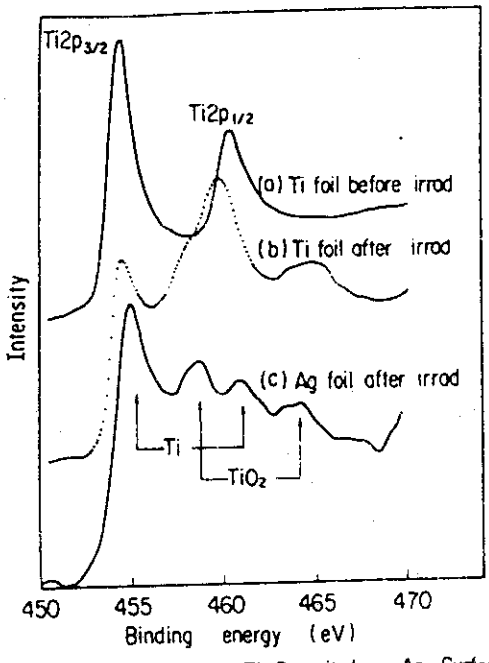

Fig.1 Oxidation Behaviors of Ti Deposited on Ag Surface

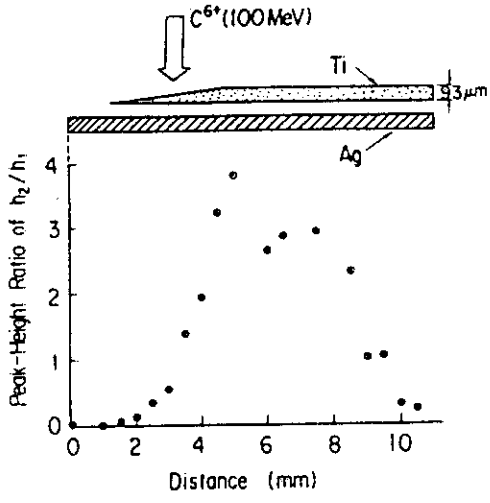

Fig.2 Ti/Ag Ratio at Various Positions of Ag Foil Surface

References

1) H.L.Bay et al.: Appl.Phys. 11(1976)289.
2) P.Mertens: Nucl.Instru.Methods 132(1976)307.
3) K.H.Ecker et al.: Phys.Rev. B18(1978)1020.
4) G.Ayrault et al.: J.Appl.Phys. 53(1982)6968.
5) T.A.Sasaki et al.: to be published.

2.2 Beam-Foil Interaction in High Energy Region

Hidenori Yamaguchi, Kunio Ozawa, Kiyoshi Kawatsura, Masao Sataka, Tetsuo Kitahara*, Akira Kikuchi**, Kenichiro Komaki***, Akio Ootsuka*** and Fuminori Fujimoto***

Department of Physics, Japan Atomic Energy Research Institute, *Yamanashi Medical University, **Faculty of Engineering, Ibaraki University and ***College of Education, University of Tokyo

Recently, availability of heavy ion accelerators and improved techniques of particle detection have given rise to renewed interests in the problems of beam-foil interactions, such as stopping power, multiple scattering, charge exchange and excitation of ions. These data are of considerable importance since they are required in many experiments using an ion beam. For heavy ions, however, there is still a lack of accurate data especially in high energy region. The stopping power and the multiple scattering are expected to have strong correlations with the charge exchange process, and also with each other. So it was scheduled to study these three processes putting together as a part of a study for beam-foil interactions.

The experimental arrangement of beam-foil spectrometer, which was installed in the 2nd Heavy-Ion Target Room, has been already reported in elsewhere[1]. A position sensitive silicon detector (PSD) is mounted on a movable arm at the end of the detection system. The beam passed through 325 cm of beam duct to the PSD after passing through the foil. The charge state of ions can be analyzed by an electrostatic deflector, which has been set up in the beam duct.

In order to detect the ion beam directly by particle detector, a technique for producing a faint beam (a few hundred counts/sec on the target) is indispensable to prevent a radiation damage to the detector, as well as pile-up of signals. We have obtained the faint beam of 150 MeV Cl^{9+} ions from JAERI tandem accelerator by limitting width of four-jaw slit set up at a position 338 cm apart from the foil. And the charge state and angular distributions of the ions after passing through thin carbon foils (3-150 $\mu g/cm^2$) were measured. An electric field of the deflector was 8 kV/cm.

Fig.1(a) and (b) represent as examples the charge state spectra for thicknesses of 3 and 10 $\mu g/cm^2$, respectively. By Bohr's criterion, a fast heavy ion penetrating through matter is expected to be stripped

its electrons which have orbital velocities less than the velocity of ions. The orbital velocity of K-shell electrons of Cl atom is comparable to the velocity of 180 MeV Cl ion. Fractions of bare (17+) and hydrogen-like (16+) ions can be recognized for 10 $\mu g/cm^2$ thickness. These highly ionized ions are expected to show further increase of their fractions for higher incident energies.

Fig.2(a) and (b) represent as examples angular distributions measured by the PSD for ions scattered by carbon foils of 10 and 150 $\mu g/cm^2$, respectively. The half angle of scattering, $\theta_{1/2}$, which is defined as that corresponding to the half width at half height of the distribution, is 0.57 mrad for 10 $\mu g/cm^2$, and 1.9 mrad for 150 $\mu g/cm^2$. The incident beam was collimated by the four-jaw slit and two apertures, and $\theta_{1/2}$ was 0.20 mrad.

We could confirm that the detection system had a satisfactory function. The study of the correlation between the multiple scattering and the charge exchange is intended to begin as a part of beam-foil studies. The measurement of the angular distribution of ions, for each outgoing charge state, scattered from very thin foils in which single collision dominates will clarify the following problems;
1)Screened Coulomb potential, 2)effective charge of ions inside solids, and 3)impact parameter dependence of charge changing cross section.

Ref. 1) JAERI TANDEM NEWS LETTER No.8 (1981)

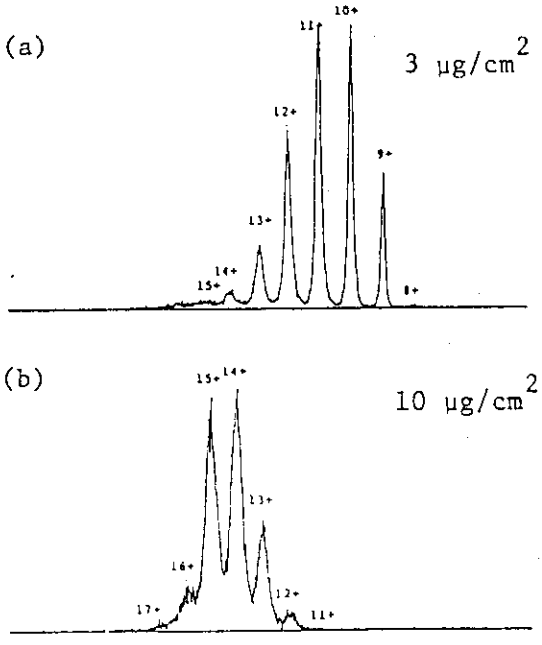

Fig. 1

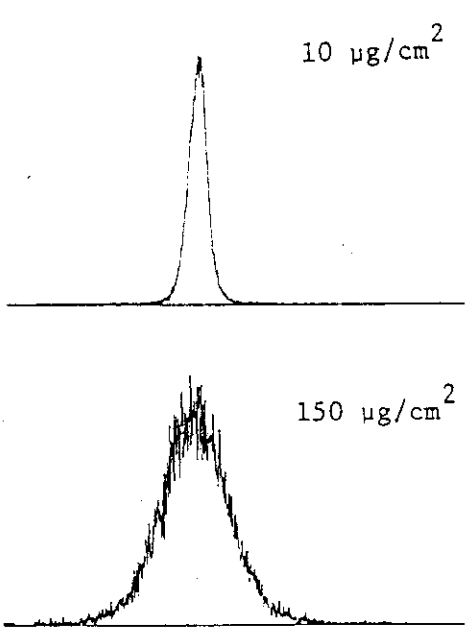

Fig. 2

2.3 Spectroscopy of Electrons and X-Rays Emitted in High-Energy Ion-Atom Collisions

Kiyoshi Kawatsura*, Masao Sataka*, Kunio Ozawa*, Hidenori Yamaguchi*, Ken-ichiro Komaki**, Akio Ootuka** and Fuminori Fujimoto**

*Department of Physics, Japan Atomic Energy Research Institute and **College of General Education, University of Tokyo.

Inelastic ion-atom collisions are studied experimentally through the measurement of the inelastic processes of ionization, excitation and electron transfer. When a highly-charged fast projectile collides with a neutral atom in a gaseous target it may, in a single collision, remove many electrons from target atom. It is possible to study inelastic ion-atom collisions of a few electron system, using JAERI tandem accelerator. In this report we present preliminary results of (1) x-ray spectroscopy and (2) electron spectroscopy for heavy ion-atom collisions.

(1) x-ray spectroscopy

Thin targets of C(67 nm) and Ag(3 μm) were mounted at 45° to the incident beam direction. A Si(Li) detector of resolution 200 eV(FWHM at 5.9 keV) was positioned inside the target chamber 5 cm from the target and 90° to the incident beam direction. A 38 μm Mylar attenuator was positioned between the target and the Be detector window to reduce contributions to the counting rate for continuum x-ray radiations at low energy. Hence x rays were required to pass through 38 μm of Mylar and 15 μm of Be before reaching the detector.

Figure 1(a) shows the measured x-ray spectrum in the low energy region for 90-MeV Cl^{8+} + Ag. The main peak at around channel 106(3.16 keV) is due to a superposition of Ag $L\alpha_1$ and $L\beta_1$ x rays. The high energy shoulder at around channel 126(3.75 keV) is due to a superposition of Ag $L\beta_{2,15}$ and $L\gamma_1$. The low energy satellite at channel 92 (2.74 keV) is projectile Cl K x-ray transitions.

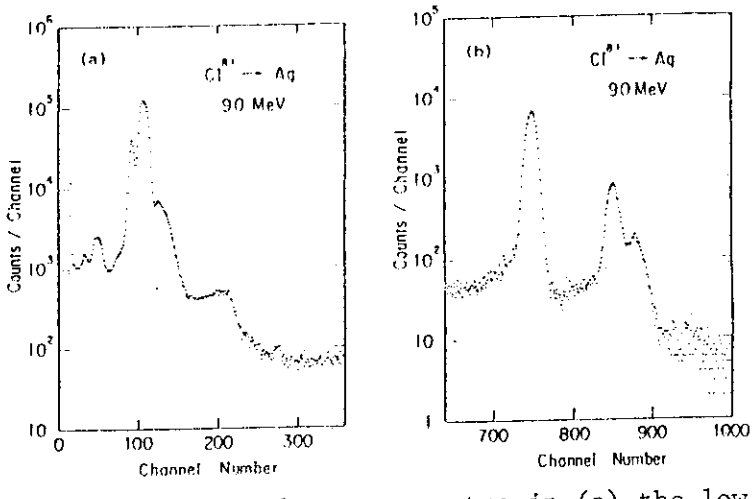

Fig. 1 The measured x-ray spectra in (a) the low energy region and (b) the high energy region.

The small peak at around channel 210 (3.3keV) is due to the pile up of Ag L x-ray pulses. Figure 1(b) shows the high energy region of the same spectrum. The strong peak at channel 749 (22.1 keV) is due to Ag $K\alpha_{1,2}$ x-ray transition. Other peaks at channel 852 (25.2 keV) and 878 (25.9 keV) are due to the transition of Ag $K\beta_1$ and $K\beta_2$ x rays, respectively.

(2) electron spectroscopy

Thin target of carbon (67 nm) was bombarded by Cl^{8+} ions with energy 90 MeV with respect to normal to the surface. Ejected electrons were energy analyzed by a 30^{o} parallel-plate electrostatic analyzer, counted by a channel electron multiplier and accumulated in a multiscaler. The electrostatic analyzer has an energy resolution of 2 % half width at half maximum, an angular resolution of 8^{o} and is rotatable over an angular range from 30^{o} to 90^{o} with respect to the beam direction. The earth magnetic field around the collision region was shielded with use of μ-metal.

In Figure 2. the observed spectra is given for 90 MeV Cl^{8+} impacts on carbon foil at electron observation angle 30^{o}. The spectrum is composed of some peaks and continuous part. The discrete peak at about 250 eV is assigned to C-Auger peak, with which energy calibration of ejected electron was carried out. The peak in the energy region near 1.3 keV is due to the loss electrons ejected from chlorine ions. The broad peak at energy region higher than 3 keV is attributed to binary encounter peak. The continuous part and the binary encounter peak are due to electrons produced by direct Coulomb interaction of the ions with electrons of the target carbon. The steep decrease as energy decrease in the lower energy region than 200 eV might be due to the defect in magnetic shield.

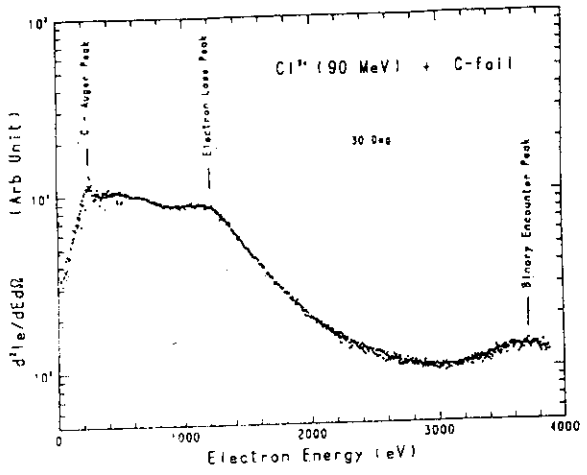

Fig. 2 The measured electron spectrum for Cl^{8+}(90MeV) - C-foil

At present time, there is no quantitative understanding of inelestic ion-atom collisions. It awaits future research.

2.4 Calorimetric Measurements of Stopping Power for ^{35}Cl and ^{12}C Ions in Nickel

Akihiro Iwase*, Shigemi Sasaki*, Tadao Iwata* and Takeshi Nihira**

*Department of Physics, Japan Atomic Energy Research Institute and
**Faculty of Engineering, Ibaraki University.

Stopping power, the energy loss of energetic ion during passing through matter has been the subject of a great deal of theoretical and experimental study. In the research of radiation damage in solids, stopping power is one of the most important parameters because the spatial distribution of radiation damage created by ions and the range of ions injected into solid are determined by the stopping power values. Much experimental work has been performed for proton, helium and heavier particles in the low energy range, but few experimental data have been obtained especially for heavy ions at high energies (above ~1MeV/amu). In the usual methods of stopping power measurements, the difference between the energy of incident beam and that of passing beam through the target foil is measured. By means of calorimetric technique,[1]) we can measure the energy loss of ions in the target foil directly instead of energy difference. This technique has the great advantage for the measurements of stopping power with high energy particles that the calorimeter is rarely damaged under heavy ion irradiation. Using this technique, we have measured the stopping powers for ^{35}Cl ions at energies ~2.7 to ~5MeV/amu and for ^{12}C ions at energies ~7 to ~8.7MeV/amu in nickel.

The principle of calorimetric technique is shown in Fig. 1.[1]) The target foil and the block which is placed behind the target foil are set on the liquid helium cryostat. Heavy ion beam accelerated by the tandem Van de Graaff accelerator at JAERI passes through the target foil and stops at the block. Heavy ions lose a certain part of energy in the target and lose all the rest of energy in the block. These energy losses cause the temperature increases of the target and the block. We detect these temperature increases using carbon resister thermometers. Immediately after irradiation, we supply the electric power into the heaters attatched to the target and the block, so that the same temperature increases as those under irradiation are reproduced. From these supplied power, we can obtain the energy loss of ions in the target foil. The thickness of the target foil is determined by

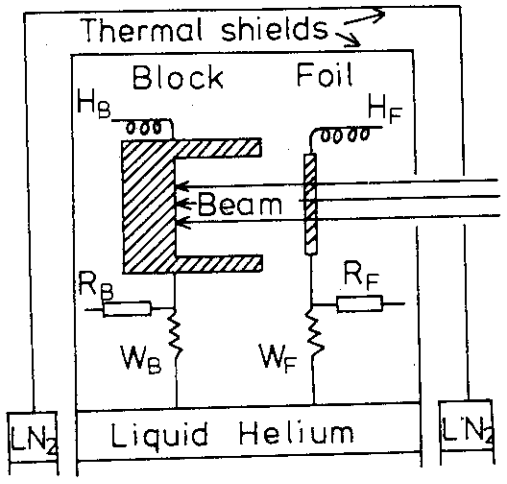

Fig. 1 Principle of calorimetric technique. W_F and W_B are thermal resistances. R_F and R_B thermometers, and H_F and H_B electrical heaters.

measuring the weight and the area. Stopping power of the target foil can be obtained by dividing the energy loss in the target by the thickness of the target.

The target was nickel foil supplied by Goodfellow Metals Ltd., and the thickness was 0.903mg/cm^2. The experimental error in our stopping power measurement consisted of the error in the determination of energy loss of ion in the target (±1.5-2.5%), the error in the determination of energy loss of ion in the block (±1.0-1.5%) and the error in the measurement of the target thickness (±2.0%). Eventually the total error in our experiment is expected to be ±5.0-5.5%.

The experimental results are shown in Fig. 2 and Fig. 3. In these figures, the values of stopping power measured by other investigators[2-5]) and the tabulated values by Northcliffe and Schilling,[6]) Ziegler[7]) and Hubert et al[8]) are also shown for the comparison with our results. In the case of ^{35}Cl ions, our results are smoothly connected to the results of Forster et al[4]) at energies below 3MeV/amu and at higher energies where there have been no experimental data up to the present, our results are in good agreement with the predicted values of Ziegler rather than those of Hubert et al or those of Northcliffe and Schilling. In the case of ^{12}C ions,

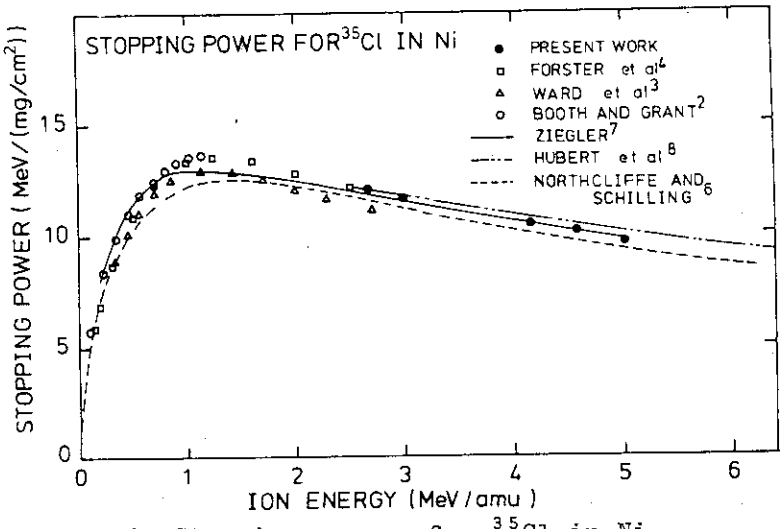

Fig. 2 Stopping powers for ^{35}Cl in Ni.

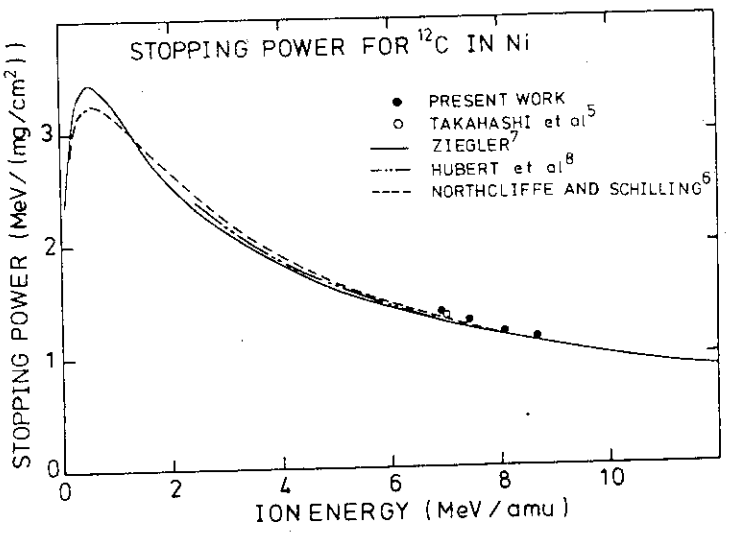

Fig. 3 Stopping powers for ^{12}C in Ni.

there were two other measurements of stopping power at the same energies as those of our experiment.[5,9] In Fig. 3, we show only one experimental result obtained by Takahashi et al.[5] They measured the stopping power for ^{12}C ion in Ni at energy ~7MeV/amu. Our result at the same energy is in good agreement with that of Takahashi et al.

From these experimental results and comparisons, we conclude that the calorimetric stopping power measurements are very useful especially for the high energy heavy ions. And at energies where there have been no experimental results, (3MeV-5MeV/amu for ^{35}Cl ions), the present results suggest that Ziegler's prediction supplies the most reliable stopping power values.

The authors are thankful to the members of Accelerators Division, Department of Physics, Japan Atomic Energy Research Institute for operating and maintaining the tandem Van de Graaff accelerator.

References

1) H. Sørensen and H. H. Andersen: Phys. Rev. B8 (1973) 1854.
2) W. Booth and I. S. Grant: Nucl. Phys. 63 (1965) 481.
3) D. Ward, R. L. Graham and J. S. Geiger: Can. J. Phys. 50 (1972) 2302.
4) J. S. Forster, D. Ward, H. R. Andrews, G. C. Ball, G. J. Costa, W. G. Davies and I. V. Mitchell: Nucl. Instr. Methods 136 (1976) 349.
5) T. Takahashi, Y. Awaya, T. Tonuma, H. Kumagai, K. Izumo, M. Nishida A. Hitachi and A. Hashizume: Phys. Rev. A27 (1983) 1360.
6) L. C. Northcliffe and R. F. Schilling: Nucl. Data Tables A7 (1970) 233.
7) J. F. Ziegler: Handbook of Stopping Cross Sections for Energetic Ions in All Elements (Pergamon, New York, 1980).
8) F.Hubert, A. Fleury, R. Bimbot and D. Gardes: Ann. Phys., Fr. 5 (1980) 1.
9) P. G. Roll and F. E. Steigert: Nucl. Phys. 17 (1960) 54.

III RADIATION EFFECTS IN MATERIALS

3.1 Irradiation Damages in Oxygen Ion Irradiated Li_2O

Kenji Noda*, Yoshinobu Ishii*, Hisayuki Matsui**,
Tomoo Kirihara** and Hitoshi Watanabe*

*Department of Fuels and Materials Research, Japan Atomic Energy Research Institute, ** Faculty of Engineering, Nagoya University.

Lithium oxide (Li_2O) is a prime candidate of solid breeding blanket materials of fusion reactors. In Li_2O irradiation damages will be enormously induced during operation of the reactor by neutrons with energy up to 14MeV (fast neutrons), tritons and helium ions produced from $^6Li(n,\alpha)^3H$ reactions. In the present study, Li_2O single crystals were irradiated with oxygen ions using tandem accelerator at JAERI and irradiation damages induced in the crystals were investigated in order to know a fundamental knowledge of irradiation damages due to the fast neutrons.

Specimens used were single crystals grown from Li_2O powder by floating zone melting method using an infrared imaging furnace. Oxygen ion irradiation was done at room temperature in high temperature irradiation chamber evacuated to ultra high vacuum (10^{-8}Torr.). After the irradiation, irradiation damages induced were observed at room temperature by ESR (electron spin resonance) method. Actually, the temperature of irradiated region was assumed to be elevated to about 450K.

ESR spectra of Li_2O single crystals irradiated to 1 to 3×10^{20}ions/m^2 by oxygen ions with energy of 100 or 112 MeV had a hyperfine structure (HFS) consisting of more than 20 peaks. The HFS was found to be dependent upon orientation of the crystals and the g-value was 2.002 ± 0.001. Such spectra are good in agreement with the spectra due to F^+-centers in Li_2O single crystals irradiated to 10^{21} to 10^{23} thermal neutrons/m^2 by thermal neutron reactors (JRR-2 and 4)[1]. Thus, the spectra of oxygen ion irradiated Li_2O can be attributed to F^+-centers (an oxygen vacancy trapping an electron).

In addition to the F^+-centers, the isotropic and narrow spectra were superimposed for the specimens irradiated to 3×10^{20}ions/m^2. The g-value of the spectra was 2.003 ± 0.001 and the line width was about 2.4G. The spectra were not dependent on the orientation of the crystal and agreed with the spectra due to Li metal colloid in Li_2O pellets irradiated to the order of 10^{23}thermal neutrons/m^2 by the thermal neutron reactor (JRR-2)[2]. In case of neutron-irradiated Li_2O pellets, Li metal colloid was assumed to precipi-

tate at grain boundaries, while it was found to precipitate in the grain for the oxygen ion irradiated Li_2O single crystal.

F^+-center content was determined by comparing the intensity of the spectra with that of diphenylpicrylhydrazyl (DPPH) in chloroform of known concentration. The volume of region induced the F^+-centers was determined by measuring the depth of colored part of the specimen using optical microscope. The concentration of the F^+-centers was calculated from the volume and the F^+-center content and is shown in Fig. 1 together with the concentration in the single crystals irradiated by the thermal neutron reactors. The F^+-centers were induced to 1 to 2×10^{25} centers/m^3 in the specimens irradiated to 1 to 3×10^{20} ions/m^2 (irradiation period; 10 to 20 h) by oxygen ions, while the F^+-centers of 10^{24} centers/m^3 was only in the specimen irradiated to the order of 10^{23} thermal neutrons/m^2 (irradiation period; 10 days) with JRR-2. This suggests that inducing rate of the F^+-centers by oxygen ion irradiation using tandem accelerator is very higher than that by the thermal neutron reactor irradiation. In respect to displacement damages, the oxygen ion irradiation is confirmed to be very useful to get a fundamental knowledge of irradiation damages of Li_2O at high fluence of the fast neutrons.

Isochronal annealing experiments were done and recovery behavior of F^+-centers and Li metal colloid was studied. The specimens were heated to 700K for 1800 sec. at intervals of about 50K. The ESR spectra of the specimens were observed at room temperature immediately after each annealing. The F^+-centers in oxygen ion irradiated specimens recovered around 570K and disappeared at 650K. Such a recovery behavior is good agreement with that of F^+-centers in neutron-irradiated specimens[1]. In comparison with the F^+-centers, Li metal colloid was stable and survived even at 700K.

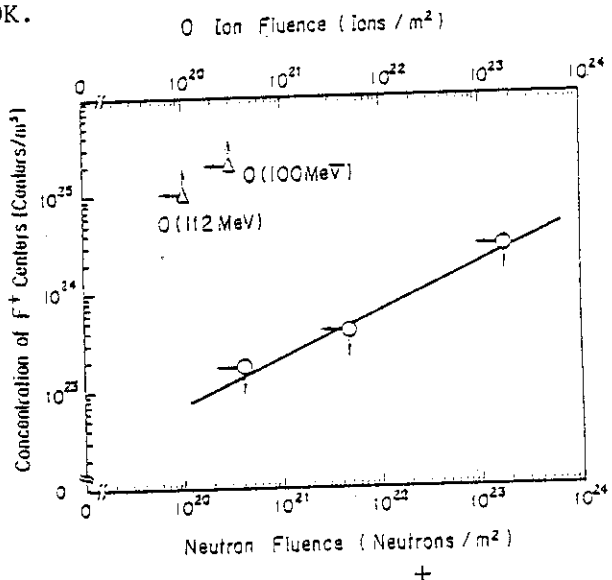

Fig. 1 Concentration of F^+-centers.

References

1) K. Noda, K. Uchida, T. Tanifuji and S. Nasu, Phys. Rev. B 24, 3736 (1981).
2) K. Noda, K. Uchida, T. Tanifuji and S. Nasu, J. Nucl. Mater. 91, 234 (1980).

3.2 Nickel-ion Irradiation to Stainless Steel

Mitsuo Tanaka, Shozo Hamada, and Kensuke Shiraishi

Department of Fuels and Materials Research, Japan Atomic Energy Research Institute

Void and/or other damage structures in structural materials is one of the major material problems for fusion power reactors. A large number of fast reactor experiment has been conducted to determine the effects of temperature and dose upon the damage structure, especially the amount of swelling in various candidate materials for fusion reactor. However the time required for the materials to recieve sufficient dose to yield significant swelling is on the order of one to several years. In order to expedite the research on void and other damage structure, high energy charged-particle irradiation has been used to simulate fast neutron damage with a resultant one-to-two order of magnitude increase in the displacement damage rate. Although the quantitative correlation of charged-particle and fast neutron has proven to be elusive goal, charged-particle experiments have provided very useful information on the mechanisms of void formation and on the relative swelling rates of different alloys.

The present study was undertaken to examine the early stage of damage structure produced in Ti-modified stainless steel by Ni-ion irradiation. The results of the examination will be compared with the damage strucutures produced by neutron irradiation. The comparison will provide some insights into the mechanisms of alloying effects on swelling and into the use of ion irradiation as a tool for alloy development of fusion reactor.

The chemical composition of the modified stainless steel in this study are shown in Table 1. The specimens of 10 mm in diameter with 0.2 mm in thickness were mechanically polished to a 0.3 μm surface-finish and then annealed for 0.5 h at 1373 K in a vacuum 10^{-3} Pa. Some of the annealed specimen were then 10%- and 15%- cold worked by rolling. After the heat-treatment and the subsequent cold work, the specimens were electropolished using a solution of 108 ml H_2SO_4, 72 ml $HClO_4$ and 20 ml C_2H_5OH at 288 K and 15 V to clean the surface. The samples were irradiated in a vacuum of 10^{-3} Pa at around 723 K with 164 MeV Ni-ions of 2.5 pnA/cm^2 in average flux by the Tandem Accelerator to fluences of 3×10^{15} and 6.7×10^{15} ions/cm^2. Using the extended E-DEP-1 computer code and assuming a displacement energy of 40 eV, the

peak doses were calculated to be 0.9 and 1.8 dpa with an average damage rate of 1.5×10^{-5} dpa/s. Variation of Ni-ion flux in this experiment is shown in Fig. 1. The heat flux carried by Ni-ion was partly converted to heat for specimen heating, so the irradiation temperature fluctuated depending on the variation of Ni-ion flux.

The irradiated specimens are now prepared in a manner of electroplating technique to observe in cross-sectional view of microstructure with a transmission electron microscope. The result of the observation will be reported in future.

Table 1 Chemical composition of Ti-modified stainless steel

(wt %)

C	Si	Mn	P	S	Ni	Cr	Mo	Ti	B	N
0.06	0.53	1.79	0.027	0.009	16.22	14.51	2.37	0.19	0.0035	0.008

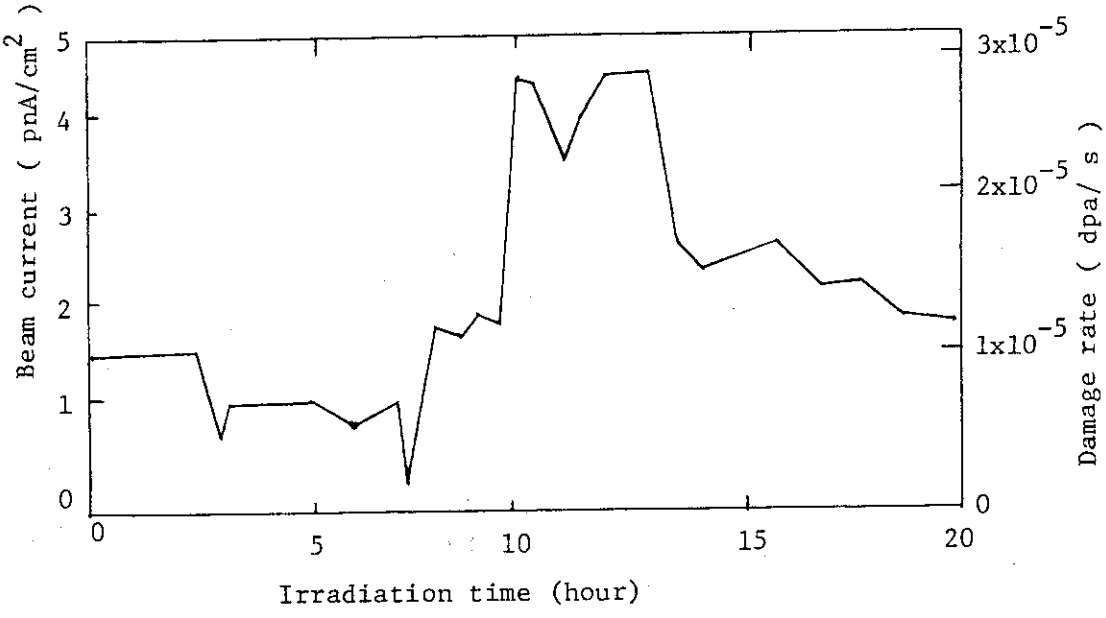

Fig. 1 Variation of beam current during the experiment.

3.3 Depth Dependent Damage Profile in Stainless Steel

Shozo Hamada, Tomotsugu Sawai and Kensuke Shiraishi

Department of Fuels and Materials Research, Japan Atomic Energy Research Institute.

In alloy development for applications to fast breeder and fusion reactors, ion irradiation experiments are useful to evaluate the radiation damage to the alloy in a short period. The radiation damage produced by ions has a strong gradient and the implanted ions affect microstructural evolution during the irradiation. Thus, understanding the damage profile produced by ion irradiation is essential for the simulation study. The damage structure produced in C-ion irradiated stainless steel are observed following to the experiment with Cl-ion irradiated pure nickel[1].

Type 316 stainless steel samples of 0.2 mm^t x 12 mm^ϕ annealed for 1 h at 1050 °C in a vacuum were electropolished in a solution of 95 % acetic acid and 5 % perchloric acid at 30 V and 15 °C, and then, irradiated with C-ions of 80 MeV in the JAERI Tandem Accelerator with a beam current of 1 $\mu A/cm^2$ to a peak concentration of 0.08 wt%. The irradiation temperature was estimated to be 600 °C from a calibration curve for a dummy disk with

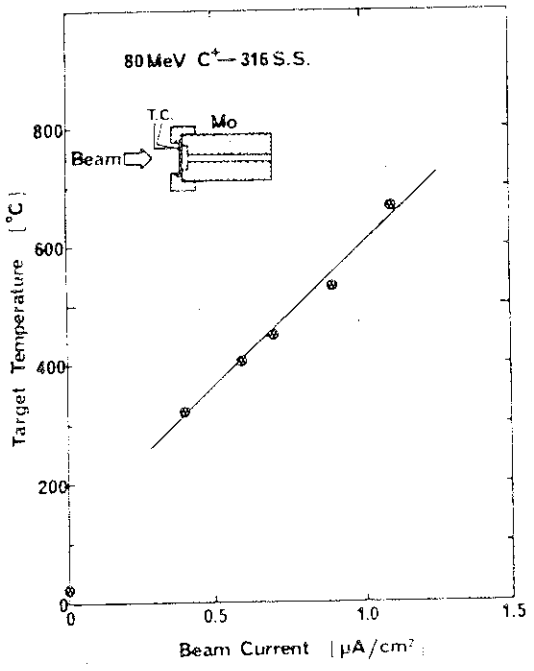

Fig.1 Beam current dependent target temperature.

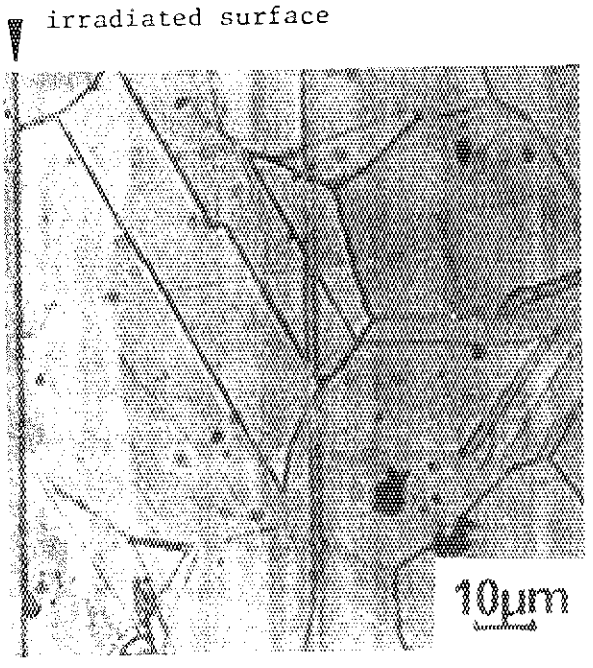

Fig.2 Microstructure view from etched surface of type 316 stainless steel irradiated with 80 MeV C-ions at 600°C.

a spot-welded thermocouple(Fig.1)

The irradiated sample was electroplated with nickel to about 3 mm thick and then sectioned parallel to the direction of the incident beam using a low speed diamond saw. The sectioned sample was mechanically polished and etched by using a saturated solution of copper chloride in aqua regia. A micrograph of the etched surface revealed a pair of parallel lines at depths of 46.2 μm and 47.7 μm from the irradiated surface(Fig.2).

The center between the parallel lines approximates the mean projected range of carbon injected into the sample as reported for He-ions injected into stainless steel[2),3)]. The observed value of 47 μm is fairly good agreement with 49.4 μm and 49.6 μm for peak positions of displacement damage and carbon concentration, respectively, calculated for 80 MeV C-ion irradiation to amorphous iron with the stopping power given by Ziegler[4)] (Fig.3).

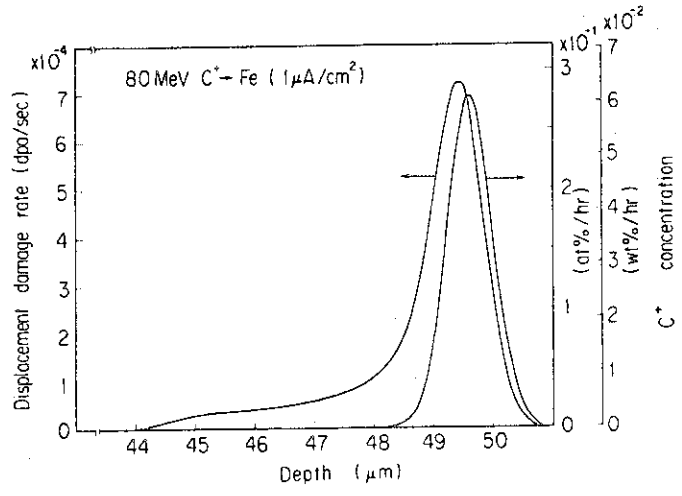

Fig.3 Displacement damage and injected carbon distributions calculated for 80 MeV C-ions to amorphous iron.

The detailed microstructure will be observed with an electron microscope to clarify the depth dependent damage profile and injected carbon atom distribution in the C-ion irradiated stainless steel sample.

References

(1) K.Shiraishi, M.Tanaka,T.Aruga and S.Hamada: Effect of Radiation on Materials, ASTM STP782 (1982) p.927

(2) 深井勝麿,白石健介：日本原子力学会誌 25 (1983) 123

(3) K.Shiraishi and K.Fukai: to be published in J. Nucl. Mater.

(4) J.F.Ziegler: Handbook of Stopping Cross-Sections for Energetic Ions in All Elements (Pergamon Press, New York,1980).

3.4 Heavy Ion Track Filter of Polyvinylidene Fluoride

Yoshihide Komaki*, Shinichi Ohno*, Hiroshi Ito**, and Matae Iwasaki***

*Department of Chemistry and **Takasaki Radiation Research Establishment, Japan Atomic Energy Research Institute, and ***Institute of Atomic Energy, Kyoto University.

We have begun an experiment for producing the heavy ion track microfilter made of polyvinylidene fluoride film(PVDF) through the irradiation of Tandem accelerator ions at JAERI.

The conditions necessary for the formation of the etchable tracks were examined first with respect to the mass and the energy of the heavy ion. After two kinds of biaxial streched films of 6 and 9 μm in thickness were vertically irradiated in a stack, each film was etched. The presence of the track holes was examined on the both sides of the etched films by means of the scanning electron micrographs. Three kinds of the heavy ions, O^{+6} (100 MeV), Cl^{+9}(160 and 110 MeV),and Ni^{+10}(150 MeV) were bombarded at the current as faint as possible for 4 to 35 sec. The maximum extent of the beam at the face of the target was over 25 to 30 mm in diameter, and the minimum limit for the current and the irradiation time were practically 10 nA and the several seconds by considering the accuracy, respectively.

Hole density ; The number of the incident particles calculated from the current density of Faraday cup was found to agree almost with the number of the etched holes observed in the film, though a large number of tracks made it difficult to count correctly.

Table 1 Irradiation conditions and Hole density in PVDF

Ions	Energy	Irrad.time	Current	Irrad.area	Track density	
	MeV	sec	nA	mm φ	cal. [cm^{-2}]	obs.
Cl^{+9}	160	4	10	8	6.3×10^{9}	4×10^{9}
O^{+6}	100	20	50	25	2×10^{10}	———
Ni^{+10}	150	35	17	25	6.3×10^{9}	8×10^{9}

Range length ; The passage penetrated through the stacked films was estimated to be about 26 μm in length at 150 MeV of the Ni^{+10}ion, from the presence of the etched holes. This value is close to the one in PET.

Criterion of track emergence ; The experimental results of the etched track emergence were plotted on the curves of the primary ionization rate of the heavy ions against the incident particle energy after R.L. Fleischer et al[1], in relation to the ions of O^{+6},Cl^{+9},and Ni^{+10}, respectively as shown in Fig. 1. Though the experimental points are not sufficient, a criterion of the track formation in PVDF seems to be estimated roughly. In PVDF, no tracks are

etched over the energy of several MeV/amu for the O^{+6} ion, but below that the more precise experiments should be carried out. The Cl^{+9} ion creates the tracks at the energy of 3 MeV/amu. The Ni^{+10} ion always creates the tracks below the energy of 2.5 MeV/amu. Figure 1 indicates that a criterion of the track formation in PVDF (a dotted line in the figure) occupies at an intermediate level between mica and PET, and that no tracks are seen in the light ions such as an alpha particle. In any case, the bombardment by the heavy ions of more than Ni with higher energy is necessary to produce the microfilter of the thick polymer films (∿50 μm in thickness).

Hole diameter ; Figure 2 indicates a scanning electron micrograph of the etched tracks in PVDF, which showed 8 x 10^9 etched holes/cm^2 in hole density after 21 hrs etching in a 10N NaOH solution at 85 °C, containing a number of hole overlaps. The apparent hole diameter is about 300 Å. The calculated bulk etching rate is 8 Å/hr, which agrees with that in FF tracks.

Reference.

1) R.L.Fleischer,P.B.Price,R.M.Walker,and E.L.Hubbard,Phys.Rev.,156,353(1967)

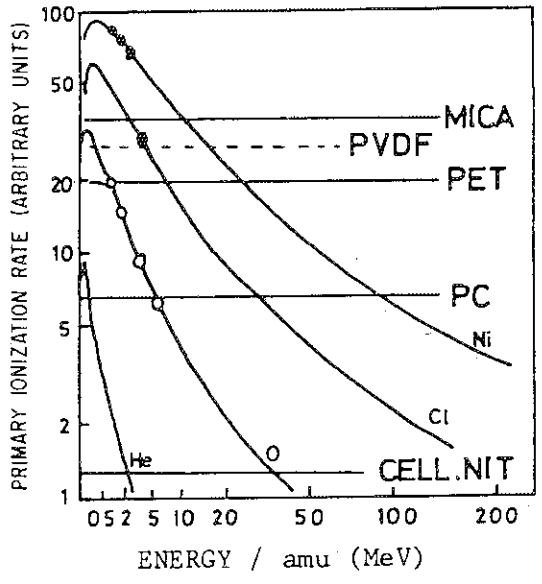

Fig. 1 Sensitivity threshholds for the O,Cl,and Ni ions.

● : 100 % track registration.
○ : no track registration.
The curves and the other level lines except PVDF follow Ref. 1.

PET : poly(ethylene-terephthalate)
PC : polycarbonate
CELL.NIT : Cellulose nitrate

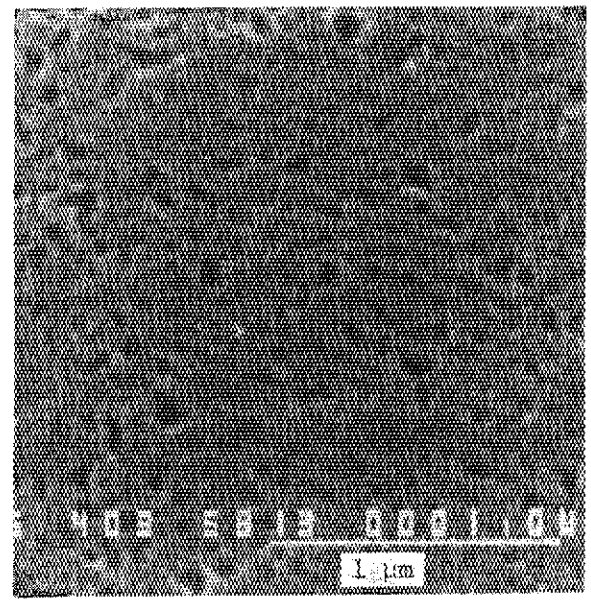

Fig. 2 A scanning electron micrograph of the Ni ion etched tracks in PVDF.

Irradiation : Ni^{+10}, 150 MeV, 35 sec, 17 nA.
Etching : 10N NaOH solution, 85 °C, 21 hrs
Hole density: 8 x 10^9/cm^2.

3.5 Heavy Ion Irradiation Experiments Using Low Temperature Irradiation Chamber

Eiji Sakai* and Yukio Kazumata**

*Department of Reactor Engineering, Japan Atomic Energy Research Institute

**Department of Physics, Japan Atomic Energy Research Institute

Various materials were irradiated at 77 K in the Low Temperature Irradiation Chamber situated at the beam line L2 with 100 MeV O^{6+}, 150 MeV Ni^{9+} and 150 MeV Cl^{9+}, as shown in Table 1. The materials irradiated were brought back to individual users' laboratories to characterize their own specimens. Two TV-cameras were purchased to monitor the beam alignment and spread by using a fused silica disc and to watch the specimens under irradiation. The electric relay in the specimen rotating circuit was burnt twice and replaced. We observed melting and decomposition of KNO_3, TGS and TGSe(MP = a few hundreds °C) and a trace of evaporation of Al-foil by irradiation heating even though the specimen-mounting-station was kept at 77 K. Care should be taken to confirm the heat resistance of the specimen as low as possible. A small hoist will be provided for holding the lid of the chamber in the next fiscal year. The results of the measurements will be described by individual users in the separate sections.

Table 1 Heavy ion irradiation experiments performed using Low Temperature Irradiation Chamber during the fiscal years 1981 and 1982

Experiment	User	Date	Heavy ion	Number of particles	Specimen	Characterization
1st	E.Sakai	29 Oct.'81	128MeV Cl^{9+}	1.32E14	Si	Induced radioactivity
				1.85E15	Si	Induced radioactivity
	K.Gesi			8.33E14	Al_2O_3	Dielectric loss
	K.Doi			1.11E15	$Pd_{80}Si_{20}$	X-ray diffraction
	K.Izui			2.86E12	Ge,MoO_3,MoS_2	T.E.M.
2nd	E.Sakai	17 Nov.'81	100MeV Cl^{8+}	4.54E15	Si	Induced radioactivity
	Y.Kazumata			4.61E15	Si,graphite	E.S.R.
3rd	K.Izui	14 Dec.'81	80MeV I^{7+}	3.46E12	Ge,Al,MoO_3,MoS_2	T.E.M.
				3.01E13	Ge,Al,MoO_3,MoS_2	T.E.M.
	E.Sakai			4.57E14	Si	Induced radioactivity
	S.Takamura			2.86E14	Ag,Cu	Hardness test
	H.Maeta			3.33E14	Mo,Cu,Al,Ge,Si	X-ray diffraction
4th	E.Sakai	1 Sept.'82	100MeV O^{6+}	1.2E16	Ge	Induced radioactivity
	K.Gesi			2.5E13	KNO_3,TGS,TGSe	Dielectric loss
	H.Naramoto			1.2E16	Si	Ion beam analysis
	S.Furuno			7.3E15	Al,Si,Ge	T.E.M.
5th	H.Naramoto	14 Jan.'83	150MeV Ni^{9+}	5.6E14	Si,LiF	Ion beam analysis
	E.Sakai			5.7E14	Ge	Induced radioactivity
	Y.Kazumata			2.8E14	graphite,TiO_2	E.S.R.
	H.Tomimitsu			2.4E14	Si	X-ray topography
6th	S.Furuno	15 Feb.'83	150MeV Cl^{9+}	3.1E15	Ge,Si,Al	T.E.M.
	H.Tomimitsu			2.8E15	Si	X-ray topography
	E.Sakai			1.8E15	Ge	Induced radioactivity
	H.Maeta			6.4E14	graphite,Fe	X-ray diffraction
	H.Naramoto			2.9E15	NaF,LiF	Ion beam analysis

3.6 Induced Radioactivities in Semiconductors and Other Materials for Solid-State Physics Research Irradiated with High-Energy Heavy Ions

Eiji Sakai

Department of Reactor Engineering, Japan Atomic Energy Research Institute

Semiconductor detectors are known to be sensitive to radiation damage which can be annealed by heating at high temperature. In the case of high-energy heavy ion detection with semiconductor detectors, fusion reactions are expected in the semiconductor materials to increase background counting rates due to long-life radioactivities produced. These radioactivities can not be annealed by heating. We have measured gamma-ray spectra from silicon and germanium irradiated with various high-energy heavy ions accelerated by 20MeV Tandem accelerator to obtain radioactivities and production cross sections of the induced nuclides. The cross sections were obtained from the observed radioactivities and the numbers of atoms of silicon and germanium in the heavy ion ranges. Figure 1 shows the gamma-ray pulse height distribution obtained from silicon irradiated with 150 MeV Cl^{9+} ions. Some results obtained from silicon and germanium are summarized in Table 1.

Radioactivities induced in other materials such as Cu, SUS-316, Mo and LiF which were irradiated by other solid-state physicists were also measured and some of the results are shown in Table 2. The effects of the presence of these newly-introduced radioactive impurities should be taken into account when the results of the solid-state physics measurements are to be interpreted.

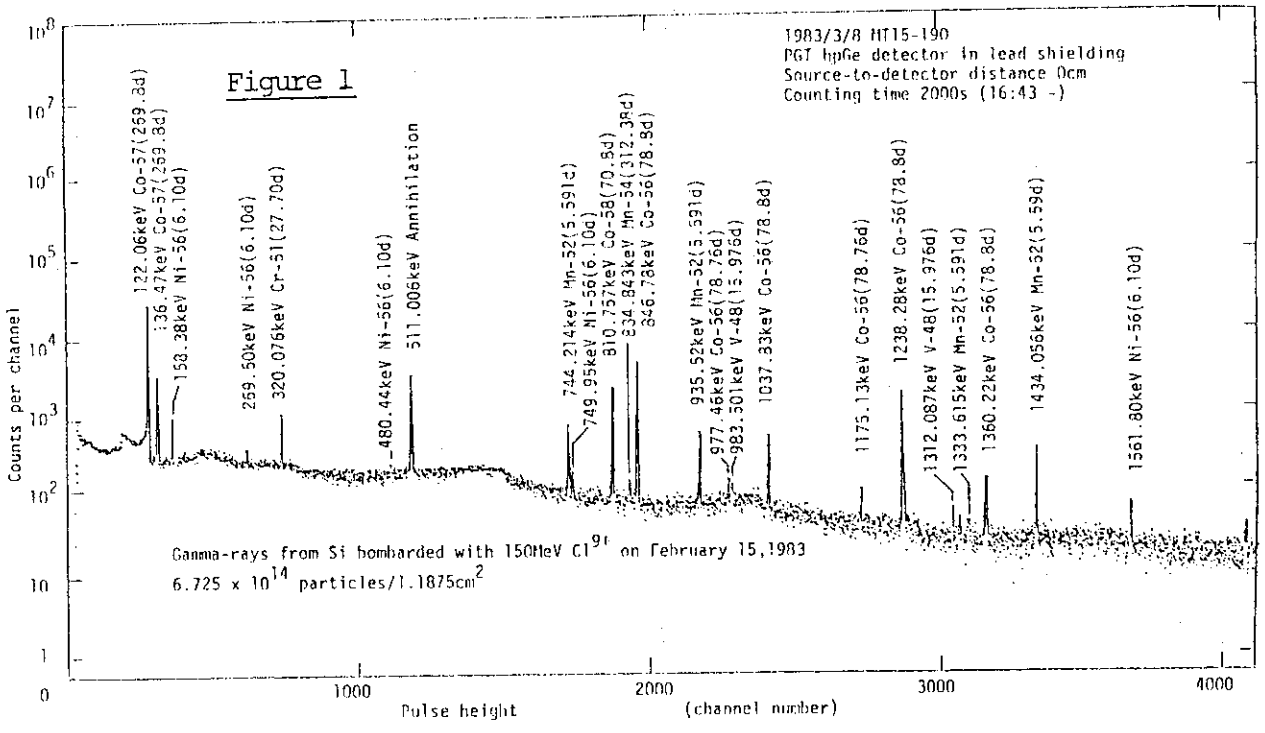

Table 1 Residual radioactive nuclides, their radioactivities, numbers of atoms and production cross sections found in silicon and germanium irradiated by high-energy heavy ions

Heavy ions	Number of particles	Irradiated material	Residual nuclide	Radioactivity(uCi)	Number of atoms	Cross section(mb)
100MeV $^{16}_{8}O^{6+}$	3.52E15 /1.42cm^2	Si	Na-22(2.6y)	1.8E-4	7.9E8	0.46
			Be-7(53.3d)	2.85E-3	7.0E8	0.41
100MeV $^{16}_{8}O^{9+}$	7.17E15 /2.90cm^2	Ge	As-73(80.3d)	4.1E-2	1.5E10	8.2
			Se-75(118.45d)	3.1E-2	1.7E10	9.3
			Rb-83(86.2d)	4.2E-1	1.66E11	89.9
			Rb-84(32.9d)	3.2E-1	3.4E10	18.3
			Sr-82(25.0d)	9.3E-1	1.1E10	5.8
			Sr-85(64.85d)	1.45E-1	1.45E11	78.3
			Y-88(106.61d)	6.0E-2	2.9E10	15.9
			Zr-88(83.4d)	5.3E-2	2.0E10	0.9
150MeV $^{35}_{17}Cl^{9+}$	6.73E14 /1.19cm^2	Si	V-48(15.976d)	6.0E-4	4.4E8	2.9
			Cr-51(27.70d)	1.5E-2	1.9E9	12.4
			Mn-52(5.591d)	2.9E-2	7.5E8	5.0
			Mn-54(312.38d)			
			Co-56(78.8d)	1.8E-2	4.6E9	30.5
			Ni-56(6.10d)	4.0E-3	7.7E7	0.5
			Co-57(269.8d)	1.4E-2	1.2E10	77.1
			Co-58(70.8d)	8.6E-3	2.0E9	12.9
150MeV $^{35}_{17}Cl^{9+}$	1.04E15 /2.84cm^2	Ge	As-71(2.54d)	4.82E-2	5.6E8	4.14
			Se-72(8.40d)	1.7E-3	4.7E7	0.34
			As-73(80.30d)	2.4E-3	6.2E8	4.6
			As-74(17.79d)	4.8E-3	2.7E8	2.0
			Se-75(118.45d)	5.1E-4	1.95E8	1.4
			Tc-96(4.35d)	8.2E-4	1.14E7	0.08
			Ru-97(2.88d)	8.14E-2	7.5E8	5.5
			Rh-99(15.0d)	1.3E-3	6.1E7	0.45
			Pd-100(3.63d)			
			Rh-101m(4.34d)	8.4E-2	1.2E9	8.5
			Ag-105(41.29d)	1.9E-2	2.5E9	18.1
			Ag-106m(8.5d)	2.4E-3	6.5E7	0.47
150MeV $^{58}_{28}Ni^{9+}$		Si	Co-56(78.76d)	2.4E-3	8.6E8	
			Co-57(271.65d)	2.2E-4	2.8E8	
			Rb-83(86.2d)	0.78	4.5E10	
			Sr-85(64.85d)	1.25E-2	5.4E9	
150MeV $^{58}_{28}Ni^{9+}$	3.67E14 /3.14cm^2	Ge	None			
80MeV $^{127}_{53}I^{7+}$	2.93E14 /3.14cm^2	Si	None			

Table 2 Residual radioactive nuclides, their radioactivities, numbers of atoms and production cross sections found in Mo, SUS-316, Cu and LiF irradiated with various high-energy heavy ions.

Heavy ion	Number of particles	Irradiated material	Residual nuclide	Radioactivity(uCi)	Number of atoms	Cross section(mb)
80MeV $^{12}_{6}C^{5+}$	7.13E14 /0.53cm^2	SUS-316	Cr-51(27.70d)	3.95E-2	3.96E6	
			Mn-52(5.591d)	2.5 E-2	6.36E8	
			Mn-54(312.20d)	1.2 E-2	1.79E10	
			Co-56(78.76d)	1.2 E-2	4.41E9	
			Co-57(271.65d)	2.9 E-2	3.43E10	
			Co-58(70.78d)	1.91E-1	6.23E10	
			Ni-56(6.10d)			
			Ni-57(1.5d)	1.04E-1	7.2 E8	
			Zn-65(244.0d)	1.6 E-1	1.77E11	
			Ga-67(3.26d)	1.35	2.04E10	
			Ge-68(288d)			
			Ge-69(1.627d)	6.5 E-1	4.78E9	
			As-71(2.542d)	8.5E-2	9.93E8	
			Se-72(8.40d)	6.4E-3	2.49E8	
			Mo-99(2.75d)			
			Ru-97(2.88d)	1.5 E-2	1.99E8	
			Rh-101m(4.34d)	5.1 E-2	1.02E8	
			Rh-105(1.478d)	2.37E-1	1.62E9	
			Pd-100(3.63d)			
			Ag-105(41.29d)			
			Ag-106m(8.5d)	1.3 E-2	5.02E8	
80MeV $^{12}_{6}C^{5+}$	3.6E15 /1.02cm^2	Mo	Nb-95(34.97d)	4.4E-2	7.12E9	12.1
			Mo-99(2.75d)	6.6E-1	8.32E9	14.1
			Tc-96(4.35d)	3.2E-1	6.38E9	10.8
			Ru-97(2.88d)	3.68	4.89E10	83.1
			Ru-103(39.35d)	2.4E-2	4.38E9	7.5
			Rh-99(15.0d)	6.0E-2	4.09E9	6.9
			Rh-101m(4.34d)	12.4	2.48E11	421
			Pd-100(3.63d)			
			Ag-105(41.29d)	1.74	3.32E11	563.7
			Ag-106m(8.5d)	2.43	9.53E10	162
150MeV $^{35}_{17}Cl^{9+}$	6.50E15 /1.77cm^2	Cu	Sc-44m(2.442d)	1.2E-1	1.36E9	14.7
			V-48(15.976d)	1.05E-4	7.72E6	0.084
			Mn-52(5.591d)	1.47E-4	3.8 E6	0.041
			Co-57(271.65d)	7.08E-5	8.86E7	0.96
			Zn-65(244.0d)	1.6E-4	1.79E8	1.93
			Ga-67(3.26d)	7.7E-3	1.16E8	1.25
			Sr-85(64.85d)			
			Y-87(3.346d)	4.6E-3	7.08E7	0.77
			Zr-88(83.4d)	8.0E-4	3.10E8	3.35
			Y-88(106.61d)	7.86E-5	3.87E7	0.42
			Zr-89(3.268d)	1.91E-2	2.87E8	3.11
			Tc-95m(61d)	9.7E-5	2.72E7	0.29
			Tc-96(4.35d)	1.5E-3	3.0E7	0.33
			Ru-97(2.88d)	1.6E-2	2.16E8	2.34
150MeV $^{35}_{28}Cl^{9+}$	6.02E13 /0.53cm^2	LiF	Co-56(78.76d)	5.7E-6	2.1 E6	
			Co-57(271.65d)	2.3E-4	2.8 E8	
			As-71(2.541d)	2.05E-2	2.4 E8	
			Se-72(8.4d)	8.08E-4	9.7 E6	
			Se-75(118.45d)	3.0E-4	1.7 E8	

3.7 ESR of Pyro-Graphite Irradiated by High Energy Ions

Yukio Kazumata* and Shigemi Yugo**

*Department of Physics, Japan Atomic Energy Research Institute.

**University of Electro-Communications.

The characteristics of defects in graphite by high energy ion bombardments are described in this paper in comparison with low energy ion and neutron irradiations. Two kinds of paramagnetic centers are observed by ESR. One of them has the character of conduction carriers in part while the other is due to localized spin centers. These centers are associated with their respective characteristic defects.

ESR spectra observed with the irradiation of various particles are shown in Fig.1. The top(Fig.1(a)) shows the spectrum from an unirradiated specimen, which is due to conduction carriers. After neutron irradiation, the g-value in a spectrum decreases to the free spin value and the width becomes somewhat smaller, as shown in Fig.1(b). This spectrum has been interpreted as conduction carriers coupled with localized spin centers produced by the irradiation. With annealing, the intensity, the g-value and the width of the spectrum are recovered to the corresponding values of before irradiation. The third shows the spectrum with the irradiation 450 keV Ar^{+} ions. The shape is symmetric and the width decreases markedly. This spectrum is interpreted as the localized spin centers which follow the Curie-type behavior of the susceptibility. In this spectrum, no change of the g-value with annealing temperature from RT to 300 °C is observed. Finally the spectrum at the bottom in Fig.1 for 100 MeV Cl^{8+} ion irradiation consists of two lines in contrast to one line in above spectra.

The line-2 in Fig.1(d) is interpreted as being due to localized spin centers since the behavior of the line with annealing temperature from RT to 300 °C and with the measuring temperature is similar to that in the Ar^{+} irradiation. The line-1, on the other hand, has the character of conduction carriers and behaves like a pectrum in neutron irradiation in the dependence on the annealing temperature. However, the change in the g-value and the width of the line-1 with measuring temperature is opposite to those in neutron irradiation; that is, for the line-1 $g_{//}(NT) < g_{//}(RT)$ and $W_{//}(NT) < W_{//}(RT)$, but for the neutron irradiation to a dose of 3.3×10^{17} nvt, $g_{//}(NT) > g_{//}(RT)$ and $W_{//}(NT) > W_{//}(RT)$, where $g_{//}(NT)$ and $g_{//}(RT)$ denote the g-values at nitrogen and room temperature, respectively, in a static magnetic field

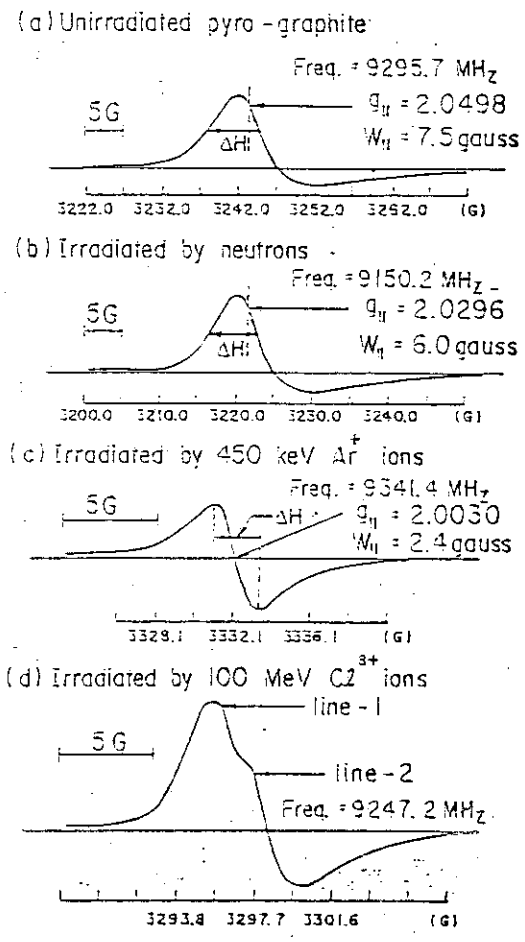

Fig.1 ESR spectra of pyro-graphite irradiated by neutrons and ions. Measurements were made at RT.
(a) Unirradiated pyro-graphite
(b) Irradiated by neutrons at 5 K to the fluence of 3.3×10^{17} nvt.
(c) Irradiated by 450 keV Ar^{+} ions to the fluence of 1.1×10^{14} Ar^{+}/cm^{2}.
(d) Irradiated by 100 MeV Cl^{8+} ions to the fluence of 2.8×10^{14} Cl^{+}/cm^{2}. The line-1 and line-2 are indicated.

parallel to the c-axis of graphite, and the similar notation applies to the width.

It is shown from the theory by McClure and Yafet[1], and from the experiments therein that the opposite change of g-value with measuring temperature as described above is related to the drop of the Fermi level into the valence band. If the concentration of acceptors produced by irradiation exceeds 100 ppm, the Fermi level drops into the valence band from the conduction band. The formation of acceptors by irradiation has been already ascertained by several experiments.[2] From this fact, the line-1 would arise from the region which contains acceptors more than 100 ppm.

The next problem to be considered is why the two different paramagnetic centers should be observed by high energy heavy ion bombardments. The scattering of projectiles by lattice atoms is governed by Coulomb potential near the surface and by Thomas-Fermi potential near the projected range of

incident ions. The number of displaced atoms for the 100 MeV Cl^{8+} ion bombardment is estimated to be 10^{-3} dpa for Coulomb potential and 5×10^{-2} dpa for Thomas-Fermi potential, respectively. Since the displacement atoms of 10^{-4} dpa produce 5~80 ppm acceptors, the amount of acceptors near the surface on the Cl^{8+} ion bombardment will be greater than 100 ppm.
Around the projected range of the ions, on the other hand, the transition from crystalline to amorphous state will be expected for the fluence of 2.8×10^{14} Cl^{+}/cm^{2} because the transition is observed at 0.06 dpa on the Ar^{+} ion bombardment.

Similar two lines are also observed by the bombardment of 150 MeV Ni^{9+} ions. The change of electronic properties in graphite with different kinds of projectiles, especially between gaseous and metallic ions, is now studied by ESR.

As a conclusion, two kinds of paramagnetic centers produced by high energy ion bombardments are interpreted as conduction carriers in a sample containing a number of acceptors produced by the bombardment and as localized spin centers in an amorphous state, respectively. From this experiment, it is proposed that the transition from conduction carriers to localized spin centers can be studied in detail by high energy ion bombardment.

(References)

1) J.W. McClure and Y. Yafet : Proceedings of the Fifth Carbon Conference, (Pergamon Press, Oxford, 1962) Vol.1, p.22
2) R.O. Dillon, I.L. Spain and J.W. McClure : J. Phys. Chem. Solids 19 (1978) 1071, and the reference therein.

3.8 Irradiation Effect with Heavy Ions on Si and Alkali Halides

Hiroshi Naramoto

Department of Physics, Japan Atomic Energy Research Institute.

Heavy ions with high energy interact with solid through the following characteristic processes; 1) nuclear reactions and/or Coulomb excitations, and 2) intense electronic excitations. The process 1 makes it possible to do the nuclear spectroscopic investigation of induced defects by recoil implantation. As the first step of this study, the influence of primary beam is investigated in a Si specimen which is sensitive to ion irradiation. The phenomena associated with the process 2 can be observed especially in semiconducting and insulating materials. Alkali halides(LiF and NaF) are chosen to investigate the energy dissipation process of heavy ions. Crystalline systems are employed so that the crystallographic information can be obtainable.

Irradiation was performed at liquid nitrogen temperature with heavy ions from JAERI tandem accelerator. Si crystal was irradiated with 100 MeV O^{+6} to 2.5×10^{15} /cm^2, and LiF and NaF crystals with 150 MeV Ni^{+9} to 1.6×10^{14} / cm^2 and 150 MeV Cl^{+9} to 5.9×10^{14} /cm^2. After irradiation, the above specimens were warmed up to room temperature, and some measurements were made. Rutherford backscattering/channeling analyses were performed on a Si crystal with 1.8 MeV He^+. The pseudo-Kikuchi patterns(so-called Coates patterns) were also taken to assess the crystal quality at the near surface region. Microstructural change of alkali halides after irradiation was detected taking optical absorption spectra and the pseudo-Kossel patterns.

Fig. 1 in the next page shows three kinds of backscattering spectra of 1.8 MeV He^+ for a Si single crystal irradiated with 100 MeV O^{+6}. The spectrum with triangles was taken at a random geometry, and the other two are the <110> aligned channeling spectra. The <110> aligned spectrum does not show any significant changes even after heavy ion irradiation(dotted curve with solid circles) except the appearance of a hump at 0.63 MeV. This yield increase corresponds to the pile-up of oxygen atoms just at the Si surface, and a comparison with the random spectrum shows no occupation of the special crystallographic sites. Contents of oxygen atoms in Si crystals depend on a condition of crystal growth, and Si specimen used here was grown by the Czochralski method [1], which implies the incorporation of oxygen impurities into Si

matrix. Judging from ion backscattering spectra in a virgin specimen, these impurities occupy the substitutional site of Si. The intense electronic excitation could make these impurities migrate to the surface of Si crystal. The area and the width of surface peak do not show any detectable change after ion irradiation. It is realized that the reconstruction of surface atoms, which is often observed in the laser-annealed Si crystals [2], is not caused in this case, and that the pile-up of oxygen impurities at the Si surface is forced by electronic loss of energetic heavy ions. The inset in Fig. 1 gives the Coates patterns in the irradiated Si crystal, which are sensitive to the introduction of lattice strain associated with crystal defects. The patterns obtained assures that this crystal is free from the lattice distortion at the near surface region even after O^{+6} irradiation. In conclusion, the influence of irradiation with oxygen ions is not so severe at the near surface of Si crystal that it is possible to utilize oxygen ions as a primary beam for the experiment of recoil implantation.

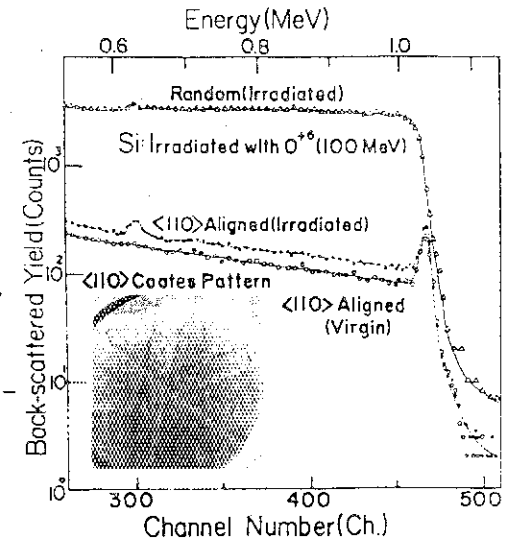

Fig. 1: Backscattering and channeling spectra of 1.8 MeV He^{+} for Si irradiated with 100 MeV O^{+6}: random(triangles), <110> aligned after irradiation(solid circles) and <110> aligned before irradiation(open circles).

The diffraction process of divergent X-rays was used to detect a change of single crystal of alkali halides. The pseudo-Kossel patterns obtained suggest the lattice expansion at the near surface region. The expansion is not uniform along depth, and it is difficult to resolve the Cu $K\alpha_1$ and $K\alpha_2$ components. Optical absorption spectra revealed the existence of rather simple defects even after heavy ion irradiation. The energy dissipation process will be revealed by a comparison of depth-distribution of color centers in alkali halides with that in other insulators in which color centers are produced only through the nuclear collisions.

References

1) See, for example, *Crystal Growth: an introduction*, edited by P. Hartman (North-Holland/American Elseviar, Amsterdam/New York, 1973).

2) D. M. Zehner, C. W. White and G. W. Ownby, Applied Physics Letters 37 (1980)456.

3.9 Electron Microscope Observations of Tracks of 128 MeV Cl^{9+} Ions in Deposited Films of Ge

Shigemi Furuno, Hitoshi Otsu and Kazuhiko Izui

Division of Chemistry, Japan Atomic Energy Research Institute

The observations of tracks of high energy heavy ions in solid materials have been made with a transmission electron microscope. The irradiation experiments for track production were carried out using specified and well collimated ion beams obtained from a tandem acceralator in order to investigate the governing factors and the mechanism for the track formation in various solid materials.[1)]

In this report, the results of observations of the tracks of Cl^{9+} ions in deposited films of Ge are shown. Thin films of 50 Å thickness were prepared by vacuum evaporation on thin collodion films supported with copper meshes. These specimens were bombarded with 128 MeV Cl^{9+} ions in the irradiation chamber cooled at liquid nitrogen temperature. After irradiation, observations of the specimens were carried out with an electron microscope of JEM 100C type operating at 100 kV.

Figures 1 and 2 show the tracks produced in deposited films of Ge by 128 MeV Cl^{9+} ions incident in the directions normal and at angle of about 10° to the surface of the specimens, respectively.

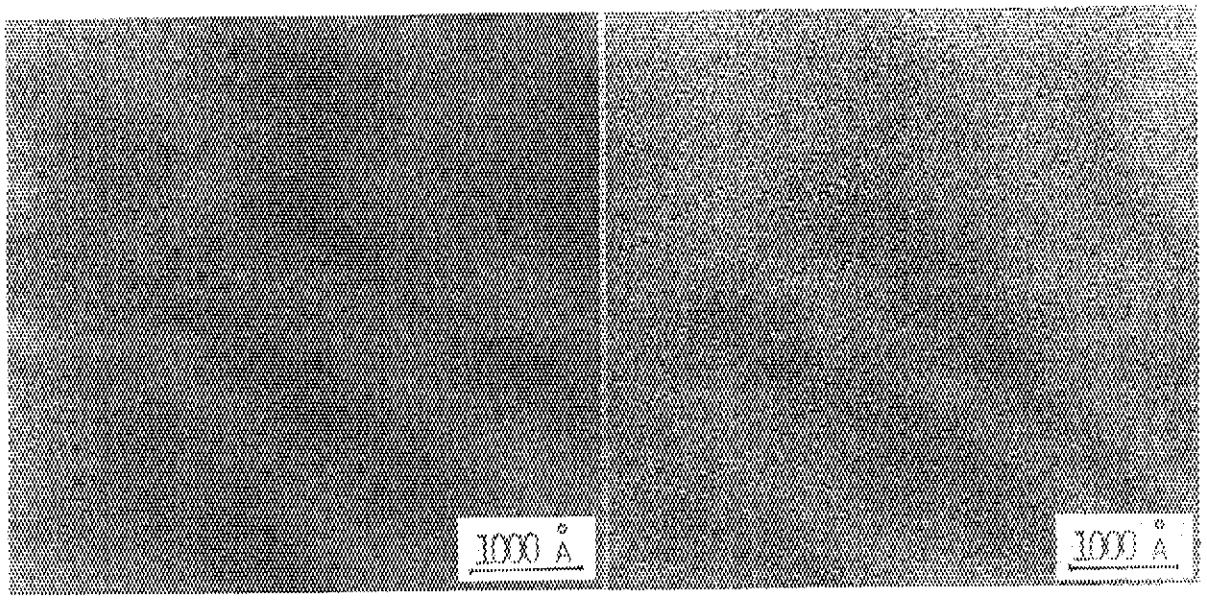

Fig. 1 Tracks of 128 MeV Cl^{9+} ions incident in the normal direction to the surface of the deposited film of Ge.

Fig. 2 Tracks of 128 MeV Cl^{9+} ions incident at the angle of about 10° to the surface of the specimen.

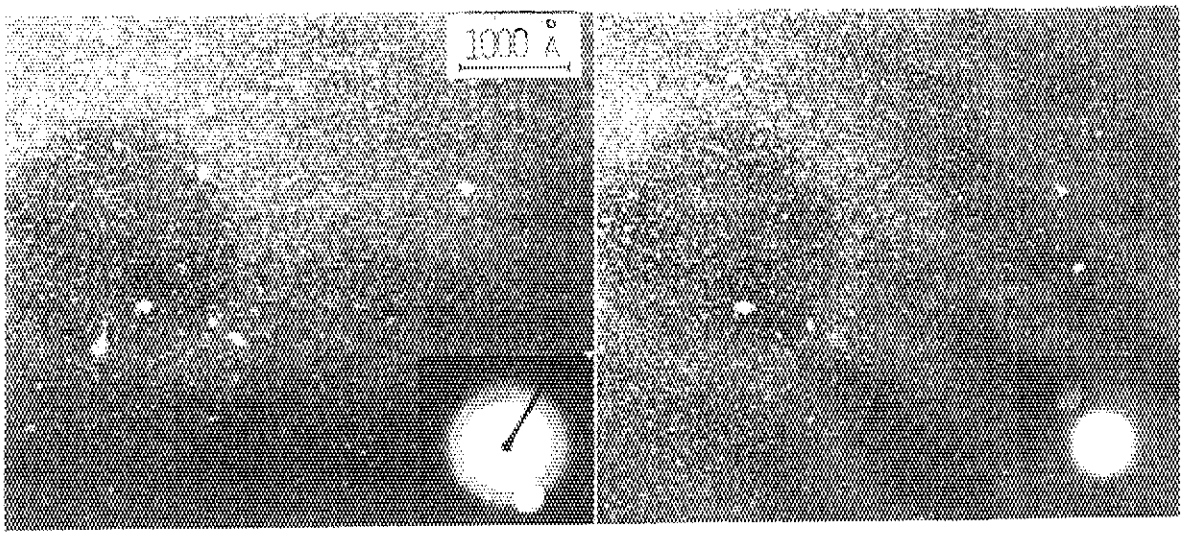

Fig. 3 Dark-field image of the tracks of 128 MeV Cl^{9+} ions incident in the normal direction to the surface of the specimen.

Fig. 4 Dark-field image of the same area as figure 3 taken with the beam of another part of the diffraction ring.

A diffraction pattern from deposited films of Ge shows a halo pattern indicating an almost amorphous structure. After irradiation, this changes into a ring pattern indicating that some parts of films recrystallize. To clarify this phenomenon, dark field image micrographs are taken. Figure 3 is taken with the beam of a part of diffraction ring by setting the objective aperture as shown in the diffraction pattern inset in this figure. Figure 4 shows the same area as figure 3 taken with the beam of another part of the diffraction ring. From this result it is concluded that these tracks consist of small crystallets of about 100 Å in diameter. This recrystallization along the tracks is considered to arise from the thermal spike effect due to the energy deposited by high energy Cl^{9+} ions.

The same kind of irradiation experiments were also carried out using 100 MeV O^{6+} ions. In this case, however, no track was observed. This result is considered to be due to less energy deposition of about a sixth than that in the case of 128 MeV Cl^{9+} ion.

Reference

1) S. Furuno, H. Otsu and K. Izui: J. Electron Microsc. 30 (1981) 327.

3.10 X-Ray Diffraction Topographic Observation of Si Single Crystals Irradiated with 150MeV Ni^{+9} and Cl^{+9} Ions

Hiroshi Tomimitsu

Department of Physics, Japan Atomic Energy Research Institute

Si single crystal used in this experiment was grown along [001] direction by Cz.method, sliced parallel to the (001) plane, chemically etched and mechanically polished, the resultant thickness being 0.3mm. It was then cut into two pieces of the rectangle with the cross-section of $3x3cm^2$. The ion-irradiation was carried out at the tandem-type accelerator of this institute. One piece of the rectangular Si wafer was irradiated with 150MeV Ni^{+9} ions with the dose of $5x10^{13}ions/cm^2$ (specimen A), and another was with 150MeV Cl^{+9} ions of $6x10^{14}ions/cm^2$ (specimen B). For both irradiation, the Si wafers were partially covered with aluminium masks of about 34μm thickness. The X-ray diffraction topography (XDT) was carried out with a conventional Lang camera set at a fine focus X-ray generator, operated at 50kV and 1.3mA with the targets of Cu and Mo.

Although the XDT-observation is yet in progress, some typical and significant results can be briefly reported as following:

1. Both of the specimen A and B became convexed towards the irradiated surface, which was concluded through the following two facts: (a) The angular position of the reflection maximum in the rocking curve moved as the position of the incident X-rays on the specimen surface was moved, and (b) A topograph taken at an angular position showed only partial images of the whole specimen crystal. This tendency of the partial images was much more marked for the specimen B than for A. By analysing the movement of the angular position of the reflection maximum in relation to the position of the incident X-ray, it was estimated to be 6sec. of arc per cm in the crystal surface, which corresponded to the radius of the surface curvature of about 33m for the specimen A, and it seemed to be much less for the specimen B.

2. The heavy lattice strains were observed at the boundaries between the irradiated and the non-irradiated areas, where the so-called black-and white contrasts were observed. In spite of the heavy strains observed, however, there was not observed any topographic images of the lattice defects like dislocations generated at the irradiation boundaries.

3. Some topographs showed the characteristic fringes (Fig.1). It was clearly

observed that the fringes appeared in the topographs taken with the reflecting plane perpendicular to the specimen surface, while they did not appear with the reflecting plane parallel to the specimen surface. These facts are obviously inconsistent with the model proposed and observed by Bonse and Hart[1] and Bonse, Hart and Schwuttke[2].

4. An interesting phenomenon was observed as for the so-called range of the energetic ions in the materials; i.e. the thickness of 34μm of the Al mask was sufficient for 150MeV Ni^{+9} ions, while it seemed to be insufficient for 150MeV Cl^{+9} ions so that the "masked" area of the specimen B had to be suffered from rather heavy damages (Fig.2). When the interpolated values for the range of Cl ions in Al are used[3], the 150MeV Cl ions lose their energy more than 140MeV in the Al-mask and they will enter into Si with the energy less than 10MeV. The observed images of the masked areas seem, further, to be much more heavily damaged than expected with the normal irradiation with the Cl ions with the energy less than 10MeV, which may be attributed to the so-called "cascade" Al atoms in the mask caused by the through-passing Cl ions.

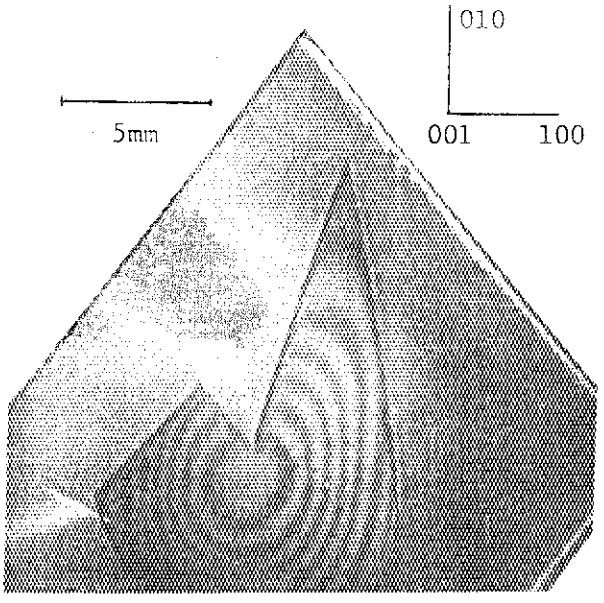

Fig.1
Systematic fringes observed at the irradiated area of the specimen A (150MeV Ni^{+9}, 5×10^{13}ions/cm^2), taken with 400 reflection by Cu-Kα1.

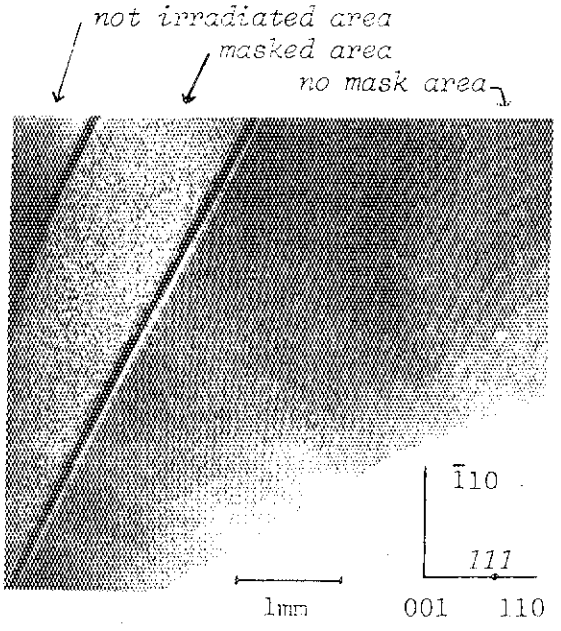

Fig.2
Topographic images of the Specimen B (150MeV Cl^{+9}, 6×10^{14}ions/cm^2), taken with 111 reflection by Cu-Kα1. Heavily damaged patterns can be observed at the masked area, while the systematic fringes at the directly irradiated area.

(References)

1. U.Bonse and M.Hart: phys.stat.sol. 33, 351 (1969).
2. U.Bonse, M.Hart and G.H.Schwuttke: *ibid.* 33, 361 (1969).
3. U.Littmark and J.F.Ziegler: *Handbook of Range Distributions for Energetic Ions in All Elements* (Pergamon, N.Y., 1980).

3.11 Microstructures Produced in 316 Stainless Steel Irradiated with 100 MeV Carbon-Ions during Irradiation Creep Experiment

Takeo Aruga and Akimichi Hishinuma

Department of Fuels and Materials Research, Japan Atomic Energy Research Institute

A thin sheet specimen of type 316 stainless steel with a geometry of 25 mm in length, 4 mm in width and 0.07 mm in thickness was solution annealed for 1 h at 1373 K. The specimen was irradiated using a irradiation creep facility installed at JAERI Tandem accelerator with 100 MeV C-ions with 1.5-2 particle-mA/m^2in current density for 18 h at 723 K under a constant uniaxial tensile stress of 100 MPa. The irradiation creep strain was monitored by measuring the distance between upper and lower grips. The details of the irradiation creep apparatus accompanied with the preliminary creep strain data will be described elsewhere.

The calculated projected range and straggling of 100 MeV C-ion in 316 steel are 67.5 and 0.5 μm,respectively. The displacement damage rate in the present irradiation condition was estimated to be 2-5x10^{-5} dpa/s at damage peak and 5-7x10^{-7} dpa/s in the region from irradiation surface to a depth of about 50 μm, as shown in Fig. 1. The specimen thickness of 70 μm was so chosen that the creep strain data obtained in the 100 MeV C-ion irradiation under stress can be considered to be representative of the whole specimen. In addition, a highly damaged region around the projected range is significant in investigating the irradiation produced microstructural development under stress.

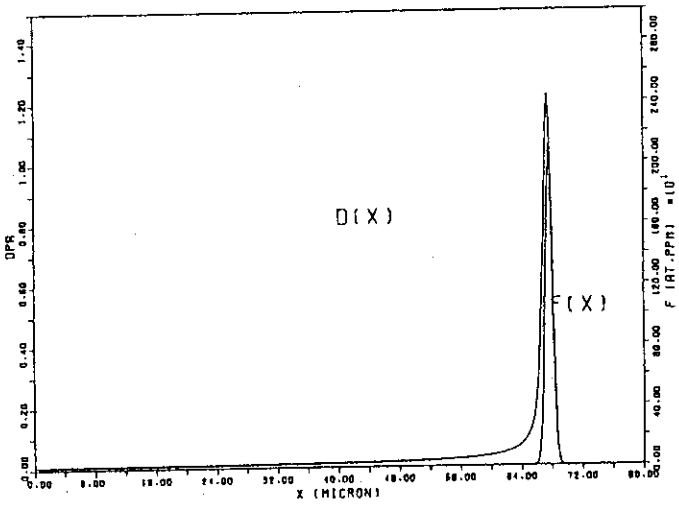

Fig. 1 Calculated damage profile (D) and stopped ion distribution(F) in 316 stainless steel irradiated with 100 MeV C-ions. The results are normalized to a current density of 10 particle-mA/m^2 in 1 h.

The total dose was estimated to be about 0.02 and 2 dpa ,in the front region of damage peak and around the peak, respectively.

The cross sectional microstructure in the irradiated specimen was examined in the direction parallel to the incident ion beam using an electron microscope operated with 1000 kV. The thickness of observed area was about 500 nm. The observational results revealed that a small angle subboundary

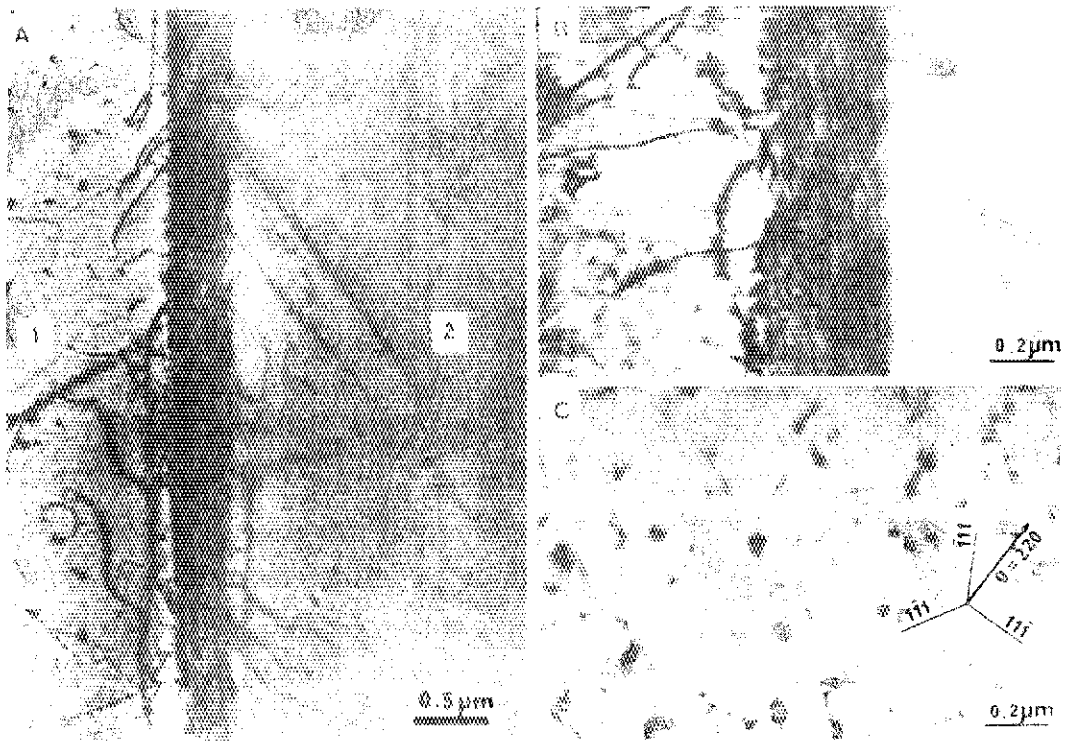

Fig. 2 Cross sectional microstructures produced in 316 stainless steel irradiated with 100 MeV C-ions at 723 K under a tensile stress of 100 MPa. A,B : subboundary formed around the depth of damage peak (the beam direction is from region marked by 1 to 2 in A and the direction of applied stress is normal to foil surface). C : dislocation loops formed in front region of damage peak to a distance of few μm.

across grains was formed, as shown in Fig. 2-A and B, along a line parallel to the irradiation surface around the projected range. The two subgrains separated by the boundary were observed to be misaligned to each other ; tilted by a small angle with a little rotation. The subboundary was consisted of networks with dislocation segments located in glide planes coplaner Burgers vector at 120°. The nucleation and growth of loops around the peak was much more pronounced than in the region far from the peak, since the damage rate at peak was higher by two orders than the other front region. The loops in a higher density around the damage peak are easy to unfault and resultant dislocation line interaction and rearrangement under stress will form dislocation networks and finally a small angle subboundary.

In the region in front of and also within a few μm behind the subboundary, the dislocation loops were observed in a density of about $5\times10^{19}/m^3$ together with dislocation lines. The loops were clearly partitioned on {111} planes (Fig.2 C). The loop distribution on each plane was summarized in Table 1. The density of loops in $(11\bar{1})$ and (111) planes was by 2-9 times larger than that in $(\bar{1}11)$ and $(1\bar{1}1)$ planes. The fact indicates that the applied stress plays a significant role in the nucleation and growth of loops on the various planes.

Table 1 Summary of transmission electron microscopy data on dislocation loop in 316 stainless steel specimen irradiated with 100 MeV C-ions to about 0.1 dpa at 723 K under a tensile stress of 100 MPa.

Crystal plane	Number density ($10^{19}/m^3$)	Fraction of density (%)	Alignment factor+	Mean diameter(nm)
$\bar{1}11$	0.2	5	0.20	82
$11\bar{1}$	1.8	43	1.77	57
111	1.5	35	1.44	50
$1\bar{1}1$	0.7	17	0.70	54

+ Ratio of each density to average

The loop densities in the outer region with 0.5 μm width in both sides on the subboundary were smaller than that in the region far from the subboundary. The local irradiation hardening due to the high density dislocation may induce the stress concentration in the region around the damage peak, which would give rise to the preferred flow of irradiation produced interstitials into or vacancy emission from the highly damaged region. As a result, the loop nucleation was considered to be suppressed in close proximity to the subboundary. Such a subboundary around the damage peak ,however, was not observed in the stress-free 316 stainless steel specimen irradiated with 1.0 MeV C-ions at 803 K to a peak dose of 10 dpa, as shown in Fig. 3 [1]. And so, the loop depleted zone observed in the present irradiated specimen seems to be caused by ion irradiation under stress.

Fig. 3 Cross sectional microstructure produced in stress-free stainless steel irradiated with 1.0 MeV C-ions at 803 K to 10 dpa at damage peak around 0.7 μm.

Reference

1) T.Aruga, Y.Katano and K.Shiraishi, to be published in J. Nucl. Mater.

IV NUCLEAR CHEMISTRY

4.1 NUCLEAR CHEMISTRY OF ACTINOIDS
Synthesis of Transuranium Nuclides from Interaction of ^{16}O with ^{238}U

Nobuo Shinohara*, Shin-ichi Ichikawa*, Shigekazu Usuda*, Toshio Suzuki*, Nobuaki Kono*, Hirokazu Umezawa*, Hiroshi Okashita*, Toshiaki Sekine**, Kentaro Hata**, Yasukazu Yoshizawa***, Takayoshi Horiguchi***, Ichiro Fujiwara****

*Department of Chemistry, **Department of Radioisotope Production, Japan Atomic Energy Research Institute; ***Department of Physics, Hiroshima University; ****Institute of Atomic Energy, Kyoto University

INTRODUCTION

In order to investigate the nuclear and chemical properties of the actinoid nuclides which have relatively short lives the questioned nuclide must be synthesized at first. The transuranium nuclides are usually produced by successive neutron capture under intense neutron flux in a nuclear reactor.[1] For the heavier nuclides this method becomes unsatisfactory because the intermediate isotopes decay so quickly that there is insufficient time for them to undergo the successive neutron capture. Besides, heavy-ion bombardment is effective to the synthesis of the elements Z>98.

In the beginning we started to understand the interaction of ^{16}O with ^{238}U by Tandem accelerator to obtain the condition for producing the aimed transuranium nuclides.

EXPERIMENTAL

The uranium target was prepared by electrodeposition onto an aluminum foil of 7 μ thickness.[2] The purity of ^{238}U was 99.98 w/o and the targets of uranium varied 300 - 2000 μg/cm^2 in thickness. The target with an aluminum catcher foil was bombarded by ^{16}O beams with energy 92 to 102 MeV and beam intensity about 0.8 to 1 μA. Typical irradiation times were from 0.5 to 3 hours. After irradiation, α- and γ-activities of the recoiled nuclei, which were collected by the aluminum catcher foil, were measured with Si-surface-barrier and Ge(Li) detectors. In order to identify the synthesized actinoid nuclide, radiochemical analysis was also performed: Both the target and the aluminum catcher foil were dissolved in mineral acid and the chemical separation was carried out by ion-exchange and co-precipitation methods, followed by α- and γ-spectrometry.

RESULTS AND DISCUSSION

The α-spectra obtained by measuring the aluminum catcher foil immediately after irradiation are shown in Fig. 1. The half-life of the 6 MeV peak was measured to be 15 ± 2 min. The 7.4 MeV peak was appeared to be due to ^{250}Fm ($T_{1/2}$ 30 min, α 7.43 MeV)[3] which was the neutron evaporation residual from the compound nucleus, ^{254}Fm. Chemical identification to those α-decay nuclides is not succeeded yet.

Figure 2 shows the α-spectra of the transplutonium fraction after ion-exchange separation of a bombarded target. Two α-activities with 6.1 MeV and 6.8 MeV energy were observed in the spectra and their half-lives were about 160 days and 35 hours, respectively. Considering their energies, half-lives and chemical properties, these activities were ascribed to ^{242}Cm and ^{246}Cf, respectively.

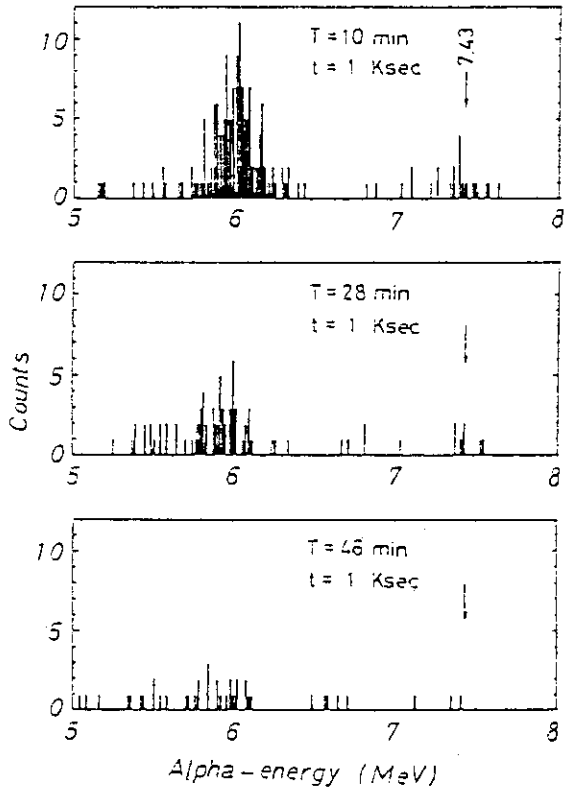

Fig.1 α-spectra of an aluminum catcher foil after bombardment with 92 MeV ^{16}O beam. T gives the starting time of counting after the end of irradiation, t the counting duration.

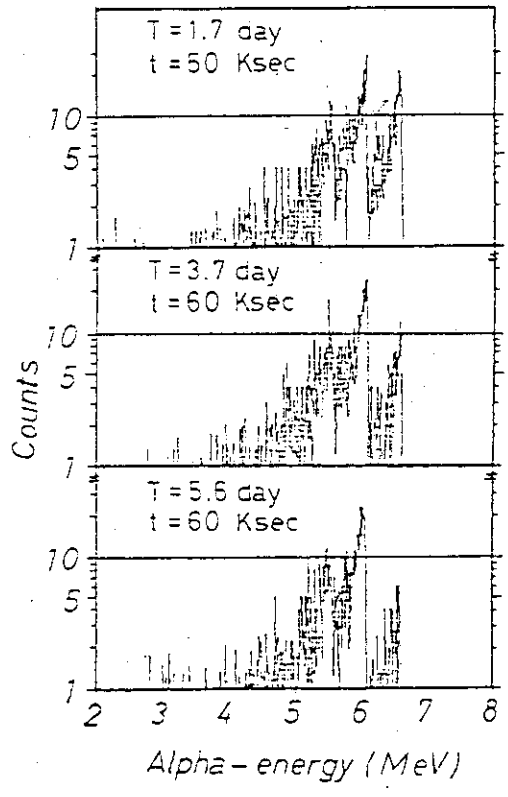

Fig.2 α-spectra of the transplutonium fraction after ion-exchange separation. ^{16}O beam energy was 97MeV. T gives the starting time of counting after the end of irradiation, t the counting duration.

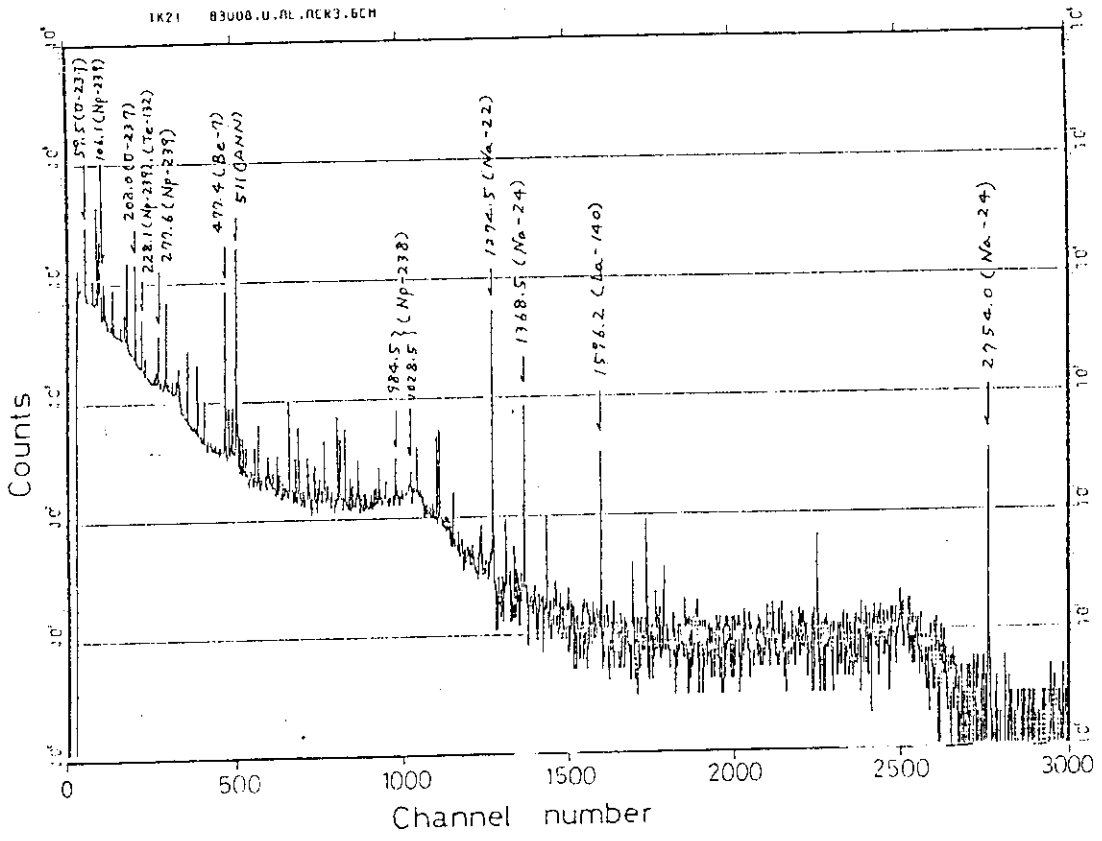

Fig.3 γ-spectrum of the target assembly after bombardment with 92 MeV ^{16}O beam. The starting time of counting after the end of irradiation was 6.7 day and the counting duration was 50 Ksec.

The γ-spectrum of the target assembly after irradiation is shown in Fig. 3. ^{238}Np, ^{239}Np and ^{237}U were identified and confirmed by chemical behavior.

So far we have identified the five actinoid nuclides with the corresponding formation cross section. However, the most of the actinoid nuclides to be made by (^{16}O,xn), (^{16}O,αxn) and other reactions were not found. Further bombardments are planned to clarify the production reaction.

REFERENCES

[1] L.J.King, J.E.Bigelow and E.D.Collins: CONF-800814-21(August,1980).

[2] S.Okazaki, et al.: private communication (1982).

[3] C.M.Lederer, V.S.Shirley, Eds.: Table of Isotopes, 7th Ed., J.Wiley & Sons, New York (1978).

[4] G.N.Akap'ev, A.G.Demin, V.A.Druin, É.G.Imaev, I.V.Kolesov, Yu.V.Lobanov, and L.P.Pashchenko: Atomnaya Énergiya, 21(1966)243.

4.2 An Experiment of Irradiated ^{197}Au with ^{16}O Ions

S.Baba*,K.Hata*,T.Sekine*,S.Ichikawa**,T.Suzuki**,N.Shinohara**,H.Baba***,
T.Saito***,A.Yokoyama***,I.Fujiwara****,N.Imanishi****

*Department of Radioisotope Production, **Department of Chemistry, Japan Atomic Energy Research Institute; ***Osaka University, ****Kyoto University

The nuclear reaction of ^{197}Au with ^{16}O has been studied by the radiochemical method. The experiment is still in progress. The main information obtained so far is the excitation functions of various product nuclides and their recoil ranges.

The Au targets of 2mg/cm^2 thick and Al catcher foils were mounted on a Faraday cup and bombarded for 0.5 - 2hours with ^{16}O beams from the tandem accelerator operated at the terminal voltage of 14MV. The incident energies to the Au targets ranged from 85 to 110MeV in the laboratory system. After the irradiation, the activities of the heavy reaction products, such as Rn, At, Po, Bi, Pb, Tl, Hg and Au isotopes, were determined by direct gamma-ray measurement of Au target and Al catcher foil, respectively, or by the measurement of radiochemically separated samples.

The obtained excitation functions were classified into three types. The first type has the typical shape for the fusion-evaporation reaction residue as shown in Fig.1, for which calculated excitation functions with ALICE[1] are presented as well for comparison. The excitation functions of the second type cannot be reproduced by the ALICE calculation with the same parameters as used in Fig.1. The third one is understood as the nuclear transfer reaction.

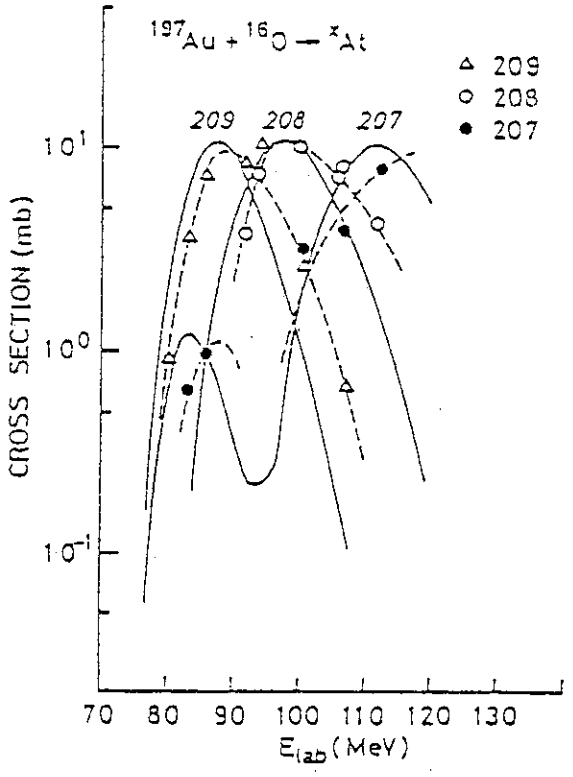

Fig.1 Some of the obtained excitation functions of the fusion-evaporation type reaction. Dashed curves are drawn through the observed data to guide the eye. Results of calculation by ALICE are also depicted with solid curve.

Figure 2 shows a typical example of the effective ranges of the

recoiled product nuclides where calculated ranges are also given with various curves corresponding to certain kinematical assumptions. The solid line represents the range of the full momentum transfer while the dotted line corresponds to the range of the so-called incomplete fusion product, that is, carbon-fusion product in which the projecting oxygen ion is assumed to break up into carbon and alpha particles before interacting with the target nucleus[2].

In the case of ^{209}At which is most likely a fusion-evaporation residue, the range is approximately equal to that of the full momentum transfer except for low energies close to the Coulomb barrier. The steep drop of the range toward the Coulomb barrier is probably explained by the scattering effect.

The range of ^{204}Po is on the contrary rather close to that of the incomplete fusion product. In the case of ^{198}Tl, the range as a function of energy shows a thoroughly different feature from that of complete or incomplete fusion as seen in Fig.2. Instead, it agrees well with the range calculated for the Rutherford scattering though the nuclear radius parameter appears to be much large as compared with the ordinary value in the heavy-ion reaction. This deviation is, however, considered to reveal the consequence of the inelasticity of the process where the range is expected to be larger than the pure elastic scattering.

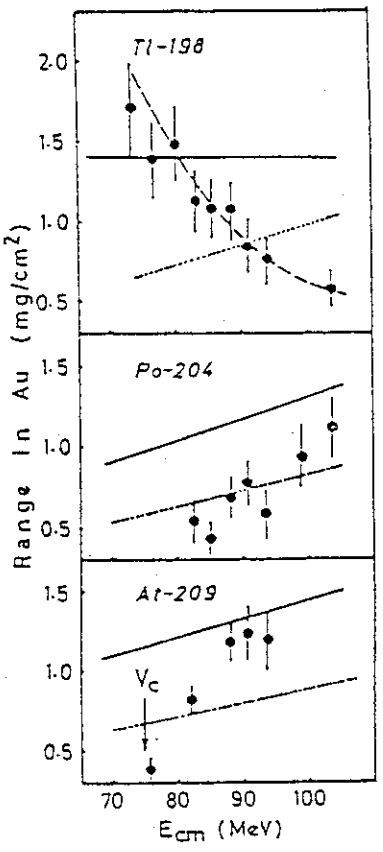

Fig.2 Ranges of the typical product nuclides. Solid and dotted curves represent calculated ranges for complete and incomplete fusion reactions, respectively, while the dashed curve is the consequence of the Rutherford scattering with r_0=1.7fm.

References

1. M.Blann, COO-3494-29 (1976).
2. T.Inamura et al., Phys.Lett., 68B, 51 (1977).

4.3 Electron Capture and Positron Decay from ^{121}Xe

T. Tamura*, M. Ohshima*, E. Minehara*, T. Sekine**, K. Hata**
S. Ichikawa***, O. Nakamura****, S. Ohya****, N. Mutsuro****

*Department of Physics, **Department of Radioisotope Production,
***Department of Chemistry, Japan Atomic Energy Research Institute;
****Faculty of Sciences, Niigata University

As the first attempt of radiactivity study utilizing a mass separator introduced from Danfysik, we planned a series of investigations of short-lived neutron-deficient isotopes of Cs, Xe, I which seemed easily ionized in the present ion source system. The EC+β^+ decay of ^{121}Xe has previously been investigated by F. Munnich et al.[1] who proposed a complex decay scheme. Lack of information in their decay scheme is the g.s. - g.s. beta-transition intensity which gave ambiguous situation for the beta branchings to all the excited state of ^{121}I (ref.2).

In the present study, radioactivities of ^{121}Xe and ^{121}I were produced by ^{107,109}Ag (^{16}O,X) reaction. A=121 mass fraction was obtained from the reaction products by using the mass separator. Examples of spectra for the mass-separated sources for A=120, 121 are shown together with the unseparated one in Fig.1. Both mass and chemical separation were performed to obtain a pure source of ^{121}I for gamma-ray study. From multiscaling of the gamma-ray spectra of mass separated and untreated sources, we deduced the g.s.-g.s. beta branchings for ^{121}Xe $\rightarrow$ ^{121}I using relative beta branching for the first excited state of ^{121}I combined with the 212-keV gamma-ray yeield (0.85 ± 0.8 γ's per decay) in the ^{121}I decay: I_β(g.s. of ^{121}Xe to g.s. of ^{121}I)$=0.29 \pm 0.5$. All the beta branchings to the ^{121}I level in the ^{121}Xe decay were calculated from this value and the gamma-ray data of Munnich et al[1]. The result is presented in Fig 3 together with log ft values. The spin and parity values for the g.s. of ^{121}Xe were deduced to be $5/2^+$ from log ft values in this experiment and from the evidence of allowed transition in ^{121}Cs g.s. ($3/2^+$) EC decay. In the study of

^{121}I decay to the ^{121}Te levels, gamma-ray energies and intensities were newly determined. Cascade relations were confirmed to eliminate the ambiguities of multiply placed gamma rays existed in the decay scheme of Bonch-Osmolovskaya et al.[3)]

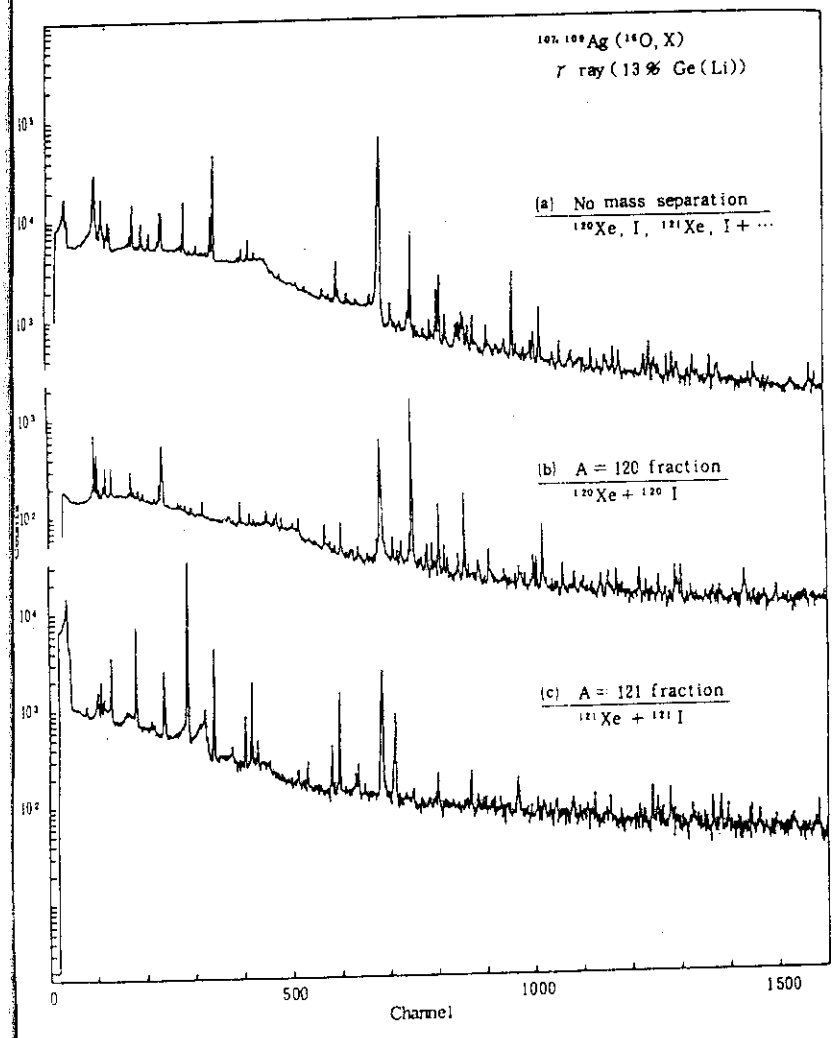

Fig. 1 Gamma-ray spectra of ^{107,109}Ag(^{16}O,x) reaction products with 13% Ge(Li) spectrometer.

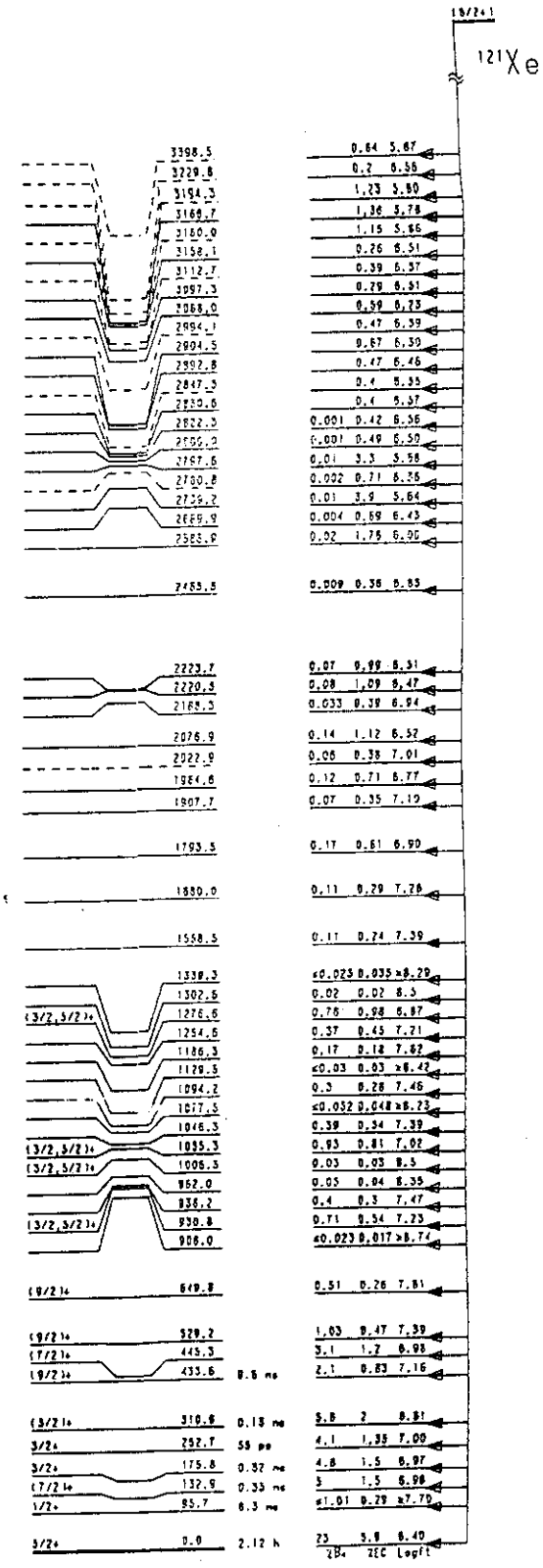

Fig.2 Levels and beta transitions in ^{121}Xe EC decay

References

1) F. Munnich, H. Kugler, H. Schrader, R. Stippler: Nucl. Phys. A215 (1973) 383

2) T. Tamura, Z. Matumoto, A. Hashizume, Y. Tendow, K. Miyana, S. Ohya, K. Kitao and M. Kanbe: Nuclear Data Sheets 26 (1979) 385

3) N.A. Bonch-Osmolovskaya, Ngo Fu An, S. Butsev, Yu.V. Norseev, M. Milanov: Izv. Akad. Nauk SSSR, Ser. Fiz. 44 (1980) 2286

4.4 Decay Scheme of ^{129g,m}Ba

T. Tamura*, M. Ohshima*, T. Sekine**, S. Ichikawa***, K. Nishimura****, S. Ohya****, N. Mutsuro***

*Department of Physics, **Department of Radioisotope Production, ***Department of Chemistry, Japan Atomic Energy Research Institute; ****Faculty of Sciences, Niigata University

The ^{129}Ba isotope is known to exist in the form of two isomers which decay by electron capture and positron emission to levels in ^{129}Cs with approximately the same half life of 2.1 h. Due to lack of effective techniques in separation of these isomers, the decay properties presented by the previous investigations[1,2] include various ambiguities: (1) level position and decay mode of g.s. and isomer; (2) gamma-ray energies and intensities from respective state, and beta branching to each level (log ft values).

In the present study, ^{129}Ba sources containing different composition of isomers were produced by three methods:

(a) ^{121}Sn (^{12}C,4n) ^{129}La (EC decay) ^{129g,m}Ba,

(b) ^{120}Sn (^{12}C,3n) ^{129g,m}Ba,

(c) ^{130}Ba (γ,n) ^{129g,m}Ba.

Gamma-ray spectra of samples (a) and (b) were measured with a 13% Ge(Li) spectrometer calibrated in the same conditions of energy per channel, distance between the source and detector, and positron absorbers. The decay characteristics of the spectra were followed to assign peaks to ^{129g,m}Ba and to obtain information necessary to establish the decay scheme. Gamma-ray spectrum corresponding to each state of isomers was obtained by mutual subtraction of the spectra taken with (a) and (b) sources by normalizing to the characteristic gamma-rays of ^{129g}Ba and ^{129m}Ba. Cascade relations of gamma rays were examined from gamma-gamma coincidence measurement using a pair of Ge detectors and an event-by-event recording system.

Tentative decay schemes of the isomeric and ground states from this study are presented in Fig. 1 (a)-(c), and Fig. 2 taking account of experimental data of ^{130}Ba(d,t) reaction[3], ^{129}La EC decay[4] and in-beam

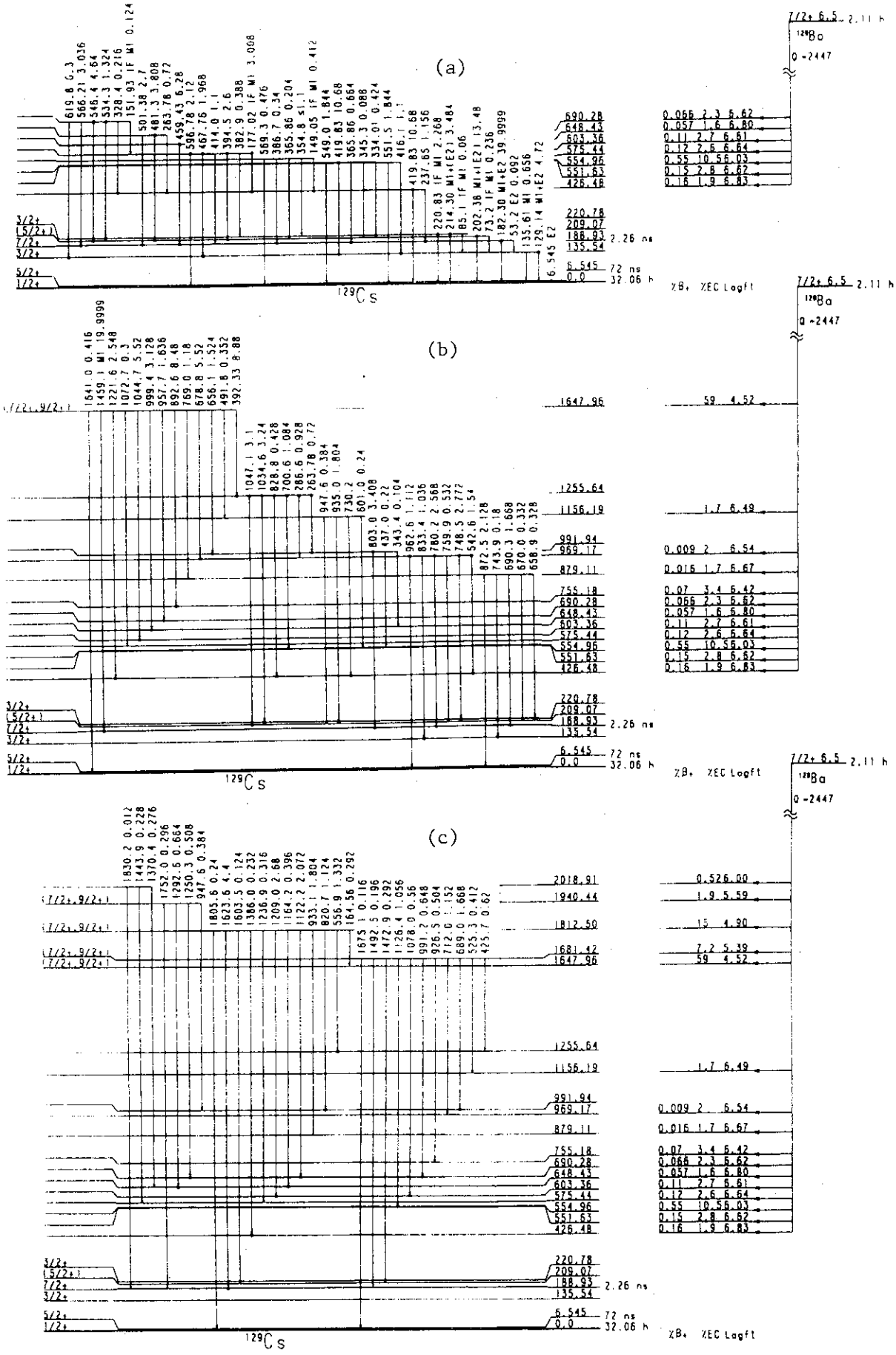

Fig. 1 Decay scheme of ^{129m}Ba

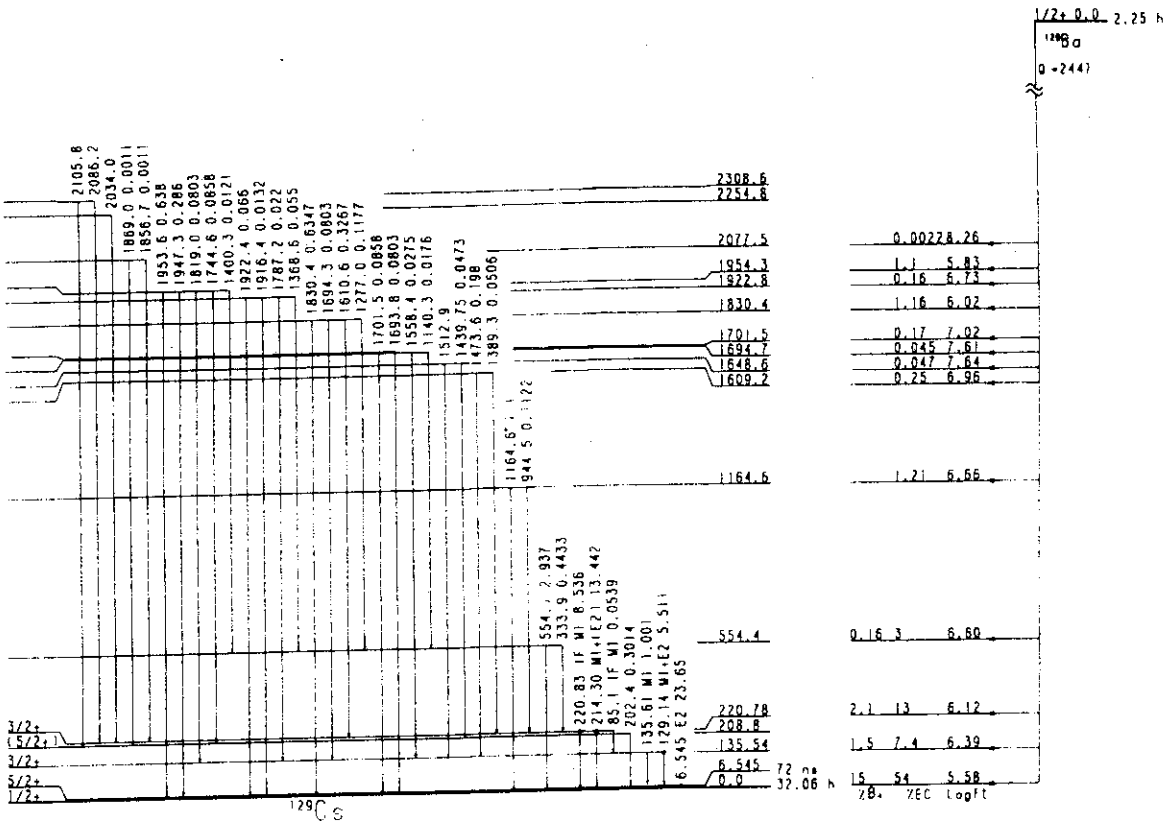

Fig. 2 Decay schme of ^{129g}Ba

gamma-ray spectroscopy on ^{129}Ba and ^{129}Cs (ref 5,6).

References

1) H. W. Taylor, B. Singh, F.S. Prato and J.D. King: Nucl. Phys. A179 (1972) 417

2) K. Ishii, T. Aoki and S. Kageyama: J. Phys. Soc. Japan 34 (1973) 285

3) R. D. Griffioen and R. K. Shline: Phys. Rev. C10 (1974) 624

4) P. Brodeur, B. P. Pathak and S. K. Mark: Z. Physik A289 (1979) 289

5) J. Chiba, R.S. Hayano, M. Sekimoto, H. Nakayama and K. Nakai: J. Phys. Soc. Japan 43 (1977) 1109

6) J. Gizon, A. Gizon and J. Meyer-ter-Vehn: Nucl. Phys. A277 (1977) 464

V NUCLEAR PHYSICS

5.1 Characteristics of a Large Hybrid Gas Counter for Use with the JAERI Magnetic Spectrograph for Heavy Ion Research

Eiko Takekoshi*, Yasuharu Sugiyama*, Hiroshi Ikezoe*, Yoshiaki Tomita*, Naomoto Shikazono*, Masayasu Sawada**, Shigeru Kubono***, Masahiko Tanaka***, Michiro Sugitani***, Seigo Kato**** and Teruo Suehiro*****.

*Department of Physics, Japan Atomic Energy Research Institute, **Institute of Physics, The University of Tsukuba, ***Institute for Nuclear Study, The University of Tokyo, ****Faculty of Science, Yamagata University, *****Division of Physics, Tohoku Institute of Technology.

A large hybrid gas counter has been constructed for use with the JAERI magnetic spectrograph for heavy ion research (ENMA)[1]. It consists of a gridded, split anode ionization chamber with three position sensitive wire proportional counters[2]. The effective values for length along the focal plane of the spectrograph, depth and height are 46 cm, 55 cm and 7 cm, respectively. The composition of the counter, the details of measurements and the characteristics of the counter with the spectrograph, which were obtained with a ^{241}Am-α source, were reported[3]. The position resolution obtained was typically 1 mm and also most of the effective length of 46 cm was in a good linearity. The characteristics of the counter, which were obtained with heavy ions, were reported[4]. Fig.1 shows a position spectrum measured with 100 MeV ^{12}C elastically scattered on ^{198}Au. The measured value of 70 keV FWHM was in good agreement with the value estimated from the contributions to finite energy resolution due to target and backing thickness and the JAERI spectrograph at 10^{o} with a beam emittance. Fig.2 shows ΔE and E spectra measured with 150 MeV Cl^{35} elastically scattered on ^{197}Au. The measured values of 580 keV and 1.6 MeV FWHM were consistent with the values estimated from the contributions of the electronic noise and straggling. Fig.3 shows a plot of ΔE.E versus $(B\rho)^2/E$ obtained by bombarding ^{12}C with 100 MeV ^{12}C and illustrates the excellent separation of the different masses and charge states of the isotopes with Z = 12 - 21. The large hybrid gas counter constructed for the focal plane detector of the JAERI spectrograph operates nicely in the precise measurements of the nuclear reactions with heavy ions.

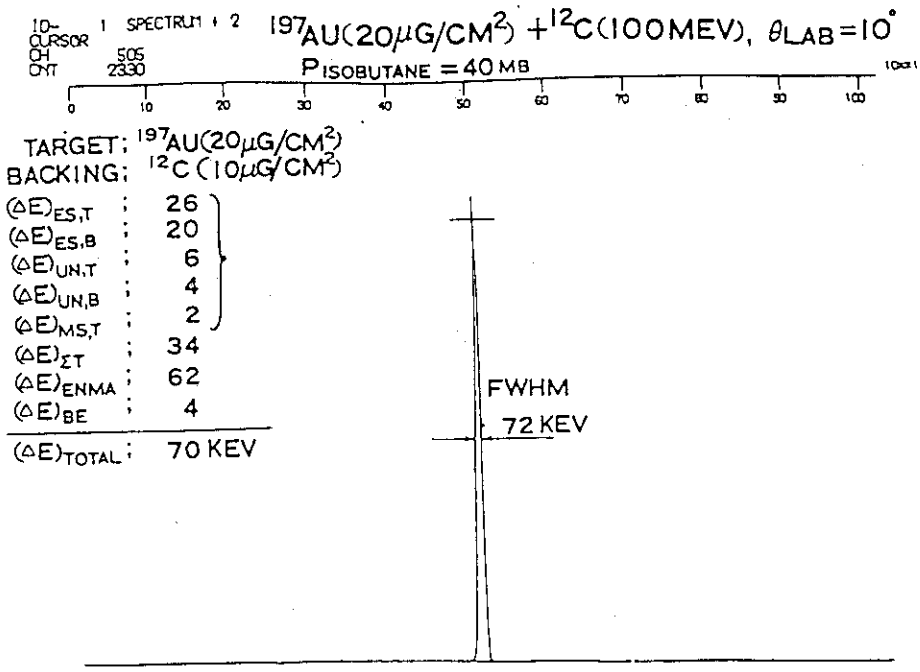

Fig.1 A position spectrum measured with 100 MeV ^{12}C elastically scattered on ^{197}Au.

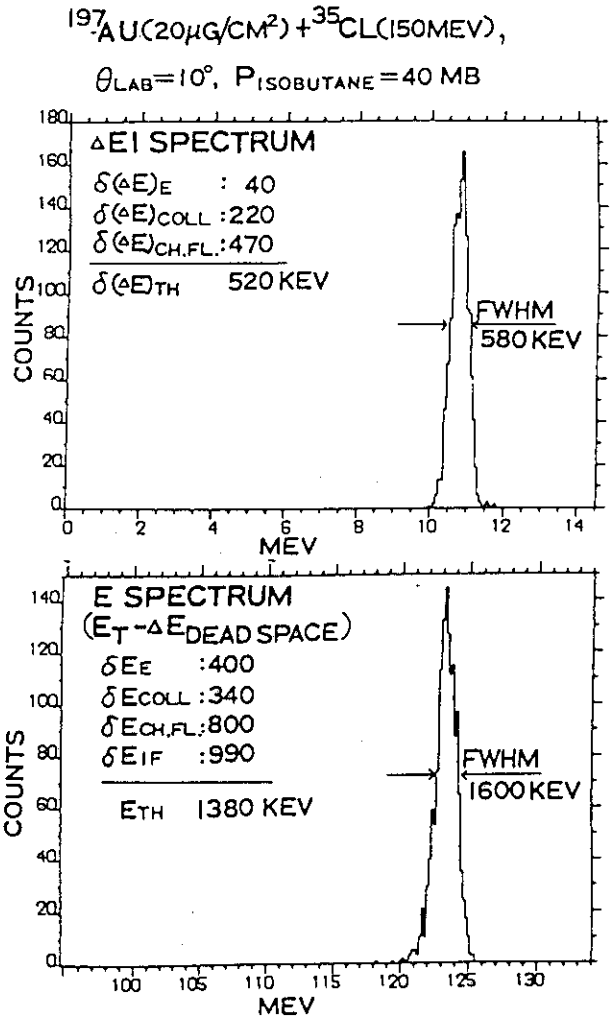

Fig.2 ΔE and E spectra measured with 150 MeV ^{35}Cl elastically scattered on ^{197}Au.

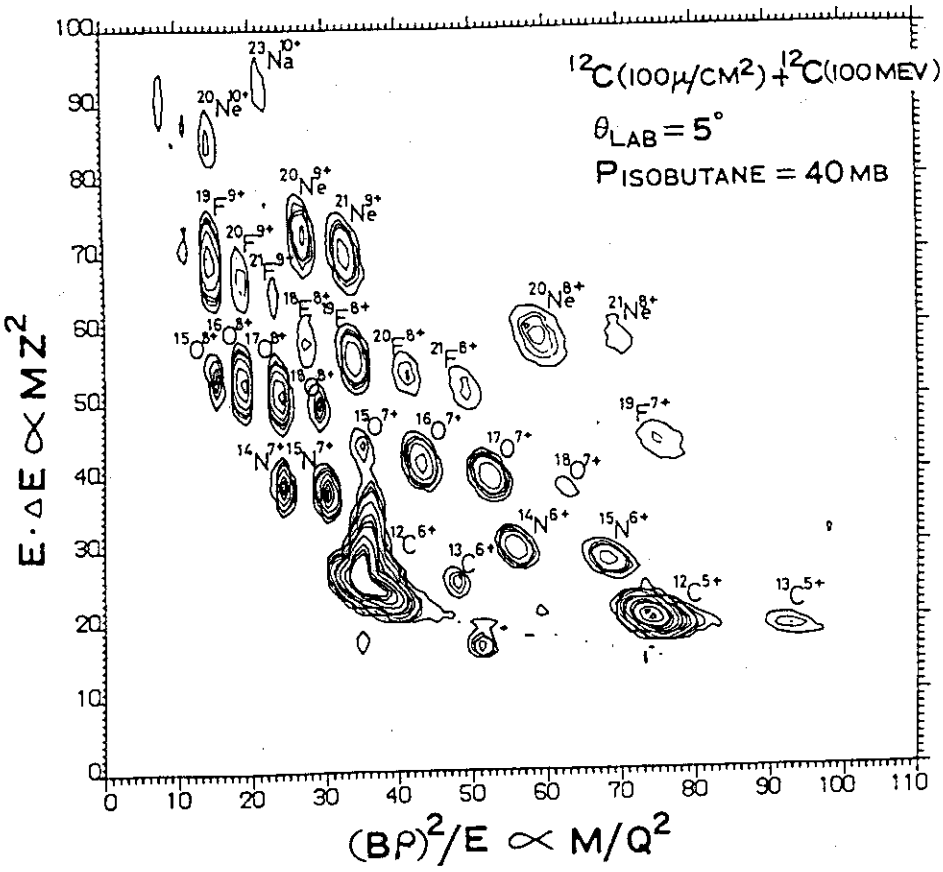

Fig.3 A plot of $\Delta E.E$ versus $(B\rho)^2/E$ obtained by bombarding ^{12}C with 100 MeV ^{12}C.

References

1). Y. Sugiyama, N. Shikazono, H. Ikezoe and H. Ikegami; Nucl. Instr. and Meth. 187 (1981) 25

2). D. Shapira, R. M. Devries, H. W. Furbright, J. Toke and M. R. Clover; Nucl. Instr. and Meth. 129 (1975) 123. J. R. Eraskine, T. H. Braid and J. C. Stoltzfus; Nucl. Instr. and Meth. 135 (1976) 67. T. R. Ophel and A. Johnson; Nucl. Instr. and Meth. 157 (1978) 461. D. Sharita, G. L. Bomar, J. L. C. Ford Jr., J. G. Gomez Del Campo and L. C. Dennis; Nucl. Instr. and Meth. 169 (1980) 77.

3). M. Sawada, Y. Sugiyama and E. Takekoshi; JAERI-M 83-014 (1983)

4). E. Takekoshi, Spring Meeting of Japan Physical Society in Tokyo, March 28, 1983. M. Sawada, Y. Sugiyama, E. Takekoshi, H. Ikezoe, Y. Tomita and N. Shikazono; Spring Meeting of Japan Physical Society in Tokyo, March 29, 1983.

5.2 JAERI Magnetic Spectrograph "ENMA" for Heavy Ion Research

Yasuharu Sugiyama*, Eiko Takekoshi*, Yoshiaki Tomita*, Hiroshi Ikezoe*, Naomoto Shikazono*, Masayasu Sawada**, Shigeru Kubono***, Masahiko Tanaka***, Michiro Sugitani***, Seigo Kato**** and Teruo Suehiro*****

*Department of Physics, Japan Atomic Energy Research Institute, **Institute of Physics, University of Tsukuba, ***Institute for Nuclear Study, University of Tokyo, ****Faculty of Science, Yamagata University, *****Division of Physics, Tohoku Institute of Technology.

A new magnetic spectrograph, named ENMA, was constructed for heavy ion reaction studies[1-3]. The spectrograph ENMA was required to have the following characteristic features.

1) A momentum resolving power $p/\Delta p$ of 7400, which is suitable for high resolution work with heavy ions, is obtainable for acceptance solid angles up to 16 msr.
2) A kinematic momentum shift k ($=dp/d\theta/p$) can be compensated from k=-0.7 to 1.0.
3) In order to obtain unique mass identification over a wide mass range in combination with the time-of-flight measurement, a path length difference ΔL is kept small.

For these requirements, extensive design studies were carried out and a separated-element-spectrograph with a QMDMDM configuration was adopted[1]. Magnetic field measurements for two dipoles, one quadrupole and three multipoles were performed and almost perfect field distributions were obtained in accordance with the design work[2].

Since the fall of the year 1981, the spectrograph ENMA has been put into operation. The solid angle of ENMA is usually set at 2.4~3.6 msr. We describe here a case of ^{12}C induced reactions as a typical example. The ^{12}C beam with an energy of 100 MeV was focused on the target in a spot of 1~2 mm in width. The overall energy resolution obtained for the elastic scattering by using a ^{12}C target of 100 $\mu g/cm^2$ is shown as a function of a kinematic momentum shift k in Fig.1. The measured values (filled circles) were in good agreements with the ones(solid line) estimated from the contributions to finite energy resolution due to the target effect (TE), the beam emittance (BE) and the JAERI spectrograph (ENMA). It is seen that the

kinematic momentum shift is compensated well in the spectrograph ENMA. Fig.2 shows a spectrum of the inelastically scattered ^{12}C for the Q-value of -4.44 MeV. The kinematic broadening (ΔE=1.96 MeV) due to the large horizontal acceptance angle is compensated well and the line shape broadened by γ emission in flight is clearly observed in addition to the sharp peak. From this spectrum it is possible to determine the spin alignment of $^{12}C_{2^+}$ (4.44 MeV) in the inelastic scattering precisely.

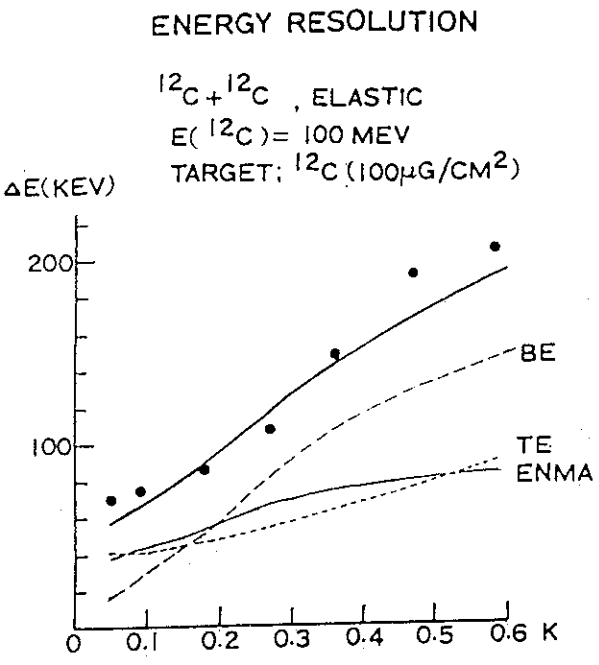

Fig.1 Energy resolution obtained for the elastic scattering of ^{12}C (100MeV) by ^{12}C(100 μg/cm^2) as a function of a kinematic shift k

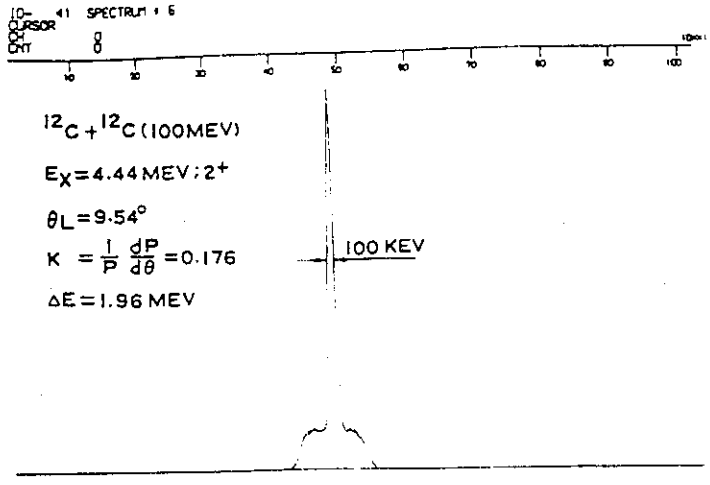

Fig.2 A spectrum of the inelastically scattered ^{12}C by ^{12}C(100 μg/cm^2) for the Q-value of -4.44 MeV.

References

1) Y.Sugiyama, N.Shikazono, H.Ikezoe and H.Ikegami; Nucl. Instr. and Meth. 187 (1981) 25.

2) Y.Sugiyama, N.Shikazono, T.Sato, T.Takayama and H.Ikegami; JAERI-M 9358 (1981). Y.Sugiyama, N.Shikazono, T.Sato and H.Ikegami; Nucl. Instr. and Meth. (1983) in press.

3) M.Sawada, Y.Sugiyama and E.Takekoshi; JAERI-M 83-014 (1983).

5.3 Elastic and Inelastic Scattering of $^{12}C + ^{12}C$ and $^{58}Ni + ^{60}Ni$

Yasuharu Sugiyama*, Naomoto Shikazono*, Yoshiaki Tomita*, Eiko Takekoshi*, Masayasu Sawada**, Shigeru Kubono***, Masahiko Tanaka***, Michiro Sugitani***, Seigo Kato**** and Teruo Suehiro*****

*Department of Physics, Japan Atomic Energy Research Institute, **Institute of Physics, University of Tsukuba, ***Institute for Nuclear Study, University of Tokyo, ****Faculty of Science, Yamagata University, *****Division of Physics, Tohoku Institute of Technology.

A large kinematic energy shift due to the center of mass motion in heavy ion reaction is one of the important factors limiting an energy resolution. The JAERI magnetic spectrograph "ENMA" constructed for heavy ion reaction studies is able to compensate for the kinematic shift of k=1[1]. Therefore the spectrograph ENMA is very powerful for high resolution works with heavy ions. In the Ni induced fusion reactions, large differences between $^{58}Ni+^{58}Ni$, $^{58}Ni+^{64}Ni$ and $^{64}Ni+^{64}Ni$ excitation functions were observed in the barrier region[2]. In JAERI, systematic studies on the elastic and inelastic scattering of ^{58}Ni by ^{58}Ni, ^{60}Ni, ^{62}Ni and ^{64}Ni are scheduled and preliminary results were obtained for the $^{58}Ni+^{60}Ni$ system at ^{58}Ni energy of 238MeV. One of the spectra is shown in Fig. 1. The energy resolution obtained was limited mainly by target effects, but the elastic and inelastic peaks were clearly resolved. The angular distributions of the eastic and inelastic scattering were measured from $\theta_{C.M.}$=20° to 110°. As results, an effect of Coulomb excitatin seems to be prominent at forward angles. Near the grazing angle, the cross sections are seem to be enhanced compared to the optical-model calculations.

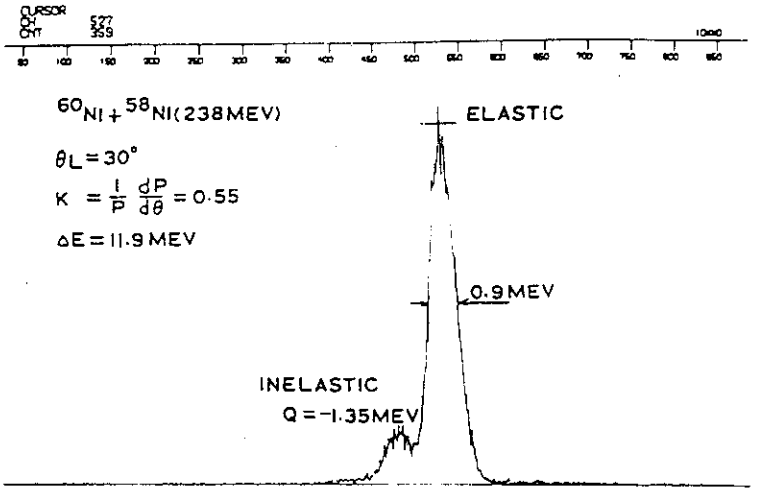

Fig.1 A spectrum of the elastic and inelastic scattering of ^{58}Ni (E_1=238 MeV) by ^{60}Ni.

In the $^{12}C + ^{12}C$ system, the line shape of the first excited state broadened by γ emission in flight was clearly observed. Fig.2 shows one of spectra of inelastically scattered ^{12}C for an incident energy of 100 MeV. The mutual excitation of the first excited state of the target and projectile (Q=-8.88 MeV) was resolved clearly from the single excitation of the 3^- state (Q=-9.64 MeV). The broadened line shapes of the mutual and single excitation of the first excited state were also measured for incident energies of 60MeV and 62.6 MeV, where a resonance occured in elastic and inelastic scatterings.

The spin alignment of the first 2^+ state in the inelastic scattering can be deduced from these line shapes. These results will provide important imformation concerning the reaction mechanisms in the $^{12}C + ^{12}C$ system.

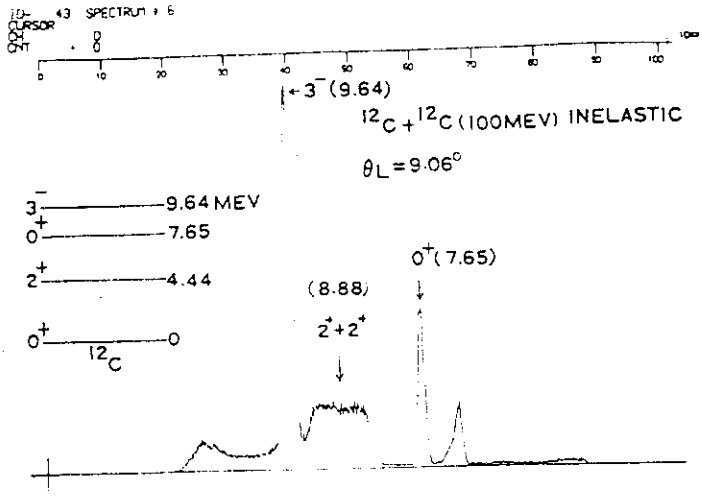

Fig.2 A spectrum of inelastically scattered ^{12}C by ^{12}C at E =100 MeV.

References

1) Y.Sugiyama, N.Shikazono,H.Ikezoe and H.Ikegami; Nucl. Instr. and Meth. 187 (1981) 25. Y.Sugiyama, N.Shikazono, T.Sato and H.Ikegami; Nucl. Instr. and Meth. (1983) in press. Y.Sugiyama et al.; contribution to this report.

2) M.Beckerman, M.Salomaa, A.Sperduto, J.D.Molitoris and A.Dirienzo; Phys. Rev. C25 (1982) 837.

5.4 Fusion and Deep Inelastic Reactions for $^{37}Cl + ^{27}Al$ and $^{16}O + ^{48}Ti$ in the Energy Region of 100 to 200 MeV

K. Ideno,* Y. Tomita,* S. Takeuchi,* S. Hanashima,*
W. Yokota,** S. M. Lee,** Y. Nagashima,** T. Nakagawa,**
Y. Fukuchi,** S. Kinouchi,** T. Komatsubara,** T. Mikumo,** and
W. Galster***

*Department of Physics, Japan Atomic Energy Research Institute,
**Tandem Accelerator Center, University of Tsukuba, and
***Hahn- Meitner Institute

With increasing energy of heavy ions for the system A = 40 - 80, large mass and energy transfer reactions begin to appear among the overwhelming fusion reaction. It is interesting to study the energy dependence of these reactions, for example, the deep inelastic reaction at an embryonic stage when its individuality is not fully developed.

Using the JAERI tandem accelerator, with two counter telescopes consisting of ΔE (ion chamber) and E (Si), we measured fusion evaporation residues at $\theta_{lab} \geq 2^\circ$ and deep inelastic fragments at $\theta_{lab} = 15^\circ - 50^\circ$ for $^{37}Cl + ^{27}Al$ and $\theta_{lab} = 11^\circ - 74^\circ$ for $^{16}O + ^{48}Ti$; both the systems have a common compound nucleus ^{64}Zn.

$^{37}Cl + ^{27}Al$: A natural Al target of 200 μg/cm^2 was used. We measured the fusion evaporation cross section at 140, 152, 162, 180 and 200 MeV (Fig. 1). The σ_{FE} values in this energy region are about 1000 mb, and the fusion reaction still dominates other reactions. Angular distributions at backward angles were measured for fragments with Z = 7 to 25 at 162, 180 and 200 MeV. In investigating the average behavior of these fragments, we assumed a binary process.[1,2] Mass division was made according to the highest Q_{gg} values. Fig. 2 shows the angular distributions for the corresponding counter parts at forward and backward angles at 200 MeV; both angular distributions fit smoothly at crossing points.

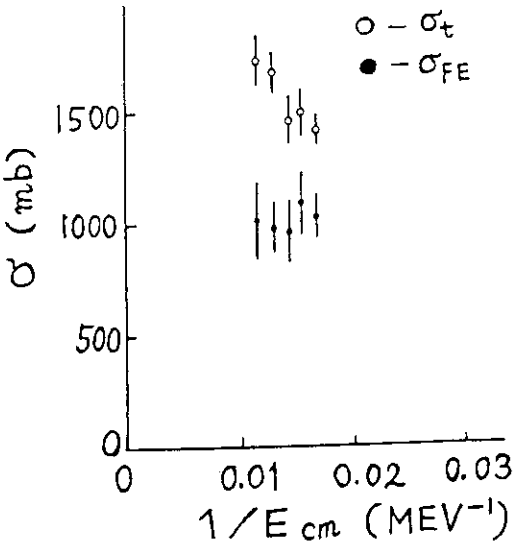

Fig. 1

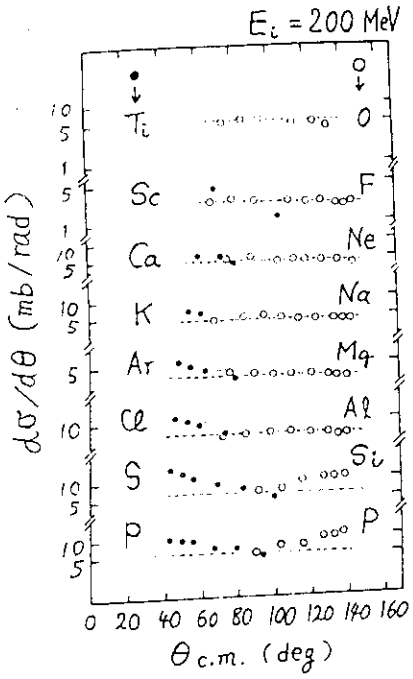

Fig. 2

It is seen that the angular distributions at backward angles follow the $1/\sin\Theta$ behavior. The most probable total kinetic energies TKE^m of the fragments for 162 to 200 MeV beams are found also to be constant at backward angles. These constant components reflect the long-time rotating composite system; they comprise 3, 9 and 11% of the fusion evaporation cross sections at 162, 180 and 200 MeV respectively. We plot these components of the TKE^m in Fig. 3, where the dependences of the TKE^m on projectile-like Z are well represented by a single solid curve caluculated from the Coulomb repulsion of two touching charges with a distance $R = 1.2 \times (A_1^{1/3} + A_2^{1/3})$ fm. Here we made no correction for light particle emission from the fragments. Analyses are still in progress for this system.

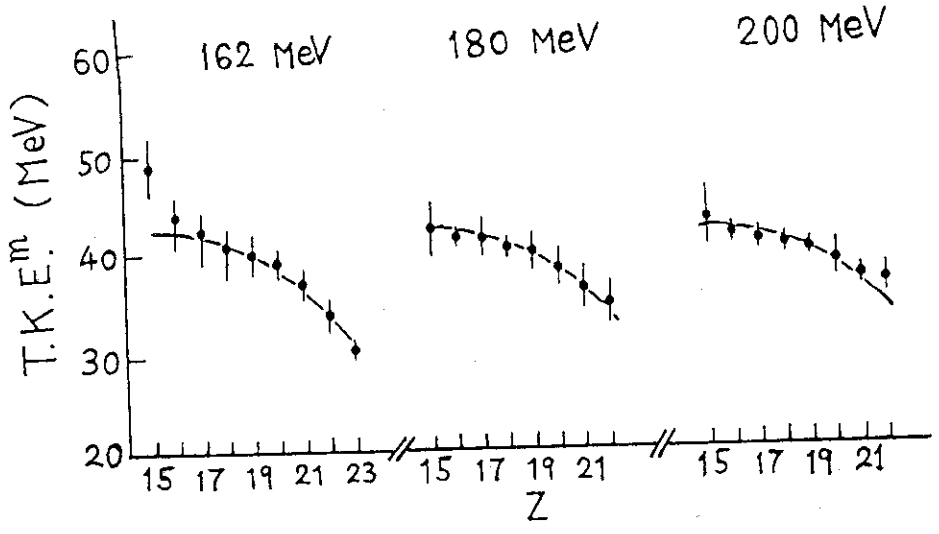

Fig. 3

$^{16}O + ^{48}Ti$: At 118 MeV we made measurements for a 99% enriched ^{48}Ti target. Preliminary analyses of the deep inelastic fragments show a similar behavior as in the $^{37}Cl + ^{27}Al$ system, but the difference lies in that we have a very large yield for carbon fragment. Further measurements in the extended energy region are planned.

1) T. M. Cormier et al., Phys. Rev. C14 (1976) 334.

2) P. Braun-Munzinger et al., Phys. Rev. Lett. 36 (1976) 849.

5.5 E0 Transition in 74-Se Isotope

Akiyasu MAKISHIMA[**], Mitsuhiko ISHII[*], Masumi OHSHIMA[*],
Hiroshi TAKETANI[**] and Minoru ADACHI[**]

[*] Department of Physics, Japan Atomic Energy Research Institute,
[**] Faculty of Science, Tokyo Institute of Technology.

We observed an E0 transition in 74-Se isotope by the use of an " lifetime filter " [1] and deduced its ρ value.

The lifetime filter is illustrated in Fig. 1. It consists of the target and a turntable with three Ta foils of 6 mg/cm^2 separated from one another by a rotation of 120°. Recoiling 74-Br atoms and others produced by bombardment of 46-Ti with a 150 MeV beam of 35-Cl were collected on one of the foils for a collection time. Then the radioactivity on the foil was analyzed in succession by two gamma-ray detectors to determine the decay rate of individual gamma-rays. A Si(Li) detector combined with a magnetic filter [2] was placed in the other side of the gamma-ray detector used for the initial counting of the radioactivities. The lifetime filter acts like a bandpass filter composed of high-pass and low-pass filters, and permits a preferential observation of some radioactivities with a mean lifetime as long as a prescribed collection time. In order to intensify the decay of 74-Br (half-life: 41 min), we chose a collection time of 4200 sec which was the sum of a counting period of 4000 sec and a pause of 200 sec.

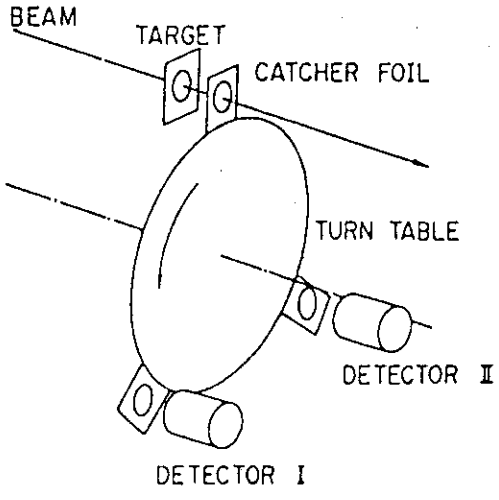

Fig. 1 A schematic drawing of the lifetime filter.

An internal conversion electron spectrum obtained is showned in Fig. 2. The 841 keV and 206 keV lines correspond to the transitions ($0_2^+ \rightarrow 0_1^+$) and ($0_2^+ \rightarrow 2_1^+$) of 74-Se isotope, respectively. From the branching ratio of these transitions together with the lifetime of the 0_2^+ state measured by R. M. Ronningen et al. [3], we deduced $\rho = (1.6 \pm 0.2) \times 10^{-1}$.

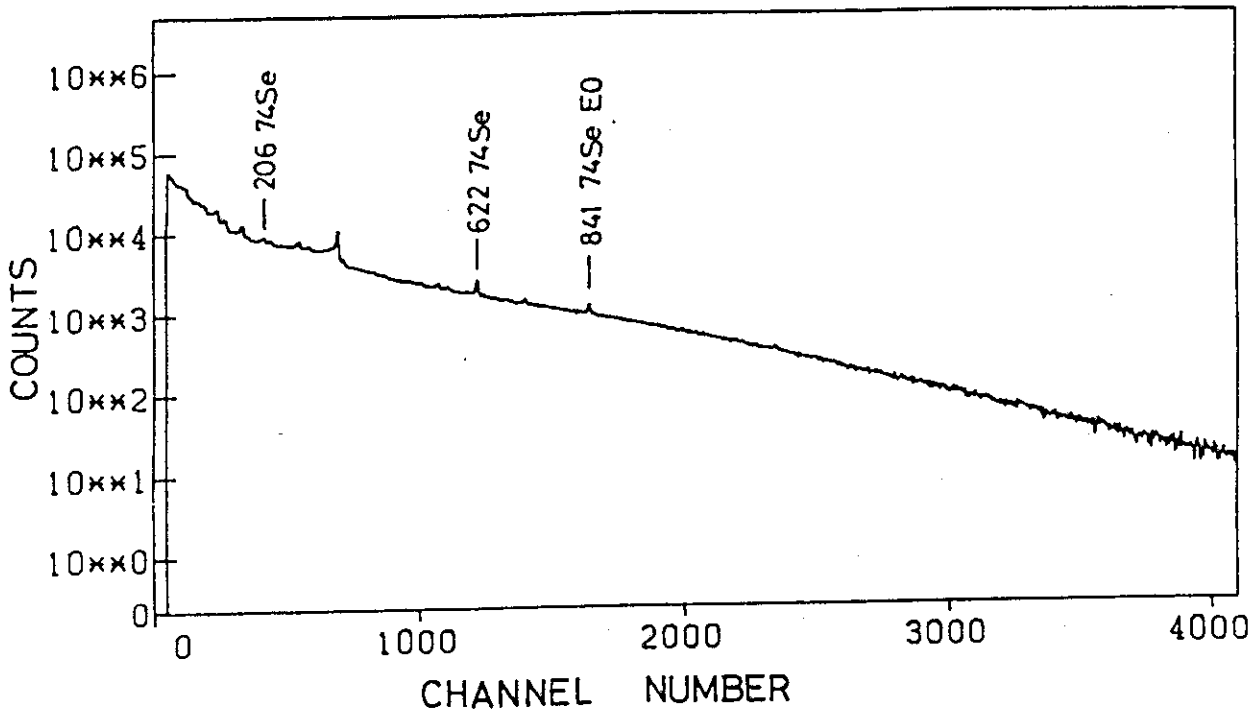

Fig. 2 Internal conversion electron spectrum observed in the time sequence of 4000 sec / 200 sec.

References

[1] A. Makishima et al., A Rotary Bandpass Filter for Lifetime Measurement of Reaction Products Induced by Heavy Ions, JAERI-M 9901 (1981), in Japanese.

[2] M. Ishii, Nucl. Instr. Meth. 127 (1975) 53.

[3] R. M. Ronningen et al., Nucl. Phys. A261 (1976) 439.

5.6 In-Beam Gamma-Ray Spectroscopy of Fusion Residues Induced by Heavy Projectiles

Mitsuhiko ISHII*, Akiyasu MAKISHIMA**, Naoki YAMADA**, Hiroshi TAKETANI** and Minoru ADACHI**

* Department of Physics, Japan Atomic Energy Research Institute,
** Faculty of Science, Tokyo Institute of Technology.

Fusion reactions induced by heavy projectiles excite the nucleus in a high spin state. So they give promise of becoming a powerful probe in the field of in-beam gamma-ray spectroscopy. However they yield much more nuclear species than those induced by light ions such as alpha-particles, 12-C and 16-O. This fact makes it difficult to identify nuclear species emitting individual gamma-rays and obscures the coincidences between gamma-rays.

We have overcome this difficulty by means of intensifying the reaction channels with a " Charged Particle Multiplicity " selector. We constructed a prototype of CPM selector shown in Fig. 1. It consists of six Si detectors placed on the faces of a half of a dodecahedron, one of which is of the annular type. They have the same diameter and thickness of 44 mm and 0.5 mm, respectively. Each one acts as a ΔE counter which discriminates between alpha-particles and protons. Information about the CPM fed from these detectors is coded into a 12 bit signal and is registered event-by-event on tape together with information about other observable quantities such as the gamma-ray energy and the lifetime.

We employed the CPM selector to study the fusion residues produced by bombarding 59-Co with a 150 MeV beam of 35-Cl. By sorting the raw data obtained, we reduced gamma-ray spectra gated with reaction channels of p, α, 2α, 2p and 3p. Combined with computational results of the ALICE, these permit us to identify isotopes emitting individual gamma-rays within an uncertainty of neutron number $N \lesssim 3$.

Furthermore the CPM selector made it feasible to search for the yrast isomer. In fact we observed yrast isomers in 90-Mo, 89-Nb and 88-Zr. Their half lifetimes were determined to be 0.80 ± 0.08 μs, 13 ± 1 ns and longer than 1 μs, respectively. As for 86-Zr, 87-Zr and 85-Y the lifetimes of their isomers are shorter than 5 ns.

In order to study high spin states of Zr isotopes in details, we

observed gamma-gamma coincidences with an annular detector which subtended $\pi/2$ steragian toward the target and intensified α-emitting channels. A preliminary analysis showed that the heavy-ion induced fusion strongly feeds yrast states at least up to 10^+ states for even Zr isotopes and $27/2^+$ for 87-Zr, and several candidates were found for transitions from higher spin states.

We are constructing a new version of CPM selector composed of ten pieces of Si detectors. It covers almost whole solid angle and is so compact as to allow the gamma-gamma coincidence measurement.

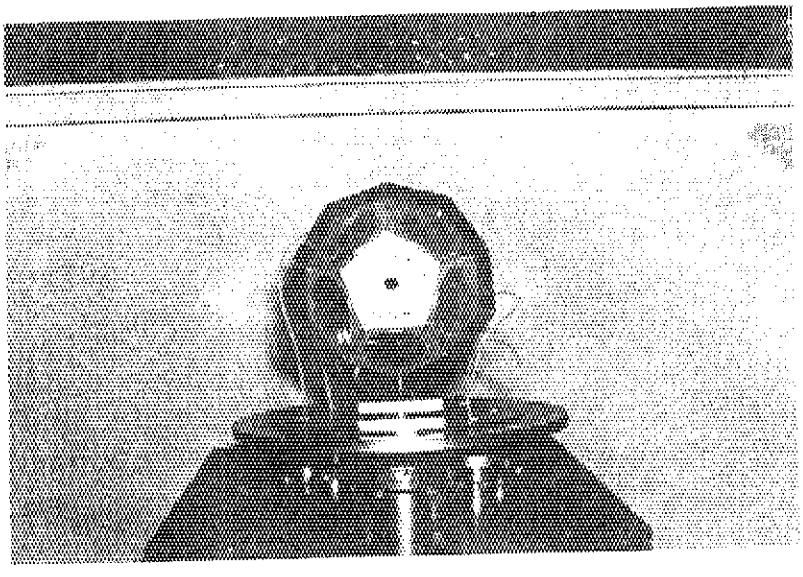

Fig. 1 Charged particle multiplicity selector

5.7 The Ground-State Rotational Band in ^{167}Er

M.Ohshima*, E.Minehara*, M.Ishii*, T.Inamura** and A.Hashizume**

* Department of Physics, Japan Atomic Energy Research Institute,

** The Institute of Physical and Chemical Research

It is well known that high-j orbits such as $i_{13/2}$ give rise to large perturbation to rotational levels of deformed nuclei. Odd-mass nuclei whose ground-state rotational bands are built on such a high-j orbit would provide important information about the perturbation effect. In order to investigate this effect on transition moments as well as level energies, we performed a multiple-Coulomb-excitation experiment on ^{167}Er, one of the typical deformed odd-mass nuclei with the ground-state rotational band built on the $i_{13/2}$-neutron orbit.

The high spin states were populated by multiple Coulomb excitation using 160-MeV ^{35}Cl ion beams from the tandem accelerator. On the basis of γ-γ coincidences and γ-ray angular distributions, a level scheme for the ground-state rotational band was established as shown in fig. 1. The levels higher than the $17/2^+$ member were newly assigned. Because there are crossover E2 transitions decaying from the $11/2^+$ to $23/2^+$ levels, ratios of experimental A2 values to calculated ones for complete alignment give nuclear alignment attenuation factors for individual levels. The attenuation factors thus obtained were used to extract multipole mixing ratios, E2/M1, in the analysis of γ-ray angular distribution and γ-γ angular distribution for stopover

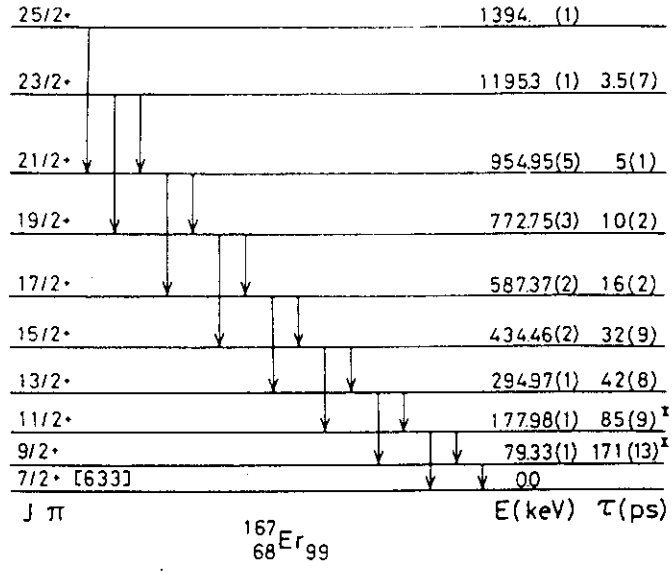

Fig.1 Level scheme of the ground-state rotational band in ^{167}Er. The values denoted by asterisk are from ref. 2.

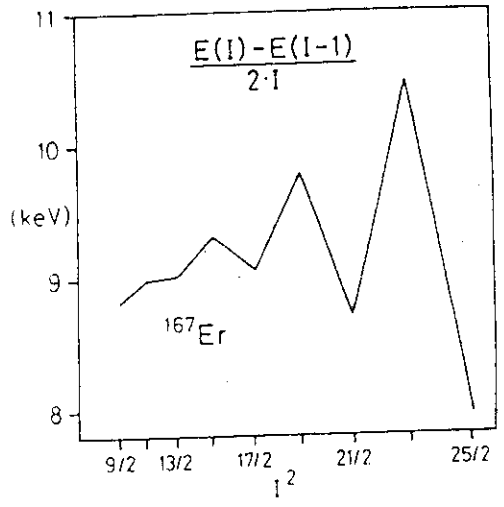

Fig.2 Energy differences of the ground-state rotational band in ^{167}Er.

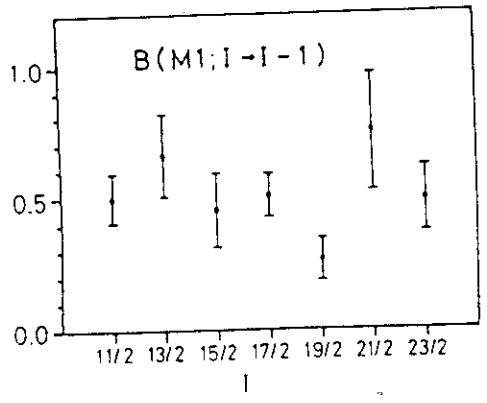

Fig.3 B(M1;I-I-1) values of ^{167}Er in units of rigid rotor values ($g_K - g_R$ = -0.57).

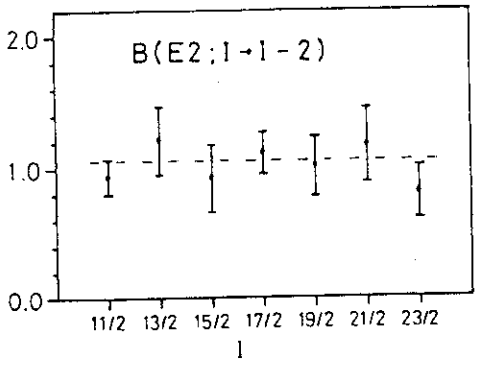

Fig.4 B(E2;I-I-2) values of ^{167}Er in units of rigid rotor values (Q_0 = 7.6 b).

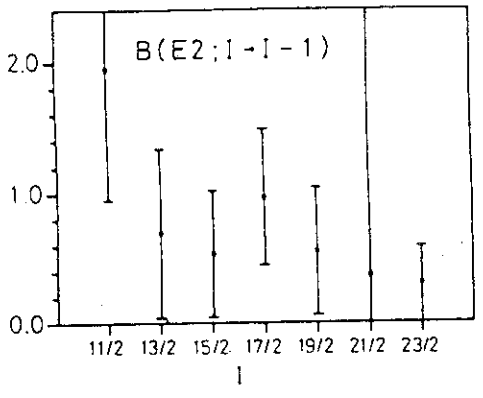

Fig.5 B(E2;I-I-1) values of ^{167}Er in units of rigid rotor values (Q_0 = 7.6 b).

transitions. Nuclear lifetimes were obtained model-independently by Doppler broadened γ-ray lineshape analysis. A γ-ray singles spectrum used for the analysis was taken with a Compton suppression spectrometer placed at 0 degree to the beam. The detailed formulation of the analysis is described in ref. 1. The results are shown at the right side of fig. 1.

Energy differences, B(M1) and B(E2) values for the ground-state

rotational band are shown in figs. 2 to 5. The rigid-rotor values in the figures are obtained by adopting g-factors[3] of $g_K = -0.39$ and $g_R = 0.18$ and an intrinsic quadrupole moment of $Q_0 = 7.6$ b. Relatively large signature dependence was observed for energy differences and B(M1) values.[4] This may be ascribed to rotational perturbation effect due to Coriolis force, which acts strongly on rotational bands based on high spin single particle orbit. The ground state of ^{167}Er is $7/2^+[633]$ Nilsson state which originates from $i_{13/2}$ neutron orbit and recent theoretical investigations predict qualitatively the same tendency for bands based on this orbit.[5,6]

References

1) T.Inamura, F.Kearns and J.C.Lisle, Nucl. Inst. Meth. 123 (1975) 529.
2) B.Harmatz, Nucl. Data Sheets 17 (1976) 143.
3) A.Bohr and B.R.Mottelson, Nuclear Structure Vol.2 (W.A.Benjamin, inc.,1975) p303.
4) M.Ohshima et al., submitted to J. Phys. Soc. Japan(1983).
5) I.Hamamoto, Phys. Lett. 102B (1981) 225.
6) E.R.Marshalek, Phys. Rev. C26 (1982) 1678.

5.8 The Ground-State Rotational Band in ^{163}Dy

M.Ohshima*, E.Minehara*, S.Kikuchi*,
T.Inamura**, A.Hashizume** and H.Kumahora***

* Department of Physics, Japan Atomic Energy Research Institute,
** The Institute of Physical and Chemical Research, *** Department of Physics, Hiroshima University

So far many experiments on multiple Coulomb excitation were performed to investigate the ground-state rotational bands of deformed nuclei. Using heavy-ion beams now available, high-spin states can be excited and transition probabilities have been extracted up to high spin. However, these studies have been rather confined to even-even nuclei and relatively few studies of odd-A nuclei have been carried out. In the present study we have performed an experiment to study the ground-state rotational bands in ^{163}Dy nuclei, which is a typical deformed nucleus with odd neutrons.

The high spin states were populated by multiple Coulomb excitation using 160-MeV ^{35}Cl and 250-MeV ^{58}Ni ion beams from the tandem accelerator. On the basis of γ-γ coincidences and γ-ray angular distributions, a level scheme for the ground-state rotational band was established as shown in fig. 1. The levels higher than the $17/2^-$ member were newly assigned. Nuclear lifetimes were obtained model-independently by Doppler broadened γ-ray lineshape analysis. A γ-ray singles spectrum used for the analysis was taken with a Compton suppression spectrometer placed at 0 degree to the beam. The detailed

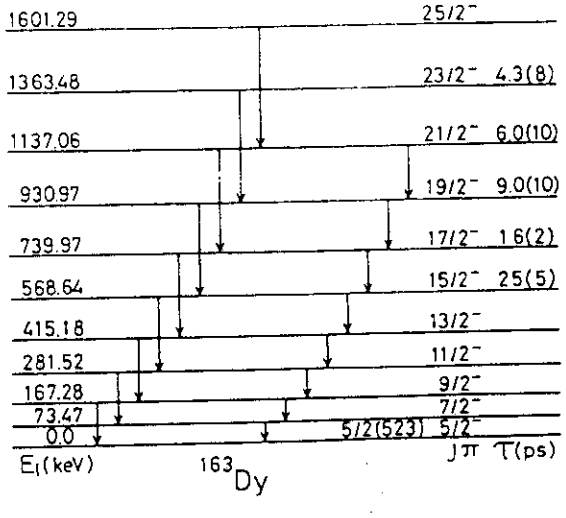

Fig.1 Level scheme of the ground-state rotational band in ^{163}Dy.

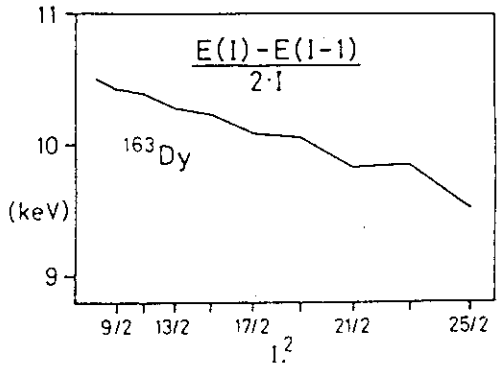

Fig.2 Energy differences of the ground-state rotational band in ^{163}Dy.

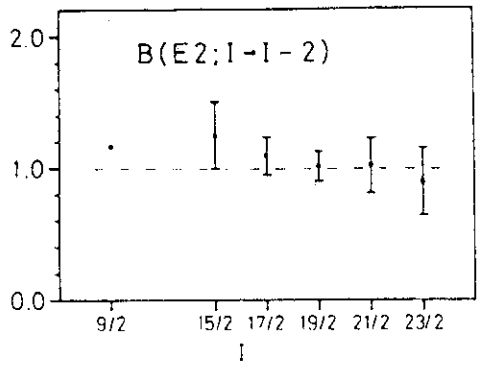

Fig.3 B(E2;I-I-2) values of ^{163}Dy in units of rigid rotor values (Q_0 = 6.8 b). The value denoted by asterisk is from ref. 3.

formulation of the analysis is described in ref. 1. The results are shown at the right of fig. 1.

Energy differences and B(E2) values for the ground-state rotational band are shown in figs. 2 and 3. The ground state of ^{163}Dy is $5/2^-$[523] Nilsson state which originates from the $f_{7/2}$ neutron orbit. Signature dependence of energy differences have turned out to be small for this band. The B(E2) values are close to the predictions of the Bohr-Mottelsson model,[2] when an intrinsic quadrupole moment of Q_0 = 6.8 b was adopted as shown in fig. 3. It would be interesting to compare the present results with the ones for ^{167}Er,[4] where signature dependence is relatively large especially for energy differences and B(M1) values. This may be ascribed to the rotational perturbation effect as suggested in ref. 3. The present results for energy differences and B(E2) values show that the rotational perturbation effect is small for this band. Further analysis for stopover transitions of ^{163}Dy is now in progress.

References

1) T.Inamura, F.Kearns and J.C.Lisle, Nucl. Inst. Meth. 123 (1975) 529.
2) A.Bohr and B.R.Mottelson, Nuclear Structure Vol.2 (W.A.Benjamin, inc.,1975).
3) J.M.Dairiki,E.Browne and V.S.Shirley, Nucl. Data Sheets 29 (1980) 653.
4) M.Ohshima et al., submitted to J. Phys. Soc. Japan(1983).

5.9 Derivation of the IBM quadrupole operator for deformed nuclei based on the "independent-pair" aspect of condensed pairs

Takaharu Otsuka

Department of Physics, Japan Atomic Energy Research Institute

It is shown that the S- and D-pairs[1] carry dominant fractions of the intrinsic quadrupole moment of the deformed nucleus, by utilizing the "independent-pair" aspect in N-condensed-pair matrix elements. A new fermion-boson mapping method is proposed based on this "independent-pair" aspect. The IBM quadrupole operator is calculated microscopically in a good agreement with phenomenological fitting.

References

1) T. Otsuka, A. Arima and N. Yoshinaga, Phys. Rev. Lett. 48, 387 (1982).

5.10 Mechanism of Cluster Emission in Nucleon-Induced Preequilibrium Reaction

Akira Iwamoto and Kichinosuke Harada
Department of Physics, Japan Atomic Energy Research Institute

A model[1] is proposed for the preequilibrium emission of light composite particles (d,t,^{3}He,α) in the nucleon-induced induced reaction of several tens of Mev energy based on the exciton model. The model contains two new points: One is the calculation of the formation factor $F_{l,m}(\epsilon)$ which stands for the probability that the composite particle of an energy ϵ is composed of l particle above the Fermi level and m particles below. Another new point is the inclusion of the pickup-type contribution in the particle emission mechanism. We allow some nucleons which constitute the complex particle to come from levels below the Fermi energy. For the calculation of $F_{l,m}(\epsilon)$, we assume a harmonic oscillator type intrinsic wave function for light composite particle and approximate it later by the Fermi gas model. The direct calculation of $F_{l,m}$ by the shell model is performed in Ref.2 and the result is very similar to the present one.

This model is applied to six kinds of (p,ϵ) reactions on ^{54}Fe, ^{118}Sn and ^{120}Sn targets. Calculated results reproduce nicely the high energy part of the experimental energy spectra , both the strength and the shape. In the figure, we show an example of ^{54}Fe(p,p') and (p,ϵ) energy spectra of incident energy 62 MeV. As is shown, the calculated spectra(solid line) reproduce well the experimental data(dashes). Largest part of the cross section comes from the $F_{1,3}$ type (three particle pickup) from 2p-1h state, but two particle pickup also contributes substantially. This holds common to all the system examined and we can say that the energy spectra of composite particle come from the pick-up reaction during the cascade process.

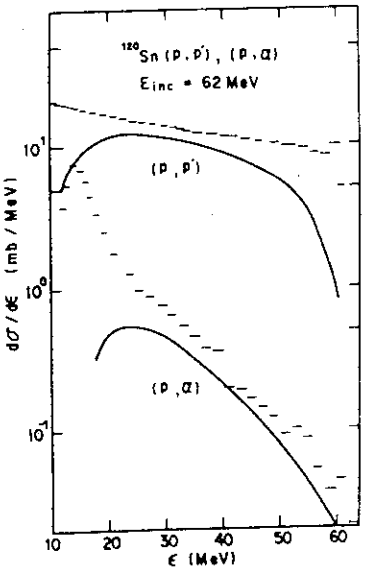

References 1) A.Iwamoto and K.Harada:
Phys.Rev.C26 (1982) 1821.
2) I.Tonozuka, A.Iwamoto and
K.Harada: JAERI-M 83-057 (1983)

5.11 Energy Spectra of Light Composite Particle

Kenichi Sato*, Akira Iwamoto** and Kichinosuke Harada**

* Division of Physics, Tohoku College of Pharmacy

** Department of Physics, Japan Atomic Energy Research Institute

A.I. and K.H. have recently developed the exciton model for the emission of light composite particle so as to include the effect of the intrinsic structure of the emitted particles and succeeded nicely in reproducing the high energy part of the experimental energy spectra of (p,α) reactions. In order to see whether the model works well not only for α but also for d,t,^{3}He emission reactions, we calculate the formation factors of the d,t,^{3}He in the same way as Ref.1 and calculate those energy spectra.[2] The values of parameters are fixed to the one used in Ref.1 for all the systems examined. The numerical calculation have been performed for the proton incident reactions with several tens of MeV on targets ^{27}Al, ^{54}Fe, ^{58}Ni, ^{89}Y, ^{120}Sn and ^{197}Au. In the figure, we show the results for d,t,^{3}He spectra from the reactions on ^{197}Au with E_p=62 MeV. Solid curves are our calculated results and short bars are the experimental data. From this figure and from other calculations, we see that the data are well reproduced by our calculation for almost all reaction systems except for the very high energy part of deuteron, where the one-step direct reaction is thought to play the dominant role. This suggests that the pre-equilibrium energy spectra of light composite particles (d,t,^{3}He,α) can be understood from our model, that is, the main part of the cross section comes from pick-up type reactions which occur in the course of equilibration process.

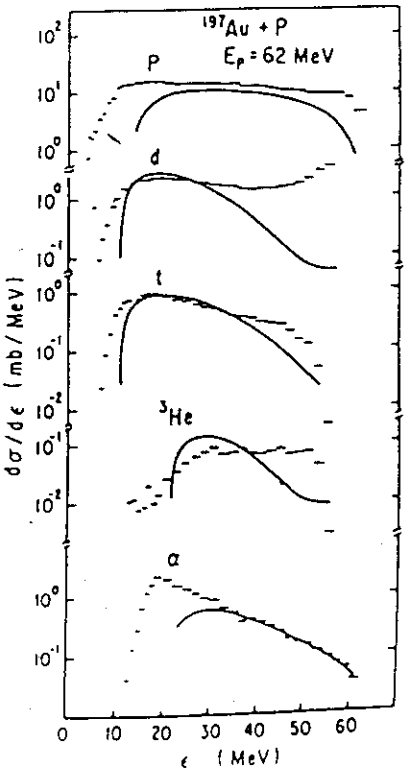

REFERENCES

1) A.Iwamoto and K.Harada ; Phys.Rev. C26 (82) 1821.

2) K.Sato, A.Iwamoto and K.Harada ; Contr. to Int. Symp. on Light Ion Reaction Mechanism, Osaka (1983).

5.12 Extension of Generalized Exciton Model and Calculation of (p,p') Angular Distribution

Akira Iwamoto and Kichinosuke Harada
Department of Physics, Japan Atomic Energy Research Institute

A formulation to calculate the angular distribution of nucleon emitted in the pre-equilibrium process was given by generalized exciton model[1] and has been used to analyze the experimental data. In order to incorporate the Fermi motion and Pauli effect in , the nucleon-nucleon cross section in nuclear matter was used in Ref.2. These models, however, contain two drawbacks. First, it happens to occur that even from the 2p-1h state (single collision) a very energetic particle can be emitted in the backward direction, which apparently contradicts to the two-body kinematics (linear momentum conservation). Second, the assumption that only the "fast" particle is allowed to change the number of exciton is too stringent.

In order to correct such points, we propose a new model[3] in which we fix not only the direction Ω but also the energy ϵ of the particle under consideration. The master equation for the probability $q(n\Omega\epsilon t)$ takes the form which is slightly more complex than the usual one. This equation is solved easily by the Legendre polynomial expansion method and the quantity $\int dt\ q(n\Omega\epsilon t)$ is given simply in the form of convolution integral, which is also easily calculated.

The numerical calculation has been done for (p,p') reaction of E_{inc}=30 62 MeV on targets ^{54}Fe, ^{120}Sn, ^{197}Au, ^{209}Bi up to 4-th step collision. In the forward angle ($\theta \lesssim 30$), the fitting to the data are much improved compared with Refs.1 and 2. Except for the backward cross section of very energetic proton, our model can reproduce the angular distribution of pre-equilibrium proton systematically well with no fitting parameter.

REFERENCES

1) G.Mantzouranis et.al.; Phys.Lett. 57B (75) 220.
2) S.Ziyang et.al.; Z.Phys. A305 (82) 61.
3) A.Iwamoto and K.Harada; Contribution to Int.Sym. Light Ion Reaction Mechanism, Osaka (1983)

5.13 Calculation of (p,α) Angular Distribution

Akira Iwamoto and Kichinosuke Harada
Department of Physics, Japan Atomic Energy Research Institute

Authors have recently developed a model to calculate the energy spectrum of composite particles emitted in the nucleon induced preequilibrium reactions.[1,2] We got a nice fitting to the data for (p,t), (p,^{3}He) and (p,α) reactions of several tens of Mev with a fixed set of parameters for all incident energies and for all targets examined. In order to calculate the energy-angle double differential cross section for (p,α) reaction, we present a model which is the extension of the generalized exciton model.[3]

We start from the generalized master equation[4] for the time evolution of the probability $q(n\Omega\epsilon t)$. In order to relate it to the angular distribution of α-particle, we assume that the latter is obtained by folding the former with the weight of the momentum distribution of α-particle intrinsic wave function. Numerical calculations have been done for several incident energies and for several targets. We show in the figure examples of them for 62MeV proton on ^{197}Au target. Although the model introduces no additional parameters, the fittingto the data is remarkably good for various outgoing energies in the angular region smaller than 90 degrees. The same quality of fitting is obtained for all systems examined.

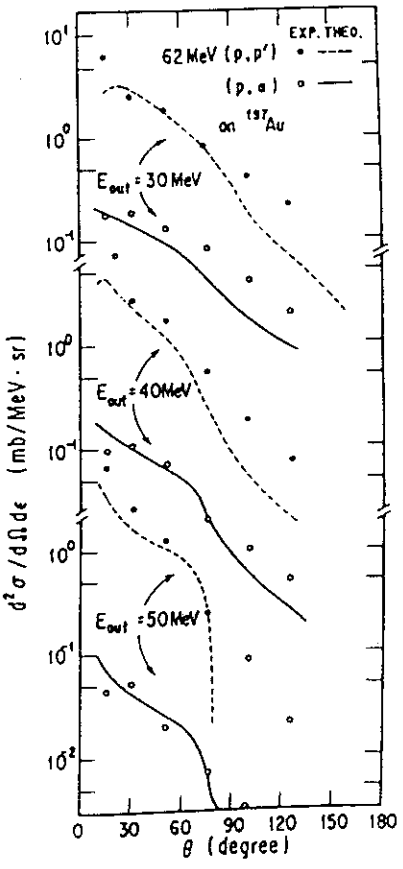

REFERENCES

1) A.Iwamoto and K.Harada: Phys.Rev.C26 (1982) 1821.
2) K.Sato, A.Iwamoto and K.Harada: Contr. to Int. Symp. on Light-Ion Reaction Mechanism, Osaka(1983).
3) A.Iwamoto and K.Harada: Contr. Int. Conf. Nuclear Physics, Florence (1983).
4) A.Iwamoto and K.Harada: Osaka Symp.(Ref.2).

VI FAST NEUTRON PHYSICS

6.1 Time Resolution of Large Scintillation Detector for Fast Neutron Measurements

Yoshimaro Yamanouti*, Masayoshi Sugimoto*, Shigeya Tanaka*,
Mikio Hyakutake**, Yutaka Furuta* and Motoharu Mizumoto*

*Department of Physics, Japan Atomic Energy Research Institute
and **Department of Nuclear Engineering, Kyushu University

One of the big four projects to be performed by the use of the JAERI tandem electrostatic accelerator is to study fast neutron physics in the energy range from 10 to 40 MeV. In order to make efficient measurements of neutrons in this energy range, a large scintillation detector has been developed. The present detector is similar in principle to the detector developed in Munich[1], i.e. both ends of the long scintillator are viewed by photomultipliers (RCA 8854) so as to compensate for increased time spread due to scintillator length. The scintillator vessel is a 10cmϕ x 80cm glass cylinder filled with NE213 liquid scintillator. The timing properties of the detector have been checked by coincidence measurements of the ^{60}Co gamma-rays with a small scintillator detector. Time resolution less than 0.9 nsec (FWHM) has been observed for an energy threshold of 1 x ^{60}Co Compton edge. The neutron gamma-ray pulse shape discrimination has been also checked using an Am-Be source.

To investigate the overall time resolution of the detector as a high energy neutron counter, neutrons from the ^{27}Al(d,n)^{28}Si reaction were observed by the pulsed-beam neutron time-of-flight technique with stop signals obtained from a beam pick-off tube. A pulsed beam of 25 MeV deuterons with a repetition rate of 4 MHz and a pulse duration of 0.86 nsec was provided by the JAERI tandem electrostatic accelerator. An 8mg/cm^2 self-supporting aluminium target was mounted on a frame at the entrance of a 3.8cm diam. by 24cm long stainless steel tube. The beam was stopped at the end of the tube. In order to shield the neutron detector from background neutrons generated at the beam stopper, an iron shadow bar about 50cm long was positioned between the stopper and the detector.

Neutrons were detected at 20° angle in an open geometry. The overall time resolution for the neutrons leading to the ground state of ^{28}Si was observed to be 1.2 nsec (FWHM). Fig.1 shows the 20° neutron time-of-flight spectrum from the $^{27}Al(d,n)^{28}Si$ reaction at E_d = 25 MeV.

Reference

1) D. Evers, E. Spindler, P. Konrad, K. Rudolph, W. Assmann and P. Sperr, Nucl. Instr. and Meth. 124 (1975) 23

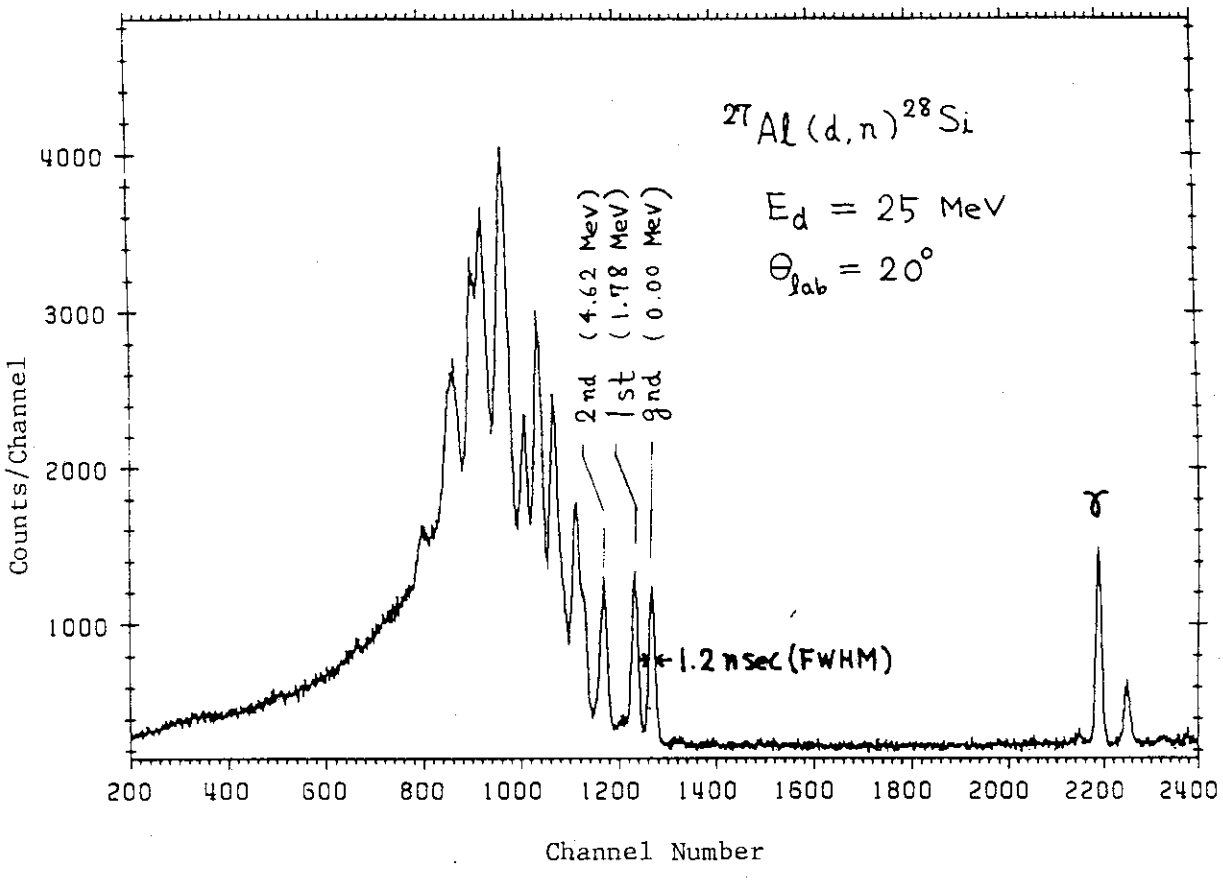

Fig.1 Time-of-flight spectrum for neutrons from the $^{27}Al(d,n)^{28}Si$ reaction at E_d=25 MeV and θ_{lab}=20°. The flight path is 9m. The width of the neutron peak leading to the ground state of ^{28}Si is 1.2 nsec (FWHM).

6.2 Neutron Emission from the d+d Reaction at 25 MeV

Masayoshi Sugimoto*, Yoshimaro Yamanouti*, Shigeya Tanaka*, Yutaka Furuta*, Motoharu Mizumoto* and Mikio Hyakutake**

*Department of Physics, Japan Atomic Energy Research Institute and
**Department of Nuclear Engineering, Fuculty of Engineering, Kyushu University

The D(d,n) reaction is an important neutron source reaction in the energy range 3 to 10 MeV. We have investigated the possibility of this reaction as the neutron source for scattering experiments in 10 to 40 MeV. The cross sections measured above 20 MeV incident energy are scarce and incomplete[1]. At 25 MeV there was one measurement of van Oers and Brockman[2] in the center-of-mass angles greater than 16 deg. In the present work the neutron emission cross sections of the $D(d,n)^3He$ and D(d,np)D reactions at 25 MeV incident energy were measured at forward angles using the neutron time-of-flight technique.

The pulsed deuteron beam was produced by the JAERI Tandem accelerator with the duoplasmatron negative ion source. The average beam current was 0.2 μA and the repetition rate was 4 MHz. The time resolution was 0.4 ns/m and the flight path was 5 m. The time reference was obtained from the beam pick-off tube at the 1 m upstream from the gas target. The gas cell of 3 cm length has a 5 μm Mo entrance window and a 1.2 mm Pt beam stop and was filled with 0.101 M Pa D_2 gas. The neutron detector was a 12.7 cm dia. x 5.1 cm thick NE213 liquid scintillator mounted on the RCA 8854 photomultiplier and the detection threshold was 5 MeV. The efficiencies were calculated by the Monte Carlo program STANTON[3]. The neutron TOF spectra were measured at 0, 1.5, 3, 5, 7.5, 20, 30 and 40 deg laboratory angles.

Fig. 1 shows the obtained differential cross sections of the $D(d,n)^3He$ reaction in the center-of-mass system and the comparison was made with the other data[2] and the evaluation[1]. The present results were agreed with the evaluation at small angles. The estimated uncertainties were 7-10 %. The double differential neutron emission cross sections in the lab system were presented in Fig. 2. The observed continuum spectra were suffered by

the large background due to the deuteron breakup in the beam stop. As the results were fluctuated by the background subtraction they were crunched by 100-200 channels. The uncertainties were 10 % or more.

References

1) M. Drosg, Nucl. Sci. Eng. 67,190(1978).
2) W. T. H. van Oers and K. W. Brockman Jr., Nucl. Phys. 48,625(1963).
3) N. R. Stanton, A Monte Carlo program for calculating neutron detection efficiencies in plastic scintillators, Ohio State University, COO-1545-92(Feb. 1971).

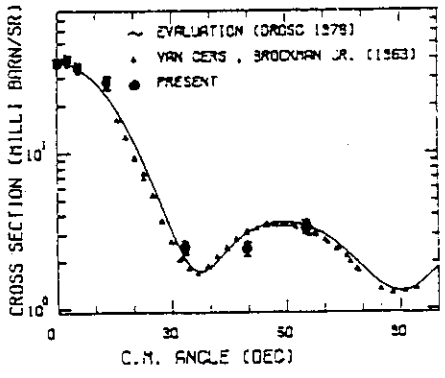

Fig. 1 Center-of-mass differential cross sections for the $D(d,n)^3He$ reaction at 25 MeV. Here, ● this work; ▲ ref.2 and —— evaluation (ref.1).

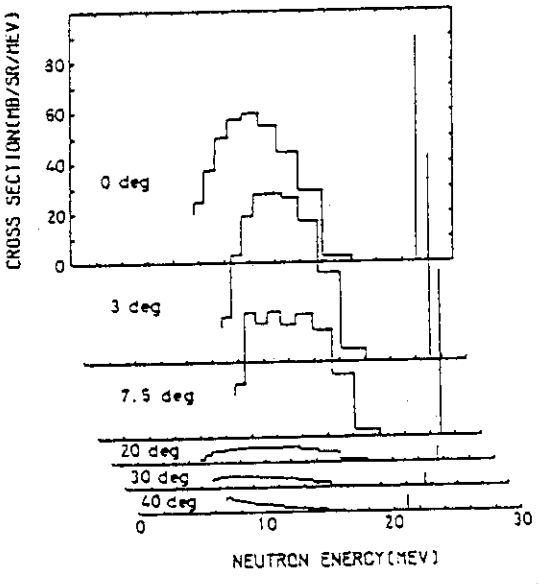

Fig. 2 Differential cross sections for the neutron emission from the d+d reaction at six laboratory angles. The single peaks at the right hand side correspond to the monoenergetic neutrons from the $D(d,n)^3He$ reaction and the bumps are from the D(d,np)D reaction.

VII PUBLICATIONS

7.1 Publications in Journals and Proceedings Articles

1. Shigemi Furuno, Hitoshi Otsu and Kazuhiko Izui
   Electron Microscope Observations of Tracks of 130 MeV Cl^{9+} Ions in Solids
   J. Electron Microsc. 30 (1981) 327

2. Susumu Hanashima
   Control System for JAERI Tandem Accelerator
   Genshikaku Kenkyu Vol. 27 No. 1, Feb. 1983

3. S. Hamada
   Effect of Irradiated Temperature on Cavity Distribution in Cl-ion Irradiated Pure Nickel
   JAERI-memo 58-003

4. Mitsuhiko Ishii, Masumi Ohshima, Tei-ichiro Matsuzaki and Hiroshi Taketani
   A Compton Polarimeter Composed of Four Planar Diodes of High-Purity Germanium
   Nucl. Instr. Meth. 196 (1982) 117

5. Akira Iwamoto and Kichinosuke Harada
   Mechanism of Cluster Emission in Nucleon-Induced Preequilibrium Reaction
   Phys. Rev. C26 (1982) 1821

6. Akira Iwamoto, Kichinosuke Harada, Shuhei Yamaji and Shiro Yoshida
   Microscopic Calculation of Friction Coefficient for Use in Heavy-Ion Reaction
   Z. Phys. A-Atom and Nuclei 302 (1981) 149

7. Yukio Kazumata and Shigemi Yugo
   ESR of Pyro-Graphite Irradiated by High Energy Ions
   J. Phys. Soc. Japan 51 (1982) 3753

8. Chiaki Kobayashi
Present Status of the JAERI Tandem Accelerator
Proc. of the 4th Symposium on Accelerator Science and Technology (November 24-26, 1982 in Tokyo) p. 325

9. Akiyasu Makishima, Hiroshi Taketani, Minoru Adachi, Masao Ogawa, Mitsuhiko Ishii, Masumi Ohshima, Shiro Kikuchi and Eisuke Minehara
A Rotary Bandpass Filter for Lifetime Measurements of Reaction Products Induced by Heavy Ions
JAERI-M-9901 (1982) in Japanese

10. Tei-ichiro Matsuzaki, Hiroshi Taketani, Mitsuhiko Ishii and Masumi Ohshima
A Compton Polarimeter with a Pair of High-Purity Ge Diodes
Nucl. Instr. Meth. 188 (1981) 63

11. Eisuke Minehara
Improvement and Development of the Negative Ion Sputter Sources for the JAERI Tandem Accelerator
Proc. Symp. on the Technical Development of Ion Source Related to the Accelerator (1981) p. 1

12. Eisuke Minehara and Shinichi Abe
Mass-Spectrometric Study of the Negatively-Charged Krypton Monofluoride
Nucl. Instr. Meth. 190 (1981) 215

13. Eisuke Minehara and Shinichi Abe
Mass-Spectrometric Study of the Negatively-Charged Krypton and Xenon Monofluorides
To be published in Nuclear Instruments and Methods

14. Eisuke Minehara, Shinichi Abe, Chiaki Kobayashi and Shiroh Kikuchi
Acceleration and Production of Various Heavy Ions at the JAERI Tandem Accelerator
Proc. 6th Symp. on Ion Sources and Ion-Assisted Technology (1981) p. 181

15. Shinichi Abe, Eisuke Minehara, Chiaki Kobayashi and Shiroh Kikuchi
Fabrication of Powder Cones for Negative Ion Sputter Sources
Proc. 6th Symp. on Ion Sources and Ion-Assisted Technology (1982) p. 185

16. Eisuke Minehara, Shinichi Abe, Chiaki Kobayashi, Shiroh Kikuchi, Susumu Hanashima, Yutaka Sato, Isao Ohuchi, Tadashi Yoshida, Susumu Kanda, Katsuzo Horie, Satoshi Tajima, Yoshihiro Tsukihashi and Shuhei Kanazawa
Production and Acceleration of Light- and Medium- Heavy Ions at the JAERI Tandem Accelerator
Proc. 4th Symp. on Accelerator Science and Technology (1982) p. 233

17. T. Mikumo, W. Yokota, S. M. Lee, Y. Nagashima, T. Nakagawa, Y. Fukuchi, K. Ideno, Y. Tomita, S. Takeuchi, S. Hanashima and W. Galster
The Reactions $^{37}Cl + ^{27}Al$ and $^{16}O + ^{48}Ti$ in the Energy Region of 100 - 200 MeV; Scission of a Composite System
Int. Symp. on Nuclear Physics at large Tandem Accelerators, Padova (1983)

18. Yuji Naruse, Hitoshi Watanabe and Kenji Noda
Irradiation Damage in Li_2O
JAERI-M 82-175
Japanese Contributions to IAEA INTOR Workshop
Phase II A ChaptèrVIII; Tritium and Blanket, p. 113

19. Kenji Noda and Hitoshi Watanabe
Irradiation Damage in Oxygen Ion Irradiated Li_2O
Progress Report on Fusion Reactor Materials Research and Development in Japan (1981) p. 106

20. Masumi Ohshima, Eisuke Minehara, Mitsuhiko Ishii, Takashi Inamura and Akira Hashizume
Multiple Coulomb Excitation of ^{167}Er
Proceedings to the INS International Conference on Dynamics of Nuclear Collective Motion (1982) p. 128

21. Masumi Ohshima, Eisuke Minehara, Mitsuhiko Ishii, Takashi Inamura and Akira Hashizume
Multiple Coulomb Excitation of ^{167}Er
submitted to J. Phys. Soc. Japan (1983)

22. Takaharu Otsuka
Rotational States and Interacting Bosons
Nucl. Phys. A368 (1981) 244

23. Takaharu Otsuka
On the Microscopic Foundation of the Interacting Boson Model
Proceeding of the 1982 INS Symposium edited by K. Tanabe and K. Ogawa

24. Takaharu Otsuka, Akito Arima and Naotake Yoshinaga
Dominance of Monopole and Quadrupole Pairs in the Nilsson Model
Phys. Rev. Lett. 48 (1982) 387

25. Takaharu Otsuka and Kichinosuke Harada
Pre-Equilibrium Description of Fast Light Particle Emission in Heavy-Ion Reactions
Phys. Lett. 121B (1983) 106

26. M. Sawada, Y. Sugiyama and E. Takekoshi
Characteristics of a Large Hybrid Gas Counter
JAERI-M 83-014 (1983)

27. K. Shiraishi, M. P. Tanaka, T. Aruga and S. Hamada
Damage Profile in Ion-Bombarded Nickel and Stainless Steel
ASTM STP 782 (1982) p. 297

28. Yasuharu Sugiyama, Naomoto Shikazono, Hiroshi Ikezoe and Hidetsugu Ikegami
JAERI Magnetic Spectrograph for Heavy-Ion Research
Nucl. Instr. Meth. 187 (1981) 25

29. Yasuharu Sugiyama, Naomoto Shikazono, Takemi Sato, Takeshi Takayama and Hidetsugu Ikegami
Magnet Design for JAERI Heavy-Ion Spectrograph
JAERI-M 9358 (1981)

30. Suehiro Takeuchi and Shuhei Kanazawa
Carbon Deposition Apparatus to Produce Long-lived Stripper Foils for the JAERI Tandem Accelerator
Nucl. Instr. Meth. 197 (1982) 267

31. Suehiro Takeuchi
Development of Long-lived Carbon Stripper Foils
Proc. of the 6th Symposium on Ion Sources and Ion-assisted Technology (June 7-9, 1982 Kyoto) p. 177

32. Suehiro Takeuchi and Shuhei Kanazawa
New Carbon Stripper Foils Less Shrinkable under Heavy Ion Bombardment
Nucl. Instr. Meth. 206 (1983) 331

33. Yoshiaki Tomita, Isao Ohuchi, Susumu Kanda, Katsuzo Horie, Yoshihiro Tsukihashi and Susumu Hanashima
Control System for JAERI Tandem Accelerator
Proceedings of the 4th Symposium on Accelerator Science and Technology (Nov. 24-26, 1982)

34. Isao Tonozuka, Akira Iwamoto and Kichinosuke Harada
Shell Model Calculation of Alpha-Formation Factor for Use in Pre-Equilibrium Alpha Emission
JAERI-M 83-057 (1983)

35. Shuhei Yamaji and Akira Iwamoto
Friction Coefficient for Deep Inelastic Heavy Ion Collision
Preprint (1983), submitted to Z. Phys. A

36. Shuhei Yamaji, Akira Iwamoto, Kichinosuke Harada and Shiro Yoshida
Microscopic Calculation of the Mass Diffusion Coefficient Using Linear Response Theory
Phys. Lett. 106B (1981) 433

37. Naotake Yoshinaga, Akito Arima and Takaharu Otsuka
Description of High-Spin States in the Interacting Boson Model
Phys. Lett. 114B (1982) 86

7.2 Contributions to Scientific and Technical Meetings

1. Hiroshi Baba et al.
   $^{197}Au + ^{16}O$ Reaction (2) Momentum Transfer and Charged Particle Emission
   The 26th Symposium on Radiochemistry in Niigata (Oct. 2-4, 1982)

2. S. Hamada, M. Tanaka and K. Shiraishi
   Effect of Irradiated Temperature on Cavity Distribution in Cl-ion Irradiated Pure Nickel
   Spring Meeting of Japan Institute of Metals in Tokyo (Apr. 1-3, 1982)

3. S. Hanashima, K. Ideno, S. Takeuchi, Y. Tomita, Y. Fukuchi, W. Galster, S. Kinouchi, S. M. Lee, T. Mikumo, Y. Nagashima, T. Nakagawa and W. Yokota
   Fusion and Many-nucleon Transfer Reactions in $^{37}Cl + ^{27}Al$
   Spring Meeting of Physical Society of Japan in Tokyo (1983)

4. Shin-ichi Ichikawa et al.
   $^{197}Au + ^{16}O$ Reaction (1) The Yields of Residual Nuclides
   The 26th Symposium on Radiochemistry in Niigata (Oct. 2-4, 1982)

5. Akira Iwamoto
   Light Ion Emission from Pre-equilibrium State
   Spring Meeting of Physical Society of Japan in Koganei (Mar. 31 - Apr. 3, 1982)

6. Akira Iwamoto, Kenichi Sato and Kichinosuke Harada
   Composite Particle Emission Based on the Exciton Model
   Autumn Meeting of Physical Society of Japan in Sapporo (Sept. 30 - Oct. 3, 1982)

7. Akira Iwamoto, Kenichi Sato and Kichinosuke Harada
   Angular Distribution of Light Composite Particles Emitted from Pre-equilibrium State
   Spring Meeting of Physical Society of Japan in Hachioji (Mar. 27-30, 1983)

8. Akira Iwamoto and Kichinosuke Harada
Evaporation Model for Composite Particles Emission Taking into Account the freedom of Intrinsic Motion
Autumn Meeting of Physical Society of Japan in Matsue (Oct. 1-4, 1981)

9. Kazuhiko Izui, Hitoshi Otsu and Shigemi Furuno
Direct Observations of Tracks of High Energy Heavy Ions in Solids
Spring Meeting of Physical Society of Japan in Hiroshima (Mar. 30 - Apr. 2, 1981)

10. Akiyasu Makishima et al.
E0 Transition in 74-Se
Spring Meeting of Physical Society of Japan in Tokyo (May 30, 1982)

11. Eisuke Minehara
A Surface Ionization Gun for the Negative Ion Sputter Source
Spring Meeting of Physical Society of Japan (Apr., 1982)

12. Eisuke Minehara and Shinichi Abe
The Negative Ion Source Test Facility for the JAERI Tandem Accelerator
Autumn Meeting of Physical Society of Japan (Oct., 1982)

13. Kenji Noda and Hitoshi Watanabe
Irradiation Damage in Lithium Oxide Irradiated by Oxygen Ions
Autumn Meeting of Atomic Energy Society of Japan (Oct. 8-10, 1982)

14. Kenji Noda and Hitoshi Watanabe
Irradiation Effects in Lithium Oxide
Topical Meeting on Irradiation Effects in Insulator, Kyoto University (Kumatori) (Dec. 10, 1982)

15. Masumi Ohshima, Eisuke Minehara, Mitsuhiko Ishii, Takashi Inamura and Akira Hashizume
Multiple Coulomb Excitation of Rare-Earth Odd-A Nuclei
Spring Meeting of Physical Society of Japan in Tokyo (March 28-30, 1982)

16. Masumi Ohshima, Eisuke Minehara, Mitsuhiko Ishii, Takashi Inamura and Akira Hashizume
Transition Probabilities of the Ground-State Rotational Band in ^{167}Er
Autumn Meeting of Physical Society of Japan in Sapporo (Sept. 30 - Oct. 3, 1982)

17. Masumi Ohshima, Eisuke Minehara Shiroh Kikuchi, Takashi Inamura, Akira Hashizume and Hiroki Kumahora
The Ground-State Rotational Band in ^{163}Dy
Spring Meeting of Physical Society of Japan in Tokyo (Mar. 27-30, 1983)

18. Eiji Sakai
Induced Radioactivities in Semiconductors Irradiated with High-Energy Heavy Ions
1983 Annual Meeting of the Atomic Energy Society of Japan, Paper C-11, Tokyo (May 28-31, 1983)

19. Eiji Sakai
Induced Radioactivities in Various Materials for Solid-State Physics Research Irradiated with High-Energy Heavy Ions
The 19th Annual Meeting on Radioisotopes in the Physical Sciences and Industry, Paper 6p-I-1, Tokyo (July 5-7, 1982)

20. M. Sawada, Y. Sugiyama, E. Takekoshi, H. Ikezoe, Y. Tomita and N. Shikazono
Characteristics of a Large Hybrid Gas Counter
Spring Meeting of Physical Society of Japan in Tokyo (Mar. 29, 1983)

21. K. Shiraishi, M. Tanaka, T. Aruga and S. Hamada
Microstructure Observation Produced by High Energy Ion Irradiation
Autumn Meeting of Japan Institute of Metals in Kyoto (Nov. 1-3, 1981)

22. Masayoshi Sugimoto and Yoshimaro Yamanouti
The general properties of the high energy neutron detectors
Autumn Meeting of Physical Society of Japan in Sapporo (Sept. 30 - Oct. 3, 1982)

23. Masayoshi Sugimoto, Yoshimaro Yamanouti, Yutaka Furuta, Motoharu Mizumoto, Shigeya Tanaka and Mikio Hyakutake
$D(d,n)^3He$ and D(d,np)D reactions at 25 MeV
Annual Meeting of the Atomic Energy Society of Japan in Tokyo (Mar. 28-31, 1983)

24. Yasuharu Sugiyama
JAERI Heavy-Ion Spectrograph "ENMA"
Spring Meeting of Physical Society of Japan in Tokyo (April, 1982)

25. Yasuharu Sugiyama, Naomoto Shikazono, Hiroshi Ikezoe, Yoshiaki Tomita and Hidetsugu Ikegami
JAERI Heavy-Ion Spectrometer ENMA
Autumn Meeting of Physical Society of Japan in Shimane (Oct., 1981)

26. E. Takekoshi
Position Sensitive Detectors for Precise Measurements of Nuclear Reactions with Heavy Ions
Spring Meeting of Physical Society of Japan in Tokyo (March 28, 1983)

27. Suehiro Takeuchi and Shuhei Kanazawa
Carbon Stripper Foils Less Shrinkable against Heavy Ion Bombardment
The World Conf. of the International Nuclear Target Development Society (Oct. 6-8, 1982 in Seattle)

28. T. Tamura, M. Ohshima, T. Sekine, S. Ichikawa, K. Nishimura, S. Ohya and N. Mutsuro
Decay Scheme of ^{129}Ba
Spring Meeting of Physical Society of Japan in Tokyo (Mar. 27-30, 1983)

29. T. Tamura, M. Ohshima, E. Minehara, T. Sekine, K. Hata, S. Ichikawa, O. Nakamura, S. Ohya and N. Mutsuro
Decays of ^{121}I, ^{121}Xe and ^{120}I
Spring Meeting of Physical Society of Japan in Tokyo (Mar. 29-31, 1982)

30. Shuhei Yamaji, Akira Iwamoto, Kichinosuke Harada and Shiro Yoshida
Analysis of Multi-nucleon Transfer Reaction by the Linear Response Theory
Autumn Meeting of Physical Society of Japan in Matsue (Oct. 1-4, 1981)

31. Shuhei Yamaji, Akira Iwamoto, Kichinosuke Harada and Shiro Yoshida
Effects of the Potential on the Width of the Mass Distribution in Deep Inelastic Collision
Spring Meeting of Physical Society of Japan in Hachioji (Mar. 27-30, 1983)

32. Y. Yamanouti, M. Sugimoto, S. Tanaka, M. Hyakutake, Y. Furuta and M. Mizumoto
Measurements of High Energy Neutrons by the Use of a Very Large Neutron Detector
Spring Meeting of Physical Society of Japan in Tokyo (Mar. 27-30, 1983)

33. W. Yokota, T. Nakagawa, Y. Nagashima, W. Galster, S. M. Lee, T. Mikumo, K. Ideno, S. Takeuchi and Y. Tomita
Many-nucleon Transfer Reactions in $^{37}Cl + ^{27}Al$
Autumn Meeting of Physical Society of Japan in Sapporo (1982)

VIII PERSONNEL AND COMMITTEES

8.1 Personnel

Department of Physics

	Kichinosuke Harada	Director
	Nobuyoshi Tsuda	Administrative Manager

Accelerators Division

Scientific Staff	Michio	Maruyama*
	Yuki	Kawarasaki
	Shiro	Kikuchi
	Suehiro	Takeuchi
	Eisuke	Minehara
	Susumu	Hanashima
Technical Staff	Chiaki	Kobayashi**
	Isao	Ohuchi
	Yutaka	Sato
	Tadashi	Yoshida
	Susumu	Kanda
	Katsuzo	Horie
	Satoshi	Tajima
	Yoshihiro	Tsukihashi
	Shinichi	Abe
	Shuhei	Kanazawa

Nuclear Physics Laboratory

Scientific Staff	Naomoto	Shikazono***
	Eiko	Takekoshi
	Tsutomu	Tamura
	Mitsuhiko	Ishii
	Yoshiaki	Tomita
	Yasuharu	Sugiyama
	Akira	Iwamoto

* Chief, Accelerators Division

** Chief, Technical Staff

*** Deputy Director, Department of Physics and Chief of Nuclear Physics Laboratory

Nuclear Physics Laboratory (continued)			
Scientific Staff	Kazumi	Ideno	
	Hiroshi	Ikezoe	
	Masumi	Ohshima	
	Takaharu	Ohtsuka	
Scholarship Fellow	Masayasu	Sawada	(University of Tsukuba)
	Akiyasu	Makishima	(Tokyo Institute of Technology)
Linac Laboratory			
Scientific Staff	Shigeya	Tanaka*	
	Yutaka	Furuta	
	Motoharu	Mizumoto	
	Yoshimaro	Yamanouchi	
	Masayoshi	Sugimoto	
Scholarship Fellow	Izumi	Tsubone	(Kyushu University)
Solid State Physics Laboratory I			
Scientific Staff	Kazuo	Geshi**	
	Kunio	Ozawa	
	Yukio	Kazumata	
	Kiyoshi	Kawatsura	
	Hiroshi	Naramoto	
	Hiroshi	Tomimitsu	
	Masao	Sataka	
Scholarship Fellow	Hidenori	Yamaguchi	(University of Tsukuba)
Solid State Physics Laboratory II			
Scientific Staff	Tadao	Iwata***	
	Akihiro	Iwase	
	Shigemi	Sasaki	

* Chief, Linac Laboratory

** Chief, Solid State Physics Laboratory I

*** Chief, Solid State Physics Laboratory II

Department of Chemistry

Nuclear Chemistry Laboratory

Scientific Staff	Hiroshi	Okashita*
	Hirokazu	Umezawa
	Toshio	Suzuki
	Shigekazu	Usuda
	Nobuaki	Kono
	Shin-ichi	Ichikawa
	Nobuo	Shinohara

Analytical Chemistry Laboratory

Scientific Staff	Yuji	Baba

Physical Chemistry Laboratory

Scientific Staff	Mutsuhide	Komaki

Solid State Chemistry Laboratory

Scientific Staff	Kazuhiko	Izui**
	Shin-ichi	Ohno
	Teikichi A.	Sasaki
	Shigemi	Furuno
	Hitoshi	Ohtsu

Department of Radioisotope Production

Scientific Staff	Hiroshi	Baba***

Production Development Division

Scientific Staff	Sumiko	Baba
	Kentaro	Hata
	Toshiaki	Sekine

* Chief, Nuclear Chemistry Laboratory

** Chief, Solid State Chemistry Laboratory

*** Present address: Faculty of Sciences, Osaka University

Department of Fuels and Materials Research

Physical Metallurgy Laboratory

Scientific Staff	Kensuke	Shiraishi*
	Akimichi	Hishinuma
	Mitsuo	Tanaka
	Takeo	Aruga
	Shozo	Hamada
	Tomotsugu	Sawai

Fuel Property Laboratory

Scientific Staff	Hitoshi	Watanabe**
	Kenji	Noda
	Yoshinobu	Ishii

Department of Reactor Engineering

Reactor Instrumentation Laboratory

Scientific Staff	Eiji	Sakai

Department of Health Physics

Technical Staff	Syoji	Izawa
	Yoshihiro	Seiki
	Futao	Niino
	Takeo	Seki

* Chief, Physical Metallurgy Laboratory

** Chief, Fuel Property Laboratory

8.2 Steering Committee

(Chairman)	Sueo Nomura	(Deputy Director General, Tokai Research Establishment)
	Takumi Asaoka	(Director, Department of Reactor Engineering)
	Junichi Shimokawa (∿ September 1982)	(Director, Department of Fuels and Materials Research)
	Kazumi Iwamoto (October 1982 ∿)	(Director, Department of Fuels and Materials Research)
	Kichinosuke Harada	(Director, Department of Physics)
	Haruo Natsume	(Director, Department of Chemistry)
	Yukio Obata	(Director, Department of Thermonuclear Fusion Research)
	Toshihiko Abe	(Director, Department of Radioisotope Production)
(Secretary)	Yoshikazu Hamaguchi (∿ May 1982)	(Deputy Director, Department of Physics)
(Secretary)	Naomoto Shikazono (June 1982 ∿)	(Deputy Director, Department of Physics)
(Secretary)	Michio Maruyama	(Chief, Accelerators Division)
(Secretary)	Nobuyoshi Tsuda	(Administrative Manager, Department of Physics)

8.3 Consultative Committee

(Chairman)	Hiroshi	Ishikawa	(Executive Director)
(Vice Chairman)	Sueo	Nomura	(Deputy Director General, Tokai Research Establishment)
(Vice Chairman)	Kichinosuke	Harada	(Director, Department of Physics)
	Hiromichi	Kamitsubo	(Principal Scientist, Institute of Physical and Chemical Research)
	Kozi	Nakai	(Associate Professor, University of Tokyo)
	Hiroyasu	Ejiri	(Professor, Osaka University)
	Shiori	Ishino	(Professor, University of Tokyo)
	Nobuo	Oda	(Professor, Tokyo Institute of Technoloty)
	Kohzoh	Masuda	(Professor, University of Tsukuba)
	Shiro	Iwata	(Professor, Kyoto University)
	Ichiro	Fujiwara	(Associate Professor, Kyoto University)
	Kenji	Sumita	(Professor, Osaka University)
	Itsuro	Kimura	(Professor, Kyoto University)
(Secretary)	Yoshikazu	Hamaguchi (∿ May 1982)	(Deputy Director, Department of Physics)
(Secretary)	Naomoto	Shikazono (June 1982 ∿)	(Deputy Director, Department of Physics)
(Secretary)	Michio	Maruyama	(Chief, Accelerators Division)
(Secretary)	Nobuyoshi	Tsuda	(Administrative Manager, Department of Physics)

8.4 Program Advisory Committee

(Chairman)	Yoshikazu Hamaguchi (∿ May 1982)	(Deputy Director, Department of Physics)
(Chairman)	Kichinosuke Harada (June 1982 ∿)	(Director, Department of Physics)
	Yoshihiro Seiki	(Chief, Radiation Control Group, Department of Health Physics)
	Kensuke Shiraishi	(Chief, Physical Metallurgy Laboratory, Department of Fuels and Materials Research)
	Hirokazu Umezawa	(Principal Scientist, Department of Chemistry)
	Kunio Ozawa	(Principal Scientist, Department of Physics)
	Naomoto Shikazono	(Deputy Director, Department of Physics)
	Shigeya Tanaka	(Chief, Linac Laboratory, Department of Physics)
	Michio Maruyama	(Chief, Accelerators Division, Department of Physics)
	Chiaki Kobayashi	(Chief, Tandem Operation Group, Department of Physics)

IX CO-OPERATIVE RESEARCHES

	Title	Co-operating Institution
2.2	Beam-Foil Interaction in High Energy Region	Faculty of Engineering, Ibaraki University* College of Education, University of Tokyo*
2.3	Spectroscopy of Electrons and X-rays Emitted in High-Energy Ion-Atom Collisions	College of General Education, University of Tokyo*
2.4	Calorimetric Measurements of Stopping Power for ^{35}Cl and ^{12}C Ions in Nickel	Faculty of Engineering, Ibaraki University*
3.1	Irradiation Damages in Oxygen Ion Irradiated Li_2O	Faculty of Engineering, Nagoya University*
3.7	ESR of Phyro-Graphite Irradiated by High Energy Ions	University of Electro-Communication
4.1	NUCLEAR CHEMISTRY OF ACTINOIDS Synthesis of Transuranium Nuclides from Interaction of ^{16}O with ^{238}U	Department of Physics, Hiroshima University* Institute of Atomic Energy, Kyoto University*
4.2	An Experiment of Irradiated ^{197}Au with ^{16}O Ions	Institute of Atomic Energy, Kyoto University*
4.3	Electron Capture and Positron Decay from ^{121}Xe	Faculty of Sciences, Niigata University*
4.4	Decay Scheme of $^{129g,m}Ba$	Faculty of Sciences, Niigata University*

5.1	Characteristics of a Large Hybrid Gas Counter for Use with the JAERI Magnetic Spectrograph for Heavy Ion Research	Institute of Nuclear Physics, University of Tokyo* Tohoku Institute of Technology Faculty of Science, Yamagata University
5.2	JAERI Magnetic Spectrograph "ENMA" for Heavy Ion Research	Institute for Nuclear Study, University of Tokyo* Faculty of Science, Yamagata Univerwity Tohoku Institute of Technology
5.3	Elastic and Inelastic Scattering of $^{12}C + ^{12}C$ and $^{58}Ni + ^{60}Ni$	Institute of Nuclear Physics, University of Tokyo* Faculty of Science, Yamagata University Tohoku Institute of Technology
5.4	Fusion and Deep Inelastic Reactions for $^{37}Cl + ^{27}Al$ and $^{16}O + ^{48}Ti$ in the Energy Region of 100 to 200 MeV	Tandem Accelerator Center, University of Tsukuba*
5.5	E0 Transition in 74-Se Isotope	Faculty of Science, Tokyo Institute of Technology*
5.6	In-Beam Gamma-Ray Spectroscopy of Fusion Residues Induced by Heavy Projectiles	Faculty of Science, Tokyo Institute of Technology*
5.7	The Ground-State Rotational Band in ^{167}Er	Institute of Physical and Chemical Research
5.8	The Ground-State Rotational Band in ^{163}Dy	Institute of Physical and Chemical Research

6.1	Time Resolution of Large Scintillation Detector for Fast Neutron Measurements	Faculty of Engineering, Kyushu University*
6.2	Neutron Emission from the d + d Reaction at 25 MeV	Faculty of Engineering, Kyushu University*

* Travel expense is supplied by JAERI